2017

ASSESSING THE CELLULAR AND ADHESIVE INTERACTIONS IN IN VITRO MODELS OF MANTLE CELL LYMPHOMA

Tucker, David

ASSESSING THE CELLULAR AND ADHESIVE INTERACTIONS IN *IN VITRO* MODELS OF MANTLE CELL LYMPHOMA

Submitted by Dr David Tucker of the Peninsula College of Medicine and Dentistry Graduate School to the Universities of Exeter and Plymouth as a thesis for the degree of Doctor of Medicine

April 2017

I certify that all material in this thesis which is not my own work has been identified and that no unchanged or acknowledged material has previously been submitted and approved for the award of a degree by this or any other University……..(signature)

AUTHOR'S DECLARATION

At no time during the registration for the degree of Doctor of Medicine has the author been registered for any other University award without prior agreement of the Graduate Sub-Committee.

Work submitted for this research degree at the Plymouth University has not formed part of any other degree either at Plymouth University or at another establishment.

Word count of main body of thesis: 36,478.

Signed:

Date:

ABSTRACT

Dr David Tucker

Assessing the cellular and adhesive interactions in *in vitro* models of mantle cell lymphoma

Mantle cell lymphoma (MCL) is a rare lymphoproliferative disorder (LPD) that has very poor survival. Like other LPDs, the neoplastic cells of MCL have an intimate dependence upon accessory cells within haematopoietic tissues. Understanding and exploiting the tissue-relationships of the mantle cells may therefore lead to further new approaches to treatment. This study work has set out to construct an *in vitro* system to model relevant aspects of the tissue-dependent behaviour of the neoplastic mantle cells, seeking to establish the link between *in vitro* behaviour and clinical phenotype, and establishing the feasibility of this system to study the effects of different therapeutic interventions.

The first experimental chapter employs relevant mouse and human stromal models to mirror the tissue environment of MCL *in vivo*. Testing relevant agents, the work establishes that the system can identify different behaviour between indolent and aggressive forms of MCL, and demonstrates a particular importance for CD40 ligand both in the proliferation and survival of the neoplastic mantle cells, but shows also how these effects are modulated by the soluble factors interleukin-4 (IL-4) and the toll-like receptor-9 ligand (TLR9-L). The second experimental chapter examines the adhesion molecules expressed on MCL cells. Considerable variation in the level of expression is observed between cases, but overall the cases express particularly high levels of the integrin receptors LFA-1 (detected by alpha chain CD11a) and VLA-4

(detected by alpha chain CD49d). Cases also showed a significant difference in overall adhesion and chemokine-receptor expression between cases that had either a nodal or leukaemic clinical pattern, although no single adhesion molecule was characteristic of clinical phenotype. The final experimental chapter looked at 3-D culture of MCL. Within tissues MCL grows in a 3-D rather than 2-D matrix and it is recognised that cells employ different forms of adhesion and migration within the different spatial environments. This chapter establishes the feasibility of growing cells in 3-D systems and looks at optimal conditions to preserve and examine the cellular characteristics of cells within a 3-D environment.

Overall, this thesis demonstrates the feasibility and pathobiological relevance of *ex vivo* culture of MCL cells giving insights into the factors that drive MCL survival and proliferation and the correlation between *in vitro* behaviour and clinical phenotype. It is proposed that this work can be expanded to examine therapeutic interventions in the disorder.

TABLE OF CONTENTS

LIST OF TABLES

LIST OF FIGURES

LIST OF ABBREVIATIONS

Abbreviation	Term	Abbreviation	Term
2-D	2-dimensional	LPD	lymphoproliferative disorder
3-D	3-dimensional	LPS	lipopolysaccharide
a.u.	arbitrary units	LTCM	Long-term culture medium
APC	Antigen presenting cells	MAPK	mitogen-activated protein kinases
APC	allophycocyanin	MCL	Mantle cell lymphoma
BCR	B-cell receptor	MFI	median fluorescence intensity
BSA	bovine serum albumin	MFIR	median fluorescence intensity ratio
BTK	Bruton's tyrosine kinase	MHC	Major histocompatibility complex
CAM	cellular adhesion molecules	MSC	Mesenchymal stromal cells
CAM-DR	Cell-adhesion mediated drug resistance	MZL	Marginal zone lymphoma
CD40-L	CD40-ligand	NBF	Neutral buffered formalin
CD40L-NT	CD40-ligand-non-transfected (murine stroma)	NF kB	nuclear factor kB
CD40L-T	CD40-ligand-transfected (murine stroma)	NHL	non-Hodgkin lymphoma
CDK	cyclin-dependent kinase	NK	Natural killer cells
CLL	chronic lymphocytic leukaemia	ODN	oligonucleotides
CpG	Cytosine-phosphate-Guanine	PBMC	Peripheral blood mononuclear cell
DAPI	4',6-diamidino-2-phenylindole	PBS	Phosphate buffered saline
DLBCL	diffuse large B-cell lymphoma	PE	phycoerythrin
DMSO	dimethyl-sulfoxide solution	PFH	Paraformaldehyde
ECM	Extracellular matrix	PI3k	phosphoinositide 3-kinase
FACS™	Fluorescence-activated cell sorting	PS	phosphatidylserine
FCS	Fetal calf serum	RB1	Retinoblastoma protein 1
FDC	Follicular dendritic cells	rpm	revolutions per minute
FITC	fluorescein isothiocyanate	RPMI	Roswell Park Memorial Institute
FN	Fibronectin	SEM	Standard Error of the Mean
FS	Forward scatter	SLL	Small lymphocytic lymphoma
FTH	Follicular T Helper cells	SSC	Side-scatter
GC	Germinal Centre	TD	thymus-dependent
G519	Granta-519	TI	thymus-independent
Gy	Gray	TLR9-L	Toll-like receptor-9 ligand
HCL	Hairy cell leukaemia	TNF	Tumour necrosis factor
ICAM	Intracellular adhesion molecule	VLA-4	Very Late Activation protein-4
IGHV	Immunoglobulin gene heavy-chain variable region		
IL-4	Interleukin-4		
IMDM	Iscove's Modified Dulbecco's Medium		
LAM	Lymphocyte associated macrophages		
LFA-1	Late functioning antigen 1		

ACKNOWLEDGEMENTS

The study of mantle cell lymphoma vitally important because it represents one of the most challenging forms of non-Hodgkin lymphomas (NHL) for patients and physicians with many unmet clinical needs. Yet the field is currently moving at a fast pace due to the recent development of novel targeted therapies and a development of understanding regarding the importance of the microenvironment. It is therefore both an exciting and rapidly developing arena for research.

I am principally indebted to my director of studies, Dr Claire Hutchinson for her tireless support and encouragement and for the invaluable assistance she has given to me during the preparation of this thesis.

I am grateful to Professor Simon Rule for his support and inspiration and for displaying faith in my abilities as a clinician and researcher. I am grateful to Dr Craig Donaldson for his supervision and suggestions and extremely thankful to Hannah Thompson for her invaluable support and friendship during my research placement.

I am grateful to the help and support provided by the staff at Derriford Hospital, Plymouth, particularly my colleagues in the nuclear physics unit for assistance with stromal irradiation and the biomedical scientists in the combined laboratories for their help with staining sections.

Finally I am most grateful to the patients who willingly provided their blood and time for my research and to the team of nurses and administrators involved in clinical haematology trials at Derriford Hospital.

DEDICATION

To my wife, Louise, for her endless support, patience and encouragement and to my children, George, Joseph and Connie.

1. CHAPTER 1 - INTRODUCTION

An Overview of Mantle Cell Lymphoma

1.1

Mantle cell lymphoma (MCL) is a non-Hodgkin lymphoma (NHL) subtype comprising 6-8% of all NHL cases with an approximate incidence of 0.4 per 100,000 in Europe and the USA. The median age at diagnosis is 68 years and the disease has a propensity for older males of approximately 3:1.[1–3] Patients with MCL typically present with diffuse lymphadenopathy. Extranodal involvement is a common feature, with the peripheral blood, bone marrow and gastro-intestinal tract all frequently involved.[4]

Mantle cell lymphoma has striking clinical and biological heterogeneity and can be broadly subdivided into classical, aggressive MCL and a less common indolent subtype.[5,6]

The classical, aggressive form of MCL has a progressive, nodal and symptomatic clinical phenotype and a striking tendency to disseminate throughout the body, infiltrating both the reticuloendothelial system and extranodal sites. It is often at an advanced stage at diagnosis requiring immediate treatment.[4,7]

The less common indolent form of MCL tends to remain quiescent and stable for prolonged periods, often years, without the need for treatment, and is characterized by a leukaemic, non-nodal and non-symptomatic clinical phenotype.[8] The MCL cells also have a distinct genetic and molecular character, including a simple karyotype and often demonstrate somatic hypermutation of the IgVH gene segments, suggesting experience of the germinal centre.[5,9,10]

Treatment for MCL depends on the fitness of the patient and the stage of the disease. Localised disease can sometimes be treated with local radiotherapy, whereas

widespread disease is generally treated with intensive cytoreductive therapy incorporating a monoclonal antibody specific for CD20 together with a high-dose cytarabine-based regimen, often consolidated by an autologous stem-cell transplant in first remission.[11–13] There is no standard of care for patients unfit for intensive therapy or for patients at relapse, however the landscape of therapy has recently been dramatically changed with the development of several novel targeted therapies

Regardless of treatment type, MCL is generally regarded as an incurable disease and most cases behave aggressively with a pattern of diminishing returns from sequential lines of therapy and ultimately, a poor prognosis.[14–16]

Mantle cell lymphoma therefore represents an unmet clinical need in haemato-oncology. Recent advances in the understanding of the molecular pathogenesis and cell-signalling pathways in MCL together with the introduction of new small molecule inhibitors have led to encouraging progress in the treatment of this disease (reviewed in Appendices 1 and 2).[17]

1.1.1 The Biological Characteristics of Mantle Cell Lymphoma

The genetic hallmark of MCL is the t(11;14)(q13;q32) chromosomal translocation. This translocation brings the cell-cycle regulator, CCND1 (11q13), under control of the immunoglobulin heavy chain (IGH) locus, (14q32) resulting in constitutive over-expression of cyclin D1.[3,7] Cyclin D1 binds to cyclin-dependent kinases 4 and 6 (CDK4 & 6) which phosphorylate retinoblastoma protein (RB1) leading to activation of the E2F transcription factors which, in turn, upregulate the progression through the early phases of the cell cycle, promoting unchecked proliferation.[7,18]

Although the t(11;14) translocation is the common pathological change and diagnostic hallmark of MCL, other genetic and molecular aberrations are probably necessary for

disease progression.[19,20] Mutations in the INK4a/CDK/RB1 and ARF/MDM2/p53 cellular pathways are often detected, as well as aberrant expression of the SOX11 transcription factor, all of which contribute to genetic instability, unregulated proliferation and inhibition of differentation.[6,19,21,22] Hypermutation of the immunoglobulin heavy chain gene is usually absent in MCL, however, a proportion of MCL cases, (up to 40% in some series) carry mutated IgVH genes, suggesting that some cases of MCL also have experience of the germinal centre. [23]

1.1.2 Histopathological Features of Mantle Cell Lymphoma

Mantle cell lymphoma cells possess distinct histological characteristics. The classical tumours show a proliferation of small to medium sized lymphocytes with irregular nuclei and inconspicuous nucleoli. Less commonly, mantle cells may have blastoid morphology with a round nucleus, finely dispersed chromatin and more prominent nucleoli. Some cases have larger cells with irregular and pleomorphic nuclei and distinct, small nucleoli (Figure 1-1).[7]

1.1.3 The Immunophenotype of Mantle Cell Lymphoma Cells

MCL cells demonstrate a mature B cell profile by immunophenotyping with moderate-strong expression of surface immunoglobulins (IgM/D, predominantly lambda), B-cell associated antigens such as CD19, CD20, CD22, CD79 and the T-cell and chronic lymphocytic leukaemia (CLL)-associated antigen CD5. However they do not usually express CD23 (a cell surface molecule for B cell activation and growth); CD10, which is expressed on germinal centre-associated lymphocytes, or BCL6, a transcription factor associated with lymphoid follicle germinal centre formation and maintenance.[3] The characteristic immunophenotype is useful in diagnosis and differentiation from other forms of B-NHL and will be used in this study to identify primary MCL cells when cultured with other cell types.

1.2 The Tissue Microenvironment in Mantle Cell Lymphoma

The tissue microenvironment is recognised as a key component in evolution of many forms of cancer.[24–26] In addition to the intrinsic proliferative capacity of MCL cells, there is growing evidence that MCL cells, like other forms of lymphoma are dependent on a complex network of signals provided by a supportive and protective niche in which the tumour cells, like their healthy counterparts, can thrive.[27–31]

The MCL microenvironment is generally limited to the adult lymphoreticular system, specifically, the primary lymphoid organs (bone marrow), and the secondary lymphoid organs (lymph nodes, spleen and mucosa-associated lymphoid tissues). Microscopically, this is characterised by populations of T cells, macrophages, follicular dendritic cells (FDCs) and mesenchymal stromal cells (MSCs) surrounded by a loose meshwork of fibrous connective tissue (or trabecula bone in the marrow) supplied by sinusoids, (enlarged, endothelium-lined spaces) through which lymph percolates. All these cellular components are present to varying degrees in the bone-marrow and primary and secondary lymphoid tissue which make up the protective niche of MCL cells.

The theory of MCL dependence on the tissue microenvironment comes from observations both of the clinical and histopathological characteristics of MCL and from direct observations of the cellular biology of the disease.

1.2.1 The microenvironment plays key roles in controlling lymphocyte adhesion and migration and a protective role against cytotoxic agents

From a clinical perspective, MCL is often at an advanced stage when symptoms or signs develop.[4] This is due, in part, to the lymphoma cell's ability to migrate to and colonise widely within the lymphoreticular system. This process of migration and homing is dependent on attraction, retention and release of lymphocytes into tissues. This

requires dynamic changes in the expression of surface receptors which can respond to chemokine gradients generated by MSCs and associated macrophages within the microenvironment. There is good evidence of the importance of this homing and migration relationship between lymphoma cells and the tissue microenvironment.[19,32–36]

An increase in resistance to cytotoxins has been demonstrated in neoplastic B cells in response to interactions with cells within the microenvironment, an observation which has been termed cell-adhesion mediated drug resistance (CAM-DR). It has been demonstrated that malignant B cells which express adhesion integrins, such as VLA-4- and VLA-5-fibronectin receptors, are relatively drug-resistant when pre-adhered to fibronectin (FN) compared with cells grown in suspension.[37] Mantle cell lymphoma cells have been shown to express high levels of surface adhesion markers, such as CXCR4, CXCR5 and VLA-4 (CD49d), which are thought to be important in maintaining the cells in their tissue microenvironment and facilitating protection from external toxins.[28] Blockade of VLA-4 and CXCR4 adhesion has been demonstrated to increase sensitivity to chemotherapy in MCL cell lines.[38] Several investigators have also demonstrated that beyond adhesion to a stromal cell layer in the *ex vivo* microenvironment, MCL cells appear to actively migrate beneath a protective stromal cell layer, a phenomenon termed pseudoemperipolesis (emperipolesis being the presence of an intact cell within the cytoplasm of another cell). Pseudoemperipolesis potentially affords further protection from chemotherapy and immune surveillence.[28,31,39]

Cell adhesion-mediated drug resistance is potentially one of the key mechanisms behind the persistence of disease after conventional chemotherapy. Indeed

protection by adhesion to accessory cells may be responsible for the characteristic relapses observed in MCL. It is possible therefore, that the use of targeted molecular therapies, which block external microenvironmental signals and impair homing and adhesion, may provide a therapeutic solution to the problem of residual disease after treatment in MCL.

1.2.2 Interactions with T-cells in the microenvironment: the importance of CD40-ligand

Follicular T helper cells (FT_H) are one of the key cellular components of the MCL microenvironment. In order for the adaptive immune system to initiate a response to antigen, a sequence of intracellular signals between B and T_H cells is required. The initial signal involves engagement of the FT_H cell receptor with either polypeptides presented on the surface of antigen presenting cells (APCs) in association with major-histocompatibility complex II (MHC II), or the binding of native antigen (i.e. one not yet processed by an APC) to the cognate B-cell receptor (BCR). This triggers the proliferative steps in B-cell development. This initiation step is unnecessary in MCL cells because of their constitutively active B-cell receptor (BCR) complex.[40]

The second signal involves co-stimulatory signals between activated T_H-cells and APCs or B cells. One of these co-stimulatory signals occurs when CD40-ligand (CD40-L) (also known as CD154), engages with the CD40-receptor on B cells. The CD40-L is a transmembrane protein (MW 32-39kDa) and a member of the tumour necrosis factor (TNF) superfamily. It is expressed primarily by activated T cells and B cells. Under certain inflammatory conditions, CD40-L is also expressed on numerous other cell types of the immune system and probably plays an essential role in multiple cellular immune processes.[41]

Histologically, engagement of CD40/CD40L initiates a germinal centre-type response stimulating the normal B cell to seed the germinal centre (GC) and undergo somatic hypermutation.[42] B cells with high antigen affinity through their BCR are subsequently engaged by FT_H cells through the BCR and CD40 synapse and encouraged to survive. So potent is the survival signal across the CD40 synapse that it has been demonstrated that GC B cells can be rescued from apoptosis in vitro by the administration of agonistic anti-CD40 antibody or CD40-L. This survival mechanism has been demonstrated to involve the induction of the pro-survival BCL proteins, thus protecting the B cell from Fas-ligand mediated apoptosis.[43,44] The engagement of CD40-L to CD40 also induces the activation of other cellular processes through upregulation of transcription factors including nuclear factor kB (NF kB); activation of the mitogen-activated protein kinases (MAPKs) and the phosphoinositide 3-kinase (PI3k) and PLC-gamma pathways.[45]

However the literature on the role of CD40-ligation in malignant B-cells is controversial. In Burkitt's lymphoma, a tumour of the GC, CD40-ligation results in Fas-induction and initiation of apoptosis.[46] Cell growth is also directly suppressed by CD40-ligation in other aggressive forms of B-cell lymphoma.[47] However, in more indolent forms, such as CLL, CD40-ligation can inhibit apoptosis and prolong cell survival *in vitro*.[48] Published data already exists supporting a role for CD40-L in the development of a model for MCL culture *ex* vivo.[49]

Therefore CD40-L could represent a mode of enhancing cell culture ex vivo, and in this study, the role of CD40-ligand will be explored.

1.2.3 The role of Toll-like Receptors

Antigen bound to the BCR can be internalised, processed and represented as peptides on the surface of the B cell in association with MHC class II molecules. This complex then engages with antigen-specific T_H cells which cause the B cell to proliferate and its progeny to differentiate into antibody secreting cells. These antigens are known as thymus-dependent (TD) antigens.

Although activated T_H cells are required for B cell responses to most protein antigens, some microbial components, such as lipopolysaccharide (LPS) can activate B-cells in the absence of a second T_H cell signal. In these cases, the second signal is provided either directly by recognition of a common microbial constituent or by a non-thymus derived accessory cell in conjunction with massive cross-linking of B cell receptors which would occur when a B-cell binds repeating epitopes on the bacterial cell. These antigens, often microbial cell-wall components, are known as thymus-independent antigens (TI antigens).

T-cell independent antigens are divided into type 1, intrinsically mitogenic, such as LPS, and type 2, non-mitogenic-repeating unit molecules such as polysaccharides or their haptenated derivatives.[50]

Toll-like receptor 9 (TLR-9) is expressed on antigen-naïve B-cells, including MCL cells and can recognise TI antigens, such as LPS, which are intrinsically mitogenic.[51] Through activation of TLR-9, T-cell independent antigens can initiate a cascade of intracellular events in B-cells, including phosphorylation of cytoplasmic tyrosine kinases resulting in enhanced proliferation and differentiation.[52–54] There is also evidence that the addition of TLR-9 with CD40-L stimulation acts synergistically to enhance proliferation and differentiation.[52,55,56]

1.2.4 The role of Interleukin 4

Interleukin 4 (IL-4) is a pleiotropic cytokine which regulates T and B cell responses, including proliferation, survival and gene expression.[57] It is produced by T-cells, mast cells and bone marrow stromal cells. It is made in response to immunologic recognition, principally by $CD4^+$ T lymphocytes, mediating much of its action in short range interactions between target cells and IL-4 producing T cells.[58] Interleukin-4 is responsible for stimulating resting B cells to undergo DNA synthesis in association with IgM activation and has the capacity to cause B cell blasts to enter S phase.[57,59] In addition to stimulating proliferative responses, IL-4 has been shown to inhibit apoptosis and maintain cell viability in B-cells, including their malignant counterparts by the upregulation of BCL-2 expression.[60–62] A combination of CD40-L and IL-4, also secreted by activated Th2 cells, is known to stimulate B cell proliferation *in vitro* and these molecules have been demonstrated to synergise in driving clonal expansion in normal B-cells and proliferative responses in MCL cells.[49,63]

These observations provide the rationale for the use of IL-4 and TLR-9 in combination with CD40-ligand as a model for stimulating proliferation and survival in primary MCL cells *ex vivo*.

1.3 Adhesion and Migration in MCL

It is agreed that the persistence of disease and early relapses observed characteristic of MCL indicate that neoplastic cells *in vivo* must be partly protected from the effect of immunochemotherapy and novel agents. One of the reasons for this relative resistance to therapy could be the ability of MCL cells to migrate from their site of origin and invade and colonise extra-nodal sites, such as the bone marrow, where the

microenvironment has protective effects.[4] This is achieved by the dynamic expression of surface adhesion molecules.

In vivo evidence of the role of adhesion in MCL comes from observations of the effects of BCR blockade within clinical trials. A rise in the peripheral blood lymphocyte count is a characteristic feature of therapy with the BTK-inhibitor, ibrutinib. In the phase II study of ibrutinib for relapsed MCL, this lymphocytosis peaked at a median of 4 weeks of treatment and gradually decreases over the subsequent 15 to 18 weeks.[64] This is associated with a reduction in the expression of the chemo-receptor, CD184 (CXCR4), (which is directly involved in B-cell homing and adhesion to the lymphoid tissues) and a fall in plasma chemokines, CCL22, CCL4 and CXCL14.[65] This rise in lymphocytes in the blood appears to be particularly marked in patients with disease involving the bone marrow, particularly those with >30% marrow involvement compared with those with no bone marrow involvement.[66]

In vitro studies have demonstrated that adhesion to cultured stromal cell layers can protect malignant B cells from apoptosis induced by chemotherapy. Equally, blockade of the BCR, which down-regulates expression of receptors, such as CXCR4 which adheres MCL cells to bone marrow and nodal stromal cells, has been shown to reverses these protective effects.[28,30,67]

It is hypothesised, therefore, that expression of adhesion receptor molecules, plays an important role in protecting MCL cells from therapy by maintaining malignant cells within the relative sanctuary of sites such as the bone marrow, leading to residual disease and early relapse. Therefore mobilisation of MCL cells away from sites of protection from chemotherapy or immune-surveillance could represent a therapeutic target.

Chapter 4 of this study examines the adhesion molecule profile of a series of cases of primary MCL, with a view to better characterising the expression of surface adhesion receptors and how this might change in response to stromal cell culture and the effect of drugs, such as ibrutinib.

1.3.1 An overview of cellular adhesion molecules

Cellular adhesion molecules (CAMs) are groups of ligands and receptors involved in cell homing and migration. Activities of cells such as adhesion, migration, homing and proliferation are controlled by dynamic expression of adhesion molecules, intracellular modification of signal transmission (inside-out signalling) and integrin clustering which results in increased affinity for ligand.[68] These processes allow the cells of the immune system to circulate freely as non-adherent cells in the blood and lymph, patrolling the body for infectious organisms and congregate as adherent cells in lymphoid organs as well as crossing endothelial and basement membrane barriers to aggregate at sites of infection.

Most CAMs belong to one of four major adhesion molecule families, comprising the integrins, the cadherins, the selectins and the immunoglobulin superfamily. The receptors which are thought to play a role in the adhesion and migration of MCL are briefly discussed below.

The integrins are a family of heterodimeric membrane glycoproteins expressed on the surface of a diverse range of cells. They act as receptors for extracellular matrix components. The term integrin was originally coined to reflect the role of this receptor in integrating the intracellular cytoskeleton with the extracellular matrix.[69] They also play an important role in intracellular adhesion , interacting with members of

the immunoglobulin superfamily such as intracellular adhesion molecules-1, -2 and -3, (ICAM-1, ICAM-2, ICAM-3) and vascular cell adhesion molecule-1 (VCAM-1).[70]

Structurally, integrins consist of two non-covalently associated sub-units, α and β. Original classification included three subfamilies, (β1 integrins or very late activation proteins (VLA); β2 integrins or leucams and β3 integrins or cyto-adhesins) in which a common β subunit interacts with a number of different subunits.[71,72]

Most integrins are able to bind more than one ligand (for example, VLA-1 binds collagen and laminin, VLA-3 binds collagen, laminin and FN). Binding requires both subunits and also requires activation of the integrin receptor by specific signals such as T cell activation resulting in a conformational change enabling the integrins to bind their ligands.[73]

1.3.2 Adhesion Molecule Expression in Mantle Cell Lymphoma

Given that many subtypes of NHL including MCL appear to arise from an equivalent stage of normal B-cell development, it would be logical to assume that malignant cells use the same CAMs in migration and homing as their non-malignant counterparts. Although most cases of MCL arise from lymphoid tissue, they can also display a leukaemic phase characterised by the presence of lymphoma cells in the peripheral blood. Changes in expression of CAMs on the cell surface are likely to have an important role in this behaviour.

Relatively little is known about the expression of CAMs on the surface of MCL cells. In an evaluation of expression of 10 adhesion molecules on a variety of NHL subtypes in the leukemic phase, including MCL, showed marked heterogeneity in expression between subtypes. Primary MCL cells demonstrated lower expression of CD11c and CD49c and higher expression of CD49d and CD11b when compared with CLL cells.

When MCL cells were compared with marginal zone lymphoma (MZL) cells, marginal B cell lymphoma demonstrated higher expression of CD11a, CD11c, CD18, CD29 and CD54.[74] A description of the cellular adhesion molecules considered relevant to MCL is presented in Table 1-1.

Adhesion Molecule	Description	Ligands
CD183 (CXCR3)	G protein-coupled transmembrane receptor expressed primarily on activated T cells and NK cells, preferentially on T_H1 cells. It binds to CXCL-9, -10 and -11 through which it is able to elicit influx of intracellular calcium and activate phosphoinositide 3-kinase and mitogen-activated protein kinase (MAPK). CXC ligands are IFN-induced and produced locally in the lymphoid microenvironment.	CXCL9, 10 and 11
CD11a Integrin alpha L, (LFA1)	Forms part of the integrin, lymphocyte function associated antigen (LFA-1), expressed on all leukocytes. Involved in extravasation, antigen presentation and T-lymphocyte alloantigen-induced proliferation.[75] Reportedly expressed on MCL and MZL cells more than CLL and thought to facilitate lymph node adhesion to FDCs via ICAM1-3.[76]	ICAM 1(CD54) ICAM2(CD102) ICAM3 (CD50)
CD49d (VLA-4)	Integrin alpha-4subunit (CD49d) combines with B1 subunit (CD29) to form VLA-4. VLA-4 is expressed on resting lymphocytes and monocytes and functions as both a matrix and cell receptor. As a matrix receptor it binds to fibronectin at a different site than that recognised by VLA-5 (CD49e). As a cell receptor, it binds to VCAM-1, which is induced by inflammatory mediators on the endothelium. Reportedly expressed on MCL and MZL cells more than CLL and thought to facilitate lymph node adhesion to FDCs via VCAM-1.[76]	Fibronectin VCAM-1
CD54 (ICAM-1)	A member of the immunoglobulin superfamily, normally with a lower expression in peripheral blood compared with lymph node mononuclear cells. Lower expression has been demonstrated to correlate with leukaemic / disseminated disease and extranodal involvement in some papers.[77–79]	CD11a
CD62L (L-selectin)	A single chain transmembrane protein found in most lymphocytes. Its low affinity binding facilitates the capture, rolling and slow-rolling steps of leukocyte recruitment to the region of inflammation which in turn is followed by firm adhesion and transmigration. Low expression demonstrated in MCL, CLL and MZL in one series.[76]	Blood vessel endothelium
CD58 (LFA-3)	A member of Ig superfamily expressed on antigen presenting cells (APCs), particularly macrophages which binds to LFA-2 on T cells and reinforces adhesion between T cells and APCs.[80] Expressed on haematopoietic and non-haematopoietic cells and overexpressed in acute lymphoblastic leukaemia.[81]	LFA-2
CD49e (Integrin alpha-5) (VLA-5)	Cd49e combines with beta 1 to form VLA-5 which binds the extracellular matrix protein fibronectin and aids adhesion within the lymph node and bone marrow.	Fibronectin
CD11c	CD11c combines with beta 2 subunit (CD18) to form Mac-1: expressed mainly on myeloid cells and is involved in phagocytosis of infectious agents, transendothelial migration of phagocytes and activation of neutrophils and monocytes. Higher rates of splenic involvement in CLL patients have been reported with strong 11c expression; over expressed in HCL and splenic marginal zone lymphoma but predominantly low level expression in MCL.[82]	ICAM1 Fibrinogen Factor X
CD184 (CXCR4)	High level expression is demonstrated on primary MCLs which is down-regulated by BTK-inhibitor ibrutinib.[65] Stromal cells in secondary lymphoid tissues constitutively express chemokines such as CXCL12, providing guidance for B cell positioning within distinct nodal compartments. CXCL12 has been demonstrated to induce actin polymerisation in MCL cells and induce a chemotactic response which can be inhibited by blocking the receptor CXCR4, indicating an important role in migration and localisation of CXCR4.[33]	CXCL12
CD185 (CXCR5)	A G protein-coupled transmembrane receptor. High level expression has been demonstrated on primary MCLs together with CXCR4 and VLA-4.[28] Thought to be used by MCL cells to disseminate by interaction, trafficking and homing to secondary lymphoid tissues via ligands CXCL12 and CXCL13. Ligands for CXCR4, 5 and VLA-4 may trigger the pseudoemperipolesis phenomenon.[33]	CXCL12, 13

Table 1-1 A summary of the adhesion molecules and their respective ligands considered important in MCL. (NK – Natural Killer cells; MZL – marginal zone lymphoma; CLL – chronic lymphocytic leukaemia; FDC – follicular dendritic cells; ICAM – intracellular adhesion molecule; HCL – hairy cell leukaemia; BTK – Brutons tyrosine kinase.

3-Dimensional Tissue Culture Models for the Study of Mantle Cell Lymphoma

1.4 The complex 3-dimensional (3-D) matrix of the lymph-node or bone marrow is critical in maintaining mantle cell lymphoma cells. Within this structure, stromal cells and other cellular components of the tissue micro-environment provide essential signals which govern tumour cell survival, migration and proliferation. However it is from a 2-dimensional (2-D) cell culture model that a large amount of data and subsequent understanding of cellular interactions in tumour biology has been gained.

It is generally recognised that 2-D models are not fully representative of the complex 3-D microenvironment found in living organisms and many of the functional structures and signals specifically developed to allow migration, proliferation, and differentiation may change significantly under 2-D conditions.

While attempts have been made to develop models with the 3-D characteristics of the bone marrow microenvironment in other diseases130,131, there is little or no published data on 3-D culture models in MCL. Given the critical importance that the micro-environment plays in MCL homeostasis and the differences observed in cellular behaviour in other malignancies between 2-D and 3-D models, it would seem logical to attempt to design and establish a 3-D model in vitro for the further study of MCL. To that end, the final chapter of this thesis will explore the development of a 3-D model for the study of MCL.

1.5

Summary of Introduction and Aims of this thesis

MCL is a rare form of NHL with a poor prognosis for patients. In addition to its intrinsic oncogenic mutations, signals from accessory cells within the lymphoma microenvironment are important in propagating survival and proliferation and in

protecting cells from therapy. Development of an *ex vivo* model for study of MCL cells and their microenvironment is therefore an important goal.

The aims of this thesis were:

- to develop and test a system to simulate MCL growth *in vitro* with particular focus on the role of accessory cells, both murine and human, in which survival and proliferation of primary MCL cells can be studied;
- to examine the effects of microenvironmental stimuli thought to be important to MCL growth within this system, specifically the relationship between MCL cells and CD40-L, IL-4 and TLR-9 ligand;
- to characterise the CAM expression profile of a series of primary human MCL cases and examine the effect of accessory-cell culture models and therapeutic interventions on this profile;
- to develop a 3-D, *ex vivo* culture model that reflects the lymphoma microenvironment and can be used for the study of MCL survival, proliferation and CAM expression.

2. CHAPTER 2 - MATERIALS AND METHODS

Introduction

2.1 The materials and methods employed for this thesis can be broadly divided into the collection, storage and culture of primary MCL cells from human donors; the culture of murine stromal cells and human stromal cells as supportive layers; the methods used to assess survival and proliferation of primary MCL cells under different conditions in different microenvironments and the use of flow cytometry to assess adhesion molecule profiling. The development of a 3-D model for the testing of primary MCL cells is a novel method and is therefore described in a separate chapter (Chapter 5).

Obtaining Primary MCL Cells

2.2 The Clinical Haematology Trials Department at Derriford Hospital, Plymouth is a major referral centre for patients with NHL with specialist interest and wide experience in the management of MCL, participating in numerous early and advanced-phase clinical trials. Between 50 and 75 patients, are referred each year for treatment opinions and many are enrolled locally in studies for the treatment of MCL. The current clinical trials portfolio includes five studies for patients with MCL, both untreated and relapsed using novel agents (defined as active compounds, complexes or molecules that have not previously been approved by the Food and Drug Administration (FDA) or European Medicines Agency (EMA) for the treatment of MCL) alone or in combination with each other or established immunochemotherapy.

The Derriford Clinical Trials department has a particular expertise in the use of BTK-inhibitors in MCL. Between January 2015 and December 2016, 29 patients with MCL

were enrolled into clinical trials at Derriford and ten patients initiated therapy using BTK-inhibitors.

It is from this general cohort of patients with MCL, that participants were recruited to donate peripheral blood for this research. After appropriate informed consent, patients with both untreated and relapsed and refractory disease were recruited to the database and then asked to donate samples of blood or bone marrow at the time of routine sampling.

Ethical Approval, Informed Consent and Confidentiality

2.3 Ethical approval for this research was sought from and granted by the NHS Health Research Authority National Research Ethics Service Committee East of England – Cambridge East following review of all documentation.

All potential participants were given a comprehensive patient information sheet with time to read and ask questions. Once the patient had read and understood the information sheet, and their questions had been answered, formal consent was obtained for tissue sample donation to the local biobank (Integrated Research Application System project I.D. number 145245). The patient information sheet and patient consent forms can be found in the Appendix.

2.3.1 Confidentiality and Record Keeping

Signed copies of the patient consent forms were duplicated and maintained in the patients clinical notes with a copy kept securely within a folder in the clinical trials office. A pseudo-anonymised database of patient samples (identified by patient initials and hospital number) was maintained on a secure, hard drive within Plymouth University and Peninsula School of Medicine and Dentistry (PUPSMD) accessible only to designated investigators directly involved in research on these samples after

appropriate Good Clinical Practice in Medical Research and Human-Tissue Authority training.

2.3.2 Collection of whole blood or bone marrow samples

The majority of the tissue samples obtained for this project were in the form of peripheral venous blood or liquid bone marrow aspirates. These samples were obtained during routine venesection or during a routine bone marrow biopsy from patients with an established diagnosis of MCL.

After obtaining informed consent, peripheral venous blood samples were collected by phlebotomy performed by the clinical research team. Liquid bone marrow samples were obtained as additional samples at the end of routine diagnostic or restaging bone-marrow biopsies. Therefore no additional invasive procedure was required. Whole blood and bone marrow samples were collected into 4.0mL *Vacutainer* plastic whole blood tubes (*BD Biosciences* Cat.) containing 7.2mg of the chelating agent K_2EDTA (di-potassium ethylenediaminetetraacetic acid) to prevent clotting within the tube. A summary of the subjects from whom primary MCL cells were obtained for this project are displayed in Table 2-1.

Case	Age, sex	Molecular data	Immuno-phenotype	Disease clinical phenotype	Prior Treatment	Indolent / aggressive disease
MCL01	66 f	t(11;14)	CD5/19+	Stage IV, nodal; WCC 300x109/L	None	Aggressive
MCL02	68 m	(t11;14) cyclin D1	CD5/19+	Stage IV, nodal; WCC 234x109/L	Immunochemotherapy and BTK-inhibitor	Aggressive
MCL03	74 m	cyclin D1	CD5/19+	Stage IV WCC $30x10^9$/L	None	Aggressive
MCL04	65 f	(t11;14)	CD19+	Leukaemic, MCL; WCC 280x109/L	None	Indolent
MCL05	63 f	t(11;14)	CD5/19+	Leukaemic MCL, splenomegaly	None	Aggressive
MCL06	64 f	t(11;14)	CD5/19+	Stage IV WCC $30x10^9$/L	None – but refractory to treatment	Aggressive
MCL07	65 m	t(11;14) cyclin D1	CD19+	Leukaemic MCL; WCC 30x109/L	None	Indolent
MCL08	56 m	t(11;14)	CD5/19+	Stage IV WCC $200x10^9$/L	Immunochemotherapy and BTK-inhibitor	Aggressive
MCL09	70 m	cyclin D1	CD5/19+	Stage IV WCC $190x10^9$/L	Immunochemotherapy	Aggressive
MCL10	54 m	t(11;14) cyclin D1	CD5/19+	Stage IV WCC variable†	Immunochemotherapy	Aggressive
MCL11	60 f	cyclin D1	CD5/19+	Stage IV	Immunochemotherapy	Aggressive
MCL12	62 f	cyclin D1	CD5/19+	Stage IV WCC $250x10^9$/L	Immunochemotherapy and BTK-inhibitor	Aggressive
MCL13	64 m	cyclin D1 t(11;14)	CD5/19+	Leukaemic; WCC 152x109/L	None	Indolent
MCL14	62 m	cyclin D1 t(11;14)	CD5/19+	Leukaemic; Stage II	Local radiotherapy	Indolent
MCL15	70 f	cyclin D1 t(11;14)	CD5/19+	Stage III, nodal	None	Aggressive
MCL16	70 f	cyclin D1 t(11;14)	CD5/19+	Stage IV, nodal	None	Aggressive
MCL17	74 m	cyclin D1 t(11;14)	CD5/19+	Stage IV, nodal	Immunochemotherapy	Aggressive
MCL18	91 m	cyclin D1 t(11;14)	CD5/19+	Stage IV, nodal	Immunochemotherapy	Aggressive
MCL19	71 m	cyclin D1 t(11;14)	CD5/19+	stage IV, nodal	Immunochemotherapy	Aggressive
MCL20	63 m	cyclin D1 t(11;14)	CD5/19+	stage III, nodal	Immunochemotherapy	Aggressive
MCL21	70 m	cyclin D1 t(11;14)	CD5/19+	stage III, nodal	Immunochemotherapy	Aggressive
MCL22	60 m	cyclin D1 t(11;14)	CD5/19+	stage IV, nodal	Multiple lines including BTK-inhibitor	Aggressive
MCL23	60 m	cyclin D1 t(11;14)	CD5/19+	stage IV, nodal	Allogeneic Stem cell transplant	Aggressive
MCL24	77 f	cyclin D1 t(11;14)	CD5/19+	stage III, nodal	None	Aggressive

Table 2-1 Primary MCL Subjects' Clinical and Biological Characteristics. MCL subject demographics, diagnostic molecular data, immunophenotyping of PBMCs and clinical disease summary of cases of MCL from which PBMCs and / or bone marrow MCL cells were obtained for use in adhesion profile experiments.

Separation of Peripheral Blood Mononuclear Cells from Whole Blood and Liquid Bone Marrow Samples

2.4 Peripheral blood mononuclear cells (PBMCs) were separated from whole blood by centrifugation using a density gradient medium.

Background

Boyum first described the method of centrifugation across a density gradient medium for mononuclear cell isolation from circulating blood and bone marrow cells in 1968.[83] The technique employs mixtures of polysaccharide and a radiopaque contrast medium such as Ficoll-paque. Ficoll-paque is a solution of polysucrose and sodium diatrizoate that has been adjusted to density of 1.077±0.001 g/mL. The use of this medium facilitates the rapid recovery of viable mononuclear cells from small volumes of blood. During centrifugation of the bilayer (one phase blood, one phase ficoll-paque) erythrocytes and granulocytes are aggregated by polysucrose and rapidly sediment; whereas, lymphocytes and other mononuclear cells remain at the plasma/ficoll-paque interface. There is negligible contamination by erythrocytes and most of the extraneous platelets are removed by centrifuging at a low speed during the washing steps.

Reagents

- sterile phosphate buffered saline (PBS) (*Fisher Scientific*)
- complete RPMI (Roswell Park Memorial Institution) media + glutamax (*Gibco*) containing 10% fetal calf serum (FCS) (heat inactivated, qualified grade, (*Fisher Scientific)*, and 1% Streptomycin penicillin (*Sigma*)
- ficoll-paque-1077 (*Fisher Scientific*) (stored at 2-8 ^{0}C and protected from light)

Materials and Equipment

- EDTA vacutainer tubes (*Becton and Dickinson*)
- centrifuge (*Heraeus Function Line* Laboratory Centrifuge)
- DFC 3000G phase contrast microscope (*Leica*)
- 15ml and 50ml Falcon conical-bottom flasks (*Fisher Scientific)*
- pipettes, 10ml serologic, (Pasteur) (*Fisher Scientific)*
- haemocytometer and trypan-blue (*Fisher Scientific)*

Complete RPMI medium was prepared by adding 5mls of streptomycin and 50mls of FCS to 450mls of RPMI 1640 medium. Blood or bone marrow aspirate was collected in EDTA vacutainers and processed within 6 hours, with the exception of cells from subject MCL08 which had to be couriered from Cardiff in EDTA vacutainers overnight. In this case, viability was assessed on arrival using flow cytometry and annexin V labelling and found to be >95% (Materials and Methods 2.8). The PBS and media were warmed in a water bath to 37^0c.

Equal amounts of PBS and anticoagulated blood were mixed in 50ml falcon tubes before 10mls of ficoll-paque was measured into 50ml centrifuge tubes. The diluted blood was then slowly dripped onto the ficoll-paque forming a layer of blood floating on the top ensuring not to disturb the interface between the two layers. The tubes were centrifuged at 2000 revolutions per minute (rpm) for 30 minutes with no brake. The serum layer was then removed and discarded.

The buffy coat (mononuclear band) was transferred into a 15 ml falcon tube and 10mls of sterile PBS was added. The tube was then centrifuged at 1400 rpm for 10 minutes

with no brake. The supernatant was discarded and the cell pellet was re-suspended in 2mls of PBS or media. The numbers of cells were counted using a haemocytometer.

2.4.1 Cell Counting

A sample of 40µL (microlitres) of cell suspension was added to an equal volume of trypan blue solution (staining dead cells blue but reduced by viable cells leaving them unstained) prior to a 10µL sample being loaded onto a graduated haemocytometer. Viable cells were counted in each quadrant to obtain an average which is doubled to account for dilution to give a cell count $x10^4$/mL.

2.5 Freezing and Storing Isolated Peripheral Blood Mononuclear Cells

Once isolated and quantified, PBMCs could be cryopreserved for future use.

Reagents

- freezing medium (FCS (heat inactivated, qualified grade, (*Fisher Scientific)* containing 10% dimethyl-sulfoxide solution (DMSO) (*Corning™)*

Materials and Equipment

- haemocytometer with trypan blue *(Fisher Scientific)*
- *CryoPure* 2.0mL sterile cryotubes (*Sarstedt*)
- *Mr Frosty™* freezing container (*Thermo Scientific*™)
- centrifuge (*Heraeus Function Line* Laboratory Centrifuge)
- DFC 3000G phase contrast microscope (*Leica*)
- vapour-phase liquid nitrogen storage system

2.5.1 Cryopreservation

The cell suspension was centrifuged at 1700 rpm for 10 minutes at room temperature. The supernatant was discarded and the cell pellet was resuspended in freezing

medium, in order to prevent cell rupture by the formation of intracellular ice crystals, at $2x10^7$/mL, volumes of 1000µL were aliquoted into sterile cryotubes. Tubes were then frozen slowly (1^oC – 3^oC per minute in a freezing container to -80^oC for 24hours before being transferred to liquid nitrogen for long-term storage.

2.5.2 Thawing Cryopreserved Cells

Cryovials were removed from liquid nitrogen storage using appropriate safety precautions. Cryovials were rapidly thawed at 37^OC water bath until only a sliver of ice remained in each vial. The entire contents of the vial were then transferred into 10mLs of pre-warmed complete RPMI medium in order to dilute any remaining DMSO. Cells were then washed by centrifugation (1700 rpm for 5 minutes, brake on) and resuspended in 10mLs of complete RPMI before a cell count was performed. The same protocol was followed for the storage of MCL cell lines.

2.6 Methods for Murine Cell Culture

For the experiments involving murine fibroblasts and primary MCL cells, RPMI medium was used. Complete RPMI medium is suitable for the culture of a variety of mammalian cells and is widely used to culture mantle cell lines and primary MCL cells. In this study the RPMI medium used was modified with the amino acid L-glutamine (300mg/L) and a phenol-red dye. RPMI contains biotin, vitamin B12 and para-aminobenzoic acid (PABA) in addition to the vitamins inositol and choline. However it contains no lipids, proteins or growth factors and therefore is routinely supplemented with 10% FCS.

Reagents

- complete RPMI 1640 with GlutaMAX™ medium (*Gibco*) (supplemented with 10% FCS (*Fisher Scientific*) and 1% penicillin/streptomycin (*Invitrogen*)

- trypsin-EDTA,(0.5% Trypsin 5.3mM EDTA 4Na) (*Invitrogen*)
- sterile PBS

Materials and Equipment

- adherent murine stromal cells: CD40-ligand-transfected (CD40L-T) and control CD40-ligand-non-transfected (CD40L-NT) cells (kind gift from Professor M Dyer, Leicester, UK)
- 25cm^2 and 75cm^2 vented flat-bottom culture flasks (*Fisher Scientific*)
- humidified incubator (*ThermoScientific*) maintained at 37^{o}C with 5% CO_2
- linear accelerator for irradiation *(Varian)*
- DFC 3000G phase contrast microscope (*Leica Microsystems*)

2.6.1 Protocol for Culture of Murine Fibroblasts

Murine-derived stromal cells cultured as an adherent monolayer on a plastic surface provide important supportive signals to human primary cells which support growth and proliferation during *ex vivo* culture.[84,85]

In these experiments, adherent murine stromal cells (CD40L-T and control CD40L-NT cells) were cultured in vented flasks as a monolayer and subsequently loosened from the plastic by trypsinisation, harvested and used to create a monolayer of stromal cells on the floor of standard 24 well plates, onto which primary MCL cells were added for co-culture experiments.

2.6.2 Passaging Murine Fibroblasts

Adherent murine stromal cells were cultured in 75cm^2 vented, flat-bottom flasks in complete RPMI medium in a humidified incubator maintained at 37^{o}C with 5% CO_2. The stromal cell layer was inspected for confluence every 48 hours and split using a 1:5 dilution with fresh media every 3 days using the following method.

The spent medium was discarded and the stromal cell layer was gently washed with sterile PBS. The adherent stromal cell layer was detached from the surface of the culture flask by the addition of 5mLs of trypsin-EDTA to a 75cm^2 flask. The flask was incubated at 37^{o}C for 5 to 10 minutes. Once the cells had been loosened from the cell surface, a 20% volume of the total suspension was then added to 25mLs of fresh media for on-going culture. The trypsin was neutralised within the fresh culture medium. The flask was labelled with the appropriate passage number and returned to the incubator. Cells were split to a maximum of 25 passages before being discarded.

2.6.3 Protocol for Seeding Murine Fibroblasts for Use with Primary Mantle Cells

Adherent murine fibroblasts were loosened from the plastic surface of the culture flask as previously described. The cell suspension was transferred from the flask to a 50mL conical-bottomed falcon tube where the cells were washed with PBS (via centrifugation and resuspension in PBS and a cell count was performed as previously described). A suspension of the desired density was then transferred in 1mL aliquots to the wells of a standard flat-bottomed 24 well plate and returned to the incubator. Once desired confluence had been achieved, (70% to 80% coverage of the floor of the well as determined by light microscopy), the plate was irradiated in order to arrest further stromal growth and prevent overgrowth of the primary MCL cells.

2.6.4 Protocol for Irradiation of Bone Marrow Fibroblasts

Murine bone marrow fibroblasts proliferate relatively quickly compared with human marrow fibroblasts or human peripheral blood mononuclear cells. Therefore a long-term coculture experiment is complicated by overgrowth and media exhaustion by the murine fibroblasts. In order to prevent this, bone marrow cells are often irradiated once monolayer achieves desired confluence in order to arrest further proliferation.[86]

The 24 well plate was transferred to a linear accelerator. The plate was then irradiated using 6MV photons at machine isocentre. The sample was at a depth of 5cm in a solid water phantom and the field size used was 20cm^2. The dose delivered to the sample was 15Gy (Gray) in a single fraction. This prevented further significant proliferation during ongoing culture.[87]

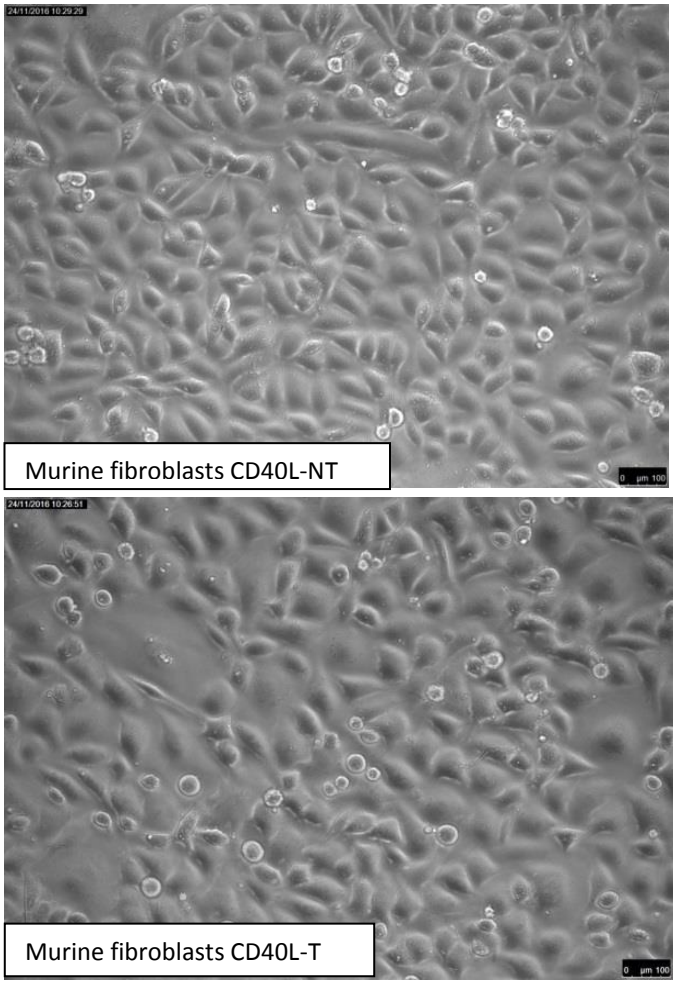

Figure 2.1. Phase-contrast images of murine fibroblast monolayers. CD40-ligand non-transfected (CD40L-NT) and transfected (CD40L-T) murine fibroblasts were seeded at 1x10^4/mL and irradiated with 15Gy when reached 70% – 80% confluence (x20 magnification).

2.6.5 Establishing Cell Surface Expression of CD40-Ligand on Stromal Cells

To demonstrate CD40L expression on the CD40L-T murine stromal cells the stromal cells were labelled with phycoerythrin (PE)-conjugated, mouse-anti-human CD40L monoclonal antibody and visualised using fluorescent microscopy (Figure 2.1).

Reagents

- adherent murine stromal cells: CD40L-T and control CD40L-NT cells (kind gift from Professor M Dyer, Leicester, UK)
- 4% paraformaldehyde (PFH) in PBS
- complete RPMI medium
- *Vectashield* hard set mounting media with DAPI (4',6-diamidino-2-phenylindole)
- PE-conjugated mouse-anti-human CD40L monoclonal antibody (*BD Pharmingen™)*

Materials and Equipment

- standard 24 well flat-bottomed culture plates (*Fisher)*
- 5mm coverslips and microscope slides (*Fisher*)
- fluorescent microscope (*Leica Microsystems*)

CD40L-NT and CD40L-T stroma were cultured on 5mm coverslips within standard 24 well plates in complete RPMI medium for 48 hours until 75% confluence. The media was discarded and the coverslips were removed from the wells. 50µL of PE-conjugated mouse-anti-human CD40-ligand monoclonal antibody was added to each coverslip and incubated in the dark for 20 minutes. The coverslips were washed with PBS before being fixed with 200µL of 4% PFH/PBS for 10 minutes. The coverslips were washed with PBS and air-dried for 24 hours. 25µL of *Vectashield* hard set mounting media with

DAPI (4',6-diamidino-2-phenylindole) mounting media was added and the slips were mounted on standard glass slides and allowed to set. The slides were then visualised by fluorescent microscopy using LAS AF Version: 2.6.3 software (*Leica Microsystems*). The images below (Figure 2-2) validate that the CD40-ligand transfected murine fibroblasts express CD40-L on their cell surface whereas the CD40-L non-transfected murine fibroblasts do not.

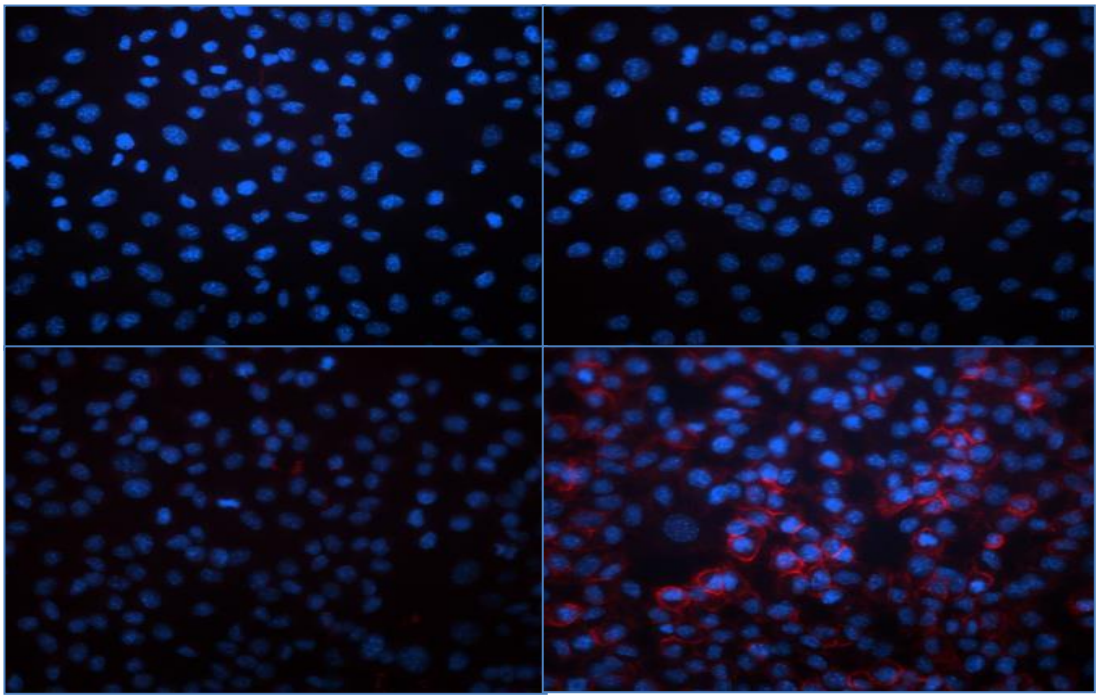

Figure 2-2. Fluorescent microscopy comparison of CD40L-transfected/non-transfected murine stromal cells. Murine stromal cells cultured until confluent then stained with PE-conjugated mouse-anti-human CD40-ligand monoclonal antibody. Cells were then fixed and mounted with prolonged DAPI . **Top images** – CD40-L non-transfected fibroblasts; bottom images – CD40-L transfected fibroblasts. **Left images** – cells stained with DAPI alone (blue); **right images** – cells stained with DAPI (blue) and PE-anti-CD40-ligand (red).

2.6.6 Co-culture of Primary MCL Cells with Murine Stromal Cells

After seeding and irradiation of a confluent layer of CD40L-NT / T murine stromal cells within a standard 24 well plate, primary human MCL PBMCs were seeded onto the monolayers and maintained at 37^{o}C with 5% CO_2 for 8 days for assessment of survival and proliferation. To selected wells, co-stimulation with 3 µM of Toll-like-receptor-9 ligand (TLR9) (tlrl-2006-1, *InvivoGen*) or 50ng/mL of recombinant human interleukin-4 (IL-4), (*AD-200-04, PeproTech*), was also applied (concentrations as per manufacturers recommendations).

2.6.6.1 Human Toll-Like Receptor-9 ligand Validation

CpG (Cytosine-phosphate-Guanine) oligonucleotides (ODNs) are TLR-ligands. They comprise of synthetic ODNs containing unmethylated CpG di-nucleotides in specific sequence contexts (*5'-Cytosine-phosphate-Guanine-3'* motifs). These motifs are present at a 20-fold greater frequency in bacterial DNA than human DNA, (where the cytosine in the dinucleotide motifs is usually methylated). Unmethylated CpG ODNs can be detected by TLRs on the lymphocyte surface and serve to trigger vigorous immune-stimulatory responses. The synthetic CpG-ODN, ODN 2006, (also known as ODN 7909) is a class-B CpG ODN which binds and activates human TLR-9 without inducing strong interferon-alpha production from dendritic cells.

In order to establish that the presence of ODNs does not induce apoptosis per se, an ODN2006 control (ODN 2137, *InvivoGen*), which contains Gp*C* (*5'-Guanine-phosphate-Cytosine-3'*) dinucleotides instead of CpGs was used as a negative control together with ODN 2006 (*InvivoGen*). This confirmed no increase in apoptosis over the DMSO vehicle control (data not shown).

Reagents

- complete RPMI 1640 with GlutaMAX^{TM} medium (*Gibco*) (supplemented with 10% FCS (*Fisher Scientific*) and 1% penicillin/streptomycin (*Invitrogen*)
- sterile PBS
- haemocytometer with trypan blue
- primary MCL PBMCs isolated and stored as previously described.

Materials and Equipment

- standard, flat-bottomed 24 well sterile plates
- adherent murine stromal cells: CD40L-T and control CD40L-NT cells (kind gift from Professor M Dyer, Leicester, UK)
- humidified incubator (*Thermo-Scientific*) maintained at 37^{o}C with 5% CO_2
- DFC 3000G phase contrast microscope *(Leica Microsystems)*
- CCD grayscale camera (Leica DFC3000 G) (*Leica Microsystems*)
- LAS AF Version: 2.6.3 software (*Leica Microsystems*)

Protocol for Co-culture

The spent medium was discarded from the wells containing the murine stromal cell layers and the monolayers were washed with 1mL of sterile PBS. The cryopreserved primary human MCL cells were thawed and resuspended in complete RPMI medium. A MCL PBMC suspension was prepared using pre-warmed complete RPMI medium and the cell density was adjusted to 4x10^{6}/mL. 1mL of the cell suspension was added to each well containing the murine stromal monolayers.

To selected wells, 3 µM of ODN 2006 human TLR9 ligand in 3µL DMSO or 50ng/mL of recombinant human IL-4 (*PeproTech*) in 5µL of DMSO was added. To the remaining wells, 5µL of DMSO was added as vehicle control.

The plates were then returned to the incubator and maintained at 37^{o}C with 5% CO_2 in the dark. The plates were inspected by light microscopy every 24 hours and the contents were assessed for survival and proliferation of MCL PBMCs after 8 days of culture.

Examples of the appearance of these co-cultures by phase-contrast light microscopy are displayed below (Figure 2-3).

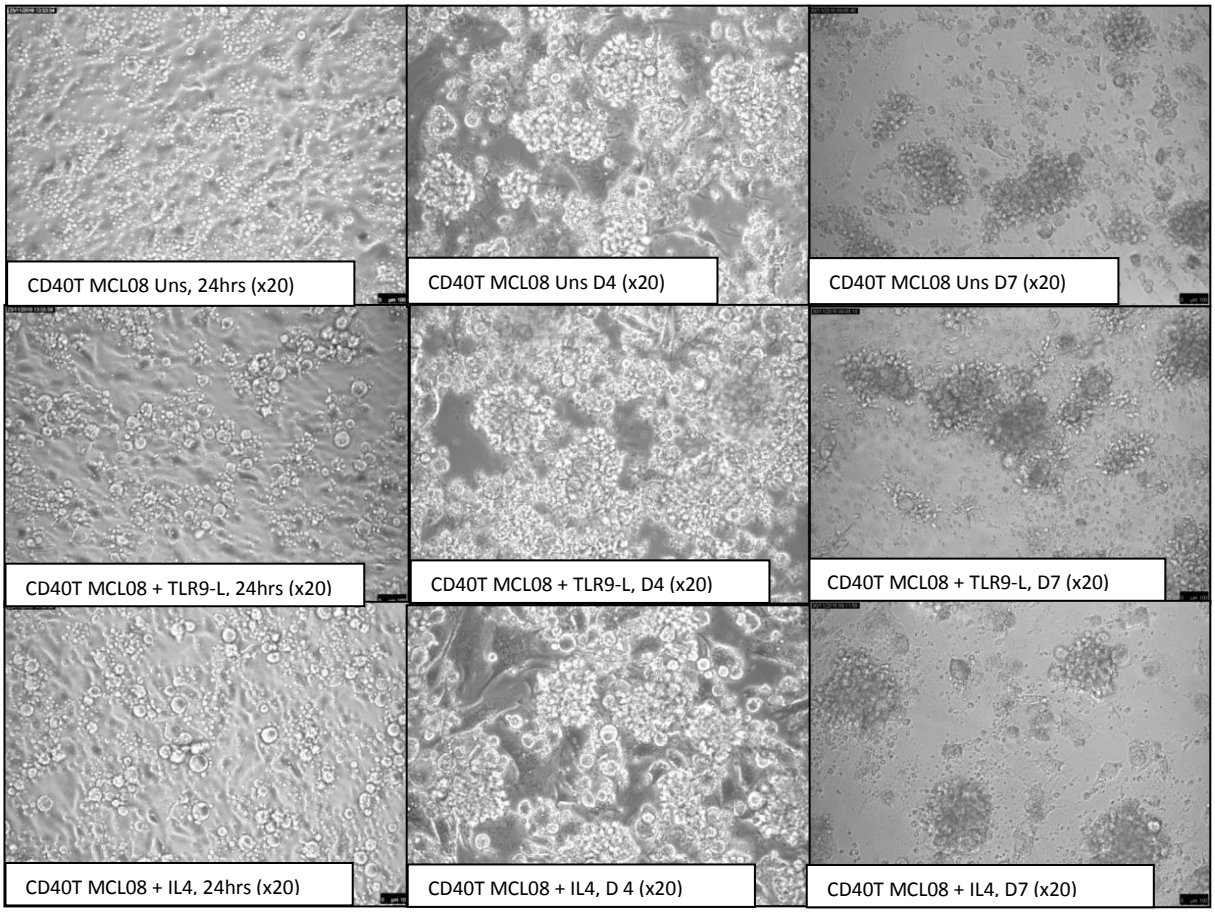

Figure 2-3. Subject MCL08 PBMCs co-cultured with CD40-ligand demonstrate evidence of cluster formation after 7 days. Cells seeded in complete RPMI at 4x10^{6}/mL on CD40-ligand-transfected (CD40L-T) murine fibroblasts after irradiation on a 24 well plate. Cultures were stimulated at baseline with 3µM TLR9 ligand (middle) and 50ng/ml Interleukin-4 (IL-4) (bottom). Images taken after 24hrs (left), 4 days (middle) and 7 days (right)

2.7 Human Bone Marrow Fibroblasts

Culture of human bone marrow stroma was performed using a protocol and culture medium based on a validated method previously published by Nicol *et al*.[88]

2.7.1 Obtaining Human Bone Marrow Fibroblasts

Liquid bone marrow aspirate was obtained as samples in excess of clinical need from patients with underlying lymphoproliferative disorders undergoing routine investigative and diagnostic bone marrow biopsies. Several variables among patients undergoing routine bone marrow sampling, such patient age, comorbidity, prior chemotherapy, current disease status and amount and quality of bone marrow sample obtained made obtaining a consistently healthy bone and abundant marrow supply challenging. Because of this, the ability of bone marrow fibroblasts to grow *in vitro* using a standard, validated long-term culture protocol, was found to be highly variable, with some patient samples growing much better than others. This was not always predicable according to disease status, age or prior therapies.

2.7.2 Separation of Human Bone Marrow Fibroblasts from Whole Bone Marrow Samples

Whole bone marrow samples were obtained from patients as previously described. The samples, (4–8 mLs of whole liquid bone marrow) were transferred from the clinic to the laboratory in EDTA-containing blood vacutainer tubes within 4 hours of sampling and processed on the same day by ficoll-separation using the method previously described.

2.7.3 Establishment of Human Bone Marrow Stroma

2.7.3.1 Preparation of complete long-term culture medium (LTCM)

Reagents

- Iscove's Modified Dulbecco's Medium (IMDM) containing 1% penicillin/streptomycin (*Invitrogen*)
- hydrocortisone – final concentration $5x10^{-7}$ M (183uM/50ml)
- 10% Qualified grade FCS (*Gibco*)
- 10% horse serum (*Gibco*)

Aliquots of IMDM were thawed when required. To each 40ml aliquot were added 5mls FCS, 5mls horse serum and 180µl working dilution hydrocortisone.

2.7.3.2 Culture of human bone marrow stromal layers

Whole bone marrow aspirate samples were ficoll-separated to produce a buffy coat layer and the plasma, fat and buffy coat layer removed from the red cells. The buffy coat preparation was either cryopreserved in qualified-grade FCS containing 10% DMSO or adjusted to $3x10^6$/ml in long-term culture medium consisting of IMDM supplemented with 10% FCS, 10% horse serum and $5x10^{-7}$M hydrocortisone (complete LTCM).

Bone marrow stromas were established in vented 25cm^2 culture flasks incubated at 37°C in 5% CO_2 for 5 days without disturbance. Marrow cultures were fed by half medium changes on days 10, 14, 21 and 28. After 1-2 weeks in culture it was usually possible to see a confluent layer of fibroblasts and engrafting cells were seen after 3-5 weeks.

2.7.3.3 Trypsinisation of marrow

Reagents

- trypsin-EDTA, (0.5% Trypsin 5.3mM EDTA 4Na) (*Invitrogen*)
- sterile PBS

Established stromal layers were removed from the flasks by trypsinisation when the stroma was fully confluent, usually between day 28 and 35 of culture. The flasks were agitated gently, the medium removed and the stroma washed twice with sterile PBS to remove any remaining supernatant cells and serum. Stromal layers were incubated at 37°C for 10 minutes with 8ml 0.5% trypsin per flask to detach the cells from the flask. The trypsin was inactivated with 1ml FCS and the cells washed twice with IMDM containing 2% FCS. It was important to work quickly through each phase of trypsinisation to avoid cell injury or death due to over trypsinisation. Care was taken to ensure that all cell clumps were disaggregated prior to the first washing step. It was possible to obtain $5x10^6$ cells from each $25cm^2$ stroma flask although yields varied according to sample quality (Figure 2-4).

2.7.3.4 Cryopreservation of established marrow stroma

Trypsinised bone marrow stromal cells were cryopreserved in FCS containing 10% DMSO (one $25cm^2$ flask per 2ml cryogenic vial). When required cryostroma were thawed rapidly in a 37°C water bath and the cryoprotectant diluted in 10mLs of LTCM. Stromal cells were washed twice before being resuspended in the appropriate medium and grown to confluence in one vented 25 cm^2 culture flask containing 10ml LTCM.

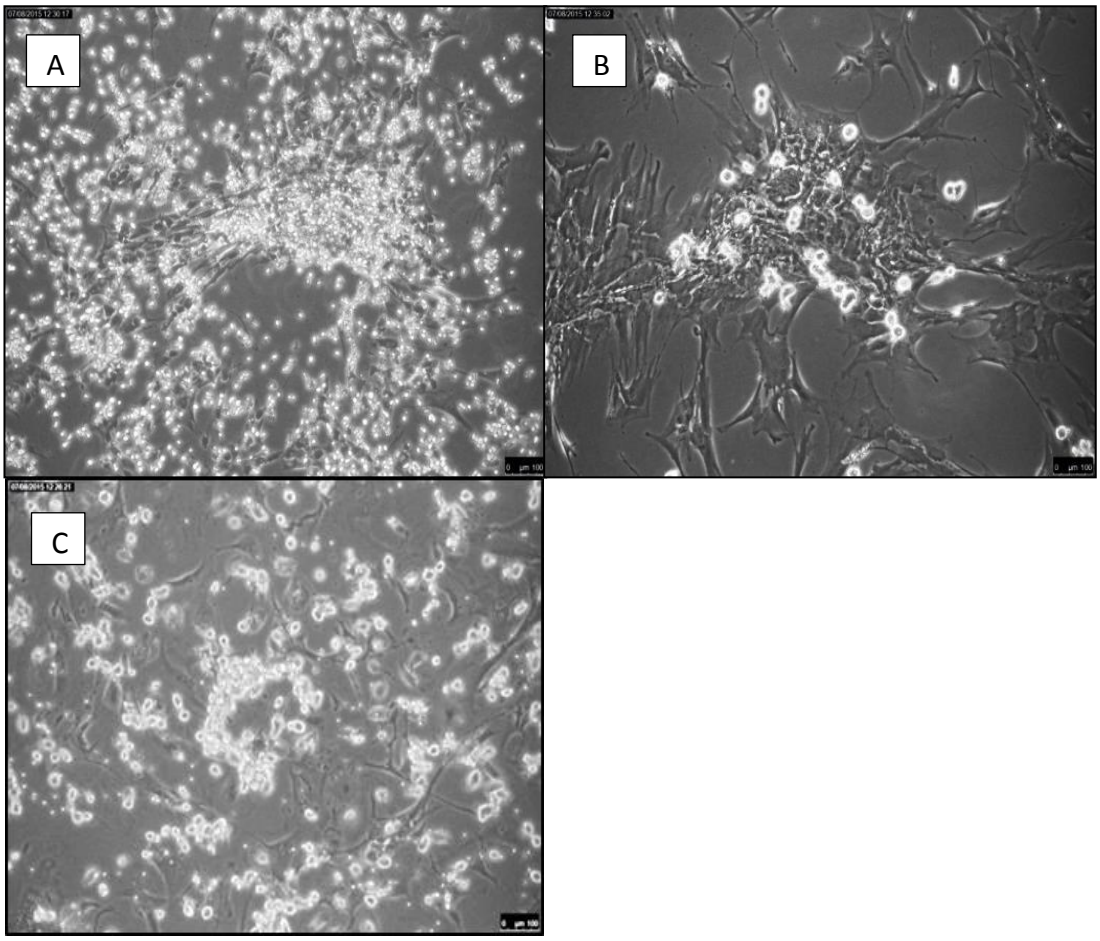

Figure 2.4. Examples of 2-D culture of human bone marrow fibroblasts from 3 different subjects (A, B, C): A: Subject following 21 days of culture; B: subject following 28 days of culture C: subject following 35 days of culture (mag. 10x). A 25cm^2 vented flasks was seeded with PBMCs from fresh human bone-marrow (density 5x10^6 cells/mL) in 10mLs of long-term culture medium after ficoll-separation from whole bone marrow aspirate. Cells were maintained at 37^{o}C, 5% CO_2 for 10 days without disturbance and then fed by half-medium separation on days 10, 14, 21, 28 and weekly thereafter.

2.8

Assessing Survival and Proliferation by Flow Cytometry

Introduction and General Principles

Flow cytometry is a laser-based method for the detection of cells suspended in a stream of fluid which carries and aligns the cells in single file through a beam of light or laser. As the cell passes through the beam, a detector converts analogue measurements of scattered light (forward-scattered (FS)) light which is proportional to the size of the cell and side-scattered (SSC) light which is proportional to the

granularity of the cell) as well as dye-specific fluorescence signals (emitted by fluorescein-conjugated antibodies) into digital signals which can be processed by a binary computer. Fluorescence-activated cell sorting (FACS™) provides a method for sorting a heterogenous mixture of cells (such as primary MCL cells, non-malignant lymphocytes and stromal cells) based upon specific light scattering and fluorescence.

Detection of Primary MCL Cells Using Cluster Differentiation Markers

Primary MCL PBMCs express a characteristic constellation of surface markers such as CD5, CD19, CD20 and FMC-7 which distinguish them from normal naïve B-lymphocytes and also from other B-cell malignancies.[3] These cells can therefore be visualised and identified by labelling these surface markers using ligand-specific monoclonal antibodies which are conjugated to a fluorochrome which will fluoresce when activated. Using fluorescence associated cell sorting (FACS™) these cells can be visualised and quantified.

Detection of Apoptosis Using Annexin-V

In addition, cells undergoing apoptosis (programmed cell death) can be distinguished from healthy cells by their surface expression of annexin-V. In normal viable cells, phosphatidylserine (PS) is located on the cytoplasmic surface of the cell membrane. During the immediate stages of apoptosis, PS translocates from the inner to the outer cell surface where it is exposed and can be detected by binding to annexin-V which can be detected when fluorescently labelled.

Detection of Proliferation Using Ki-67

The antigen Ki-67 is a nuclear protein associated with cellular proliferation and ribosomal transcription and can be used as a cell marker of proliferation. During the

active phases of the cell cycle, Ki-67 is present but is absent from resting cells. Monoclonal antibodies directed against human Ki-67 can be used to determine proliferation levels within a population of cells by FACS when conjugated to a fluorochrome. The method is complicated by the need to fix the cell and permeabilise the cell membrane to allow the antibody to bind its nuclear target. This can result in loss of cells and therefore a larger quantity of cell suspension is generally required for this assay.

Detection of Multiple Fluorochrome-Conjugated Antibodies on the Same Cell

Because of the laser/filter configuration of the flow cytometer and the fact that different fluorochromes fluoresce at different wave-lengths it is possible to design an experiment to detect multiple fluorochrome-labelled antibodies on the same cell. This is particularly useful in determining survival or proliferation of primary MCL cells when cultured on murine fibroblasts because MCL specific cluster differentiation markers can be used as well as the cell surface markers of survival and proliferation, allowing for more accurate determination of the desired population of cells.

For example, mouse-anti-human CD19 antibody conjugated to the fluorochrome APC (allophycocyanin), mouse-anti-human CD5 antibody conjugated to PE and annexin-V conjugated to FITC could all be added to the same sample and used to gate on the desired population of MCL with confidence that other cell types were reliably excluded from analysis.

2.8.1 Reagents, Materials and Equipment

Reagents

- fluorescein-conjugated, anti-human monoclonal antibodies and cellular probes (Table 2.2)
- annexin-V binding buffer (BD-Biosciences)
- FACS binding buffer (for non-annexin-V FACS) (0.5% bovine serum albumin (BSA) in 1x PBS solution)
- PBS
- staining buffer for Ki-67 Assay: 0.5% BSA/PBS 0.2% triton-X
- 4% PFH/PBS solution
- 0.5% Triton-X/PBS for cell permeabilisation

Materials and Equipment

- Accuri C6 Flow Cytometer(*BD Biosciences*)
- Accuri C Flow Plus Software (*BD Biosciences*)
- 1.5mL Eppendorf tubes (*Fisher Scientific*)
- vortex (*VortexGenie-2, Scientific Industries*)

Description	Cat. No.	Source	Fluoro-chrome	µL / test
CD19 mouse anti-human IgG1k	555412	BD Biosciences	FITC	10
CD19 mouse anti-human IgG1k	555413	BD Biosciences	PE	10
CD19 mouse anti-human IgG1k	555415	BD Biosciences	APC	10
CD5 mouse anti-human IgG1k	555355	BD Biosciences	APC	10
CD5 mouse anti-human IgG1k	555353	BD Biosciences	PE	10
CD3 mouse anti-human IgG2ak	555342	BD Biosciences	APC	10
Annexin V	556419	BD Biosciences	FITC	5
Ki-67 mouse anti-human IgG1k	556026	BD Biosciences	FITC	10
CD11c mouse anti-human IgG1k	555392	BD Biosciences	PE	10
CD62L (L-selectin) mouse anti-human IgG1k	555544	BD Biosciences	PE	10
CD49d (Integrin α4 chain) mouse anti-human IgG1k	555503	BD Biosciences	PE	10
CD49e (Integrin α5 chain) mouse anti-human IgG1k	555617	BD Biosciences	PE	10
CD11a (LFA 1α; ITGAL) mouse anti-human IgG1k	555384	BD Biosciences	PE	10
CD58 (LFA-3) mouse anti-human IgG2ak	555921	BD Biosciences	PE	10
CD54 (ICAM-1) mouse anti-human IgG1k	555511	BD Biosciences	PE	10
CD183 (CXCR3) mouse anti-human IgG1k	557185	BD Biosciences	PE	10
CD184 (CXCR4) mouse anti-human IgG2ak	555974	BD Biosciences	PE	10
CD185 (CXCR5) mouse anti-human IgG2b	FAB190P-100	R & D Systems	PE	10
Mouse anti-human IgG1k isotype control	556026	BD Biosciences	FITC	10
Mouse anti-human IgG1k isotype control	559320	BD Biosciences	PE	10
Mouse anti-human IgG1k isotype control	555751	BD Biosciences	APC	10
Mouse anti-human IgG2aκ isotype Control	555574	BD Biosciences	PE	10
Mouse Anti-Human CD154	555697	BD Biosciences	PE	10

Table 2-2 Fluorescein-conjugated human monoclonal antibodies /probes employed in labelling, survival, proliferation and adhesion experiments including isotype controls. FITC - fluorescein isothiocyanate; PE - phycoerythrin; APC –allophycocyanin.

2.8.2 Protocol for Apoptosis Assay

Two aliquots of 100µL of cell suspension were transferred from the culture well into two 1.5mL Eppendorf tubes. To one tube, 10µL of fluorescein-conjugated mouse anti-human CD5 and mouse anti-human CD19 were added. To the second tube, 10µL of the appropriate isotype control antibody were added. The tubes were gently vortexed and transferred to the dark at room temperature to permit binding. After 20 minutes 5µL of FITC-conjugated annexin-V was added to the first tube and the tube was gently vortexed. 300µL of annexin-V binding buffer was added to the tubes before being transferred to the flow-cytometer for FACS analysis.

2.8.3 Protocol for Proliferation Assay

Two aliquots of 200µL of cell suspension from each sample were transferred to labelled 1.5mL Eppendorf tubes. To one tube, 10µL of anti-CD19 and anti-CD5 antibodies were added, to the second tube, appropriate isotype controls were added. The tubes were vortexed and incubated at room temperature in the dark for 20 minutes. Both tubes were then centrifuged at 7000 rpm for 3 minutes until a cell pellet was visible. The supernatant was removed and the cells were resuspended in 200µL of 4% PFH/PBS, gently vortexed and incubated in the dark at room temperature for 10 minutes to fix the cells.

***NB**. An initial experiment was conducted to determine the optimal time to fix the cells (i.e. before or after labelling with anti-CD5 / CD19 surface marker antibodies). This experiment revealed that labelling the cells prior to fixation led to better visualisation of the surface markers by FACS after fixation and permeabilisation (data not shown).*

After a 10 minute fixation incubation the cells were washed (1mL of PBS was added and the tubes were centrifuged at 7000 rpm for 3 minutes to pellet the cells). The cells were then resuspended in 100µL of 0.5% triton-X/PBS and gently vortexed before

being incubated on ice for 10 minutes to permeabilise the cell membrane. 1mL of Ki-67 stain buffer was added and the cells were washed and resuspended in 100µL of Ki-67 stain buffer. 10µL of FITC-conjugated anti-human Ki-67 monoclonal antibody was added to the test tube and 10µL of isotype control added to the control tube. The tubes were vortexed and incubated in the dark for 25 minutes at room temperature. The cells were then washed and resuspended in 300µL of stain buffer prior to FACS analysis.

2.8.4 Protocol for Cellular Adhesion Marker Assay

For analysis of CAM profiles, 10µL of the target adhesion marker antibody or its corresponding isotype control were added to two separate 1.5mL Eppendorf tubes (Table 2.2). In addition to labelling the target CAM, the cells were co-labelled with anti-CD5 / CD19 monoclonal antibodies. 100µL of cell suspension was transferred to the labelled Eppendorf tube and the tube was gently vortexed and incubated at room temperature in the dark for 25 minutes. 300µL of stain buffer was then added and the tube vortexed and transferred to the flow cytometer for FACS analysis.

Method for Cytospin, fixation and Staining

2.9 In order to further assess the morphology of the primary MCL PBMCs during the co-culture experiments a sample of the cell suspension from each well of a series of four cases of MCL was spun onto a standard microscope slide, fixed and stained with modified Wright's stain (kindly performed by staff at the Derriford Combined Laboratories) for light microscopic examination.

Reagents

- cell suspension of human MCL PBMCs from co-culture experiments
- 4% paraformaldehyde / PBS solution
- mounting media (*Histomount*).

Materials and Equipment

- glass microscope slides & cover slips (*Fisher Scientific*)
- Statspin Cytofuge Centrifuge (+ cartridges and filters) (*Tissue-Tek®*)
- glassware for staining slides (*Fisher Scientific*)
- conical bottomed 15mL falcon tubes (*Fisher Scientific*)
- DFC 3000G phase contrast microscope (*Leica Microsystems*)

On day 7 of co-culture experiments, the cells were agitated within the well using a pipette. 100µL of media containing the co-culture from designated wells was retrieved and added to a sterile falcon tube. The empty well was visualised to ensure all cells have been retrieved and any remaining cells were retrieved by washing with PBS. 200µL of the cell suspension was added to labelled funnels loaded with filters and slides within the cytofuge. The funnels were spun gently (7000 rpm for 5 minutes) and the slides retrieved from the cartridges for labelling and inspection. The cells on the

slides were examined by light microscopy to ensure a consistent cell density was achieved (defined as cells in loose contact but not overlapping to optimise visualisation of morphology). Slides with excessive cell numbers were discarded, an appropriate dilution of the cell suspension was performed and the method was repeated until a satisfactory cell layer was achieved. The slides were then labelled and a diamond tipped pen was used to draw round the cell layers before being air-dried overnight. 200µL of 4% PFH/PBS was then dropped onto the cell layers and the slides were fixed for 15 minutes before being washed with PBS. The slides were stained with modified Wright's stain by laboratory staff in the combined laboratories at Derriford Hospital then cover-slipped using histomount and examined by light microscopy.

Cellular Adhesion Molecule Profiling of Primary MCL Cells

2.10

For the profiling of mononuclear cells from peripheral blood and bone marrow from subjects with MCL, FACS analysis of labelled cells was performed. The cells were suspended in culture medium, labelled with anti-CD5 and CD19 monoclonal antibodies and also with a monoclonal antibody against one of a panel of CAMs before being incubated and then analysed by flow cytometry.

The median fluorescence intensity (MFI) of each adhesion molecule expressed on the surface of the primary MCL cells was used for data analysis because the distribution of fluorescence intensity was not always Gaussian.

Reagents

- complete RPMI 1640 with GlutaMAX^{TM} medium (*Gibco*) (supplemented with 10% FCS (*Fisher Scientific*) and 1% penicillin/streptomycin (*Invitrogen*));
- fluorescein-conjugated mouse-anti-human monoclonal antibodies (Table 2.2)
- stain buffer (0.5% BSA in PBS) (*Fisher Scientific*)

Materials and Equipment

- Accuri C6 Flow Cytometer (*BD Biosciences*)
- Accuri CFlow Plus Software (*BD Biosciences*)
- 1.5mL Eppendorf tubes, tips and pipettes (*Fisher Scientific*)
- vortex (*VortexGenie-2, Scientific Industries*)

Peripheral blood mononuclear cells or marrow mononuclear cells were harvested from consenting subjects with MCL and separated from blood and plasma as previously described.

Mononuclear cells were resuspended in warmed, complete RPMI medium and cell density was adjusted to $1x10^6$/100µL. Ten microlitres of FITC- or APC-conjugated mouse anti-human CD5 and CD19 mononuclear antibody were added to 12 labelled 1.5mL Eppendorf tubes. To the first ten tubes, 10 µL of PE-conjugated, mouse anti-human monoclonal antibody specific to an individual adhesion molecule was added. To two tubes, 10µL of appropriate isotype control antibodies were added and one tube was labelled as an unstained control. A list of the monoclonal antibodies used is displayed in Table 2-2.

To each labelled tube, 100µL of cell suspension was added and the tubes were gently vortexed to mix before being incubated at room temperature in the dark for 20 minutes. Three hundred microlitres of staining buffer (0.5% BSA/PBS) was added to each tube before analysis by FACS™.

2.10.1 Analysing Flow Cytometry Data

An example of the plots and gates used to derive the median fluorescent intensity for each surface adhesion marker is displayed in Figure 2-5.

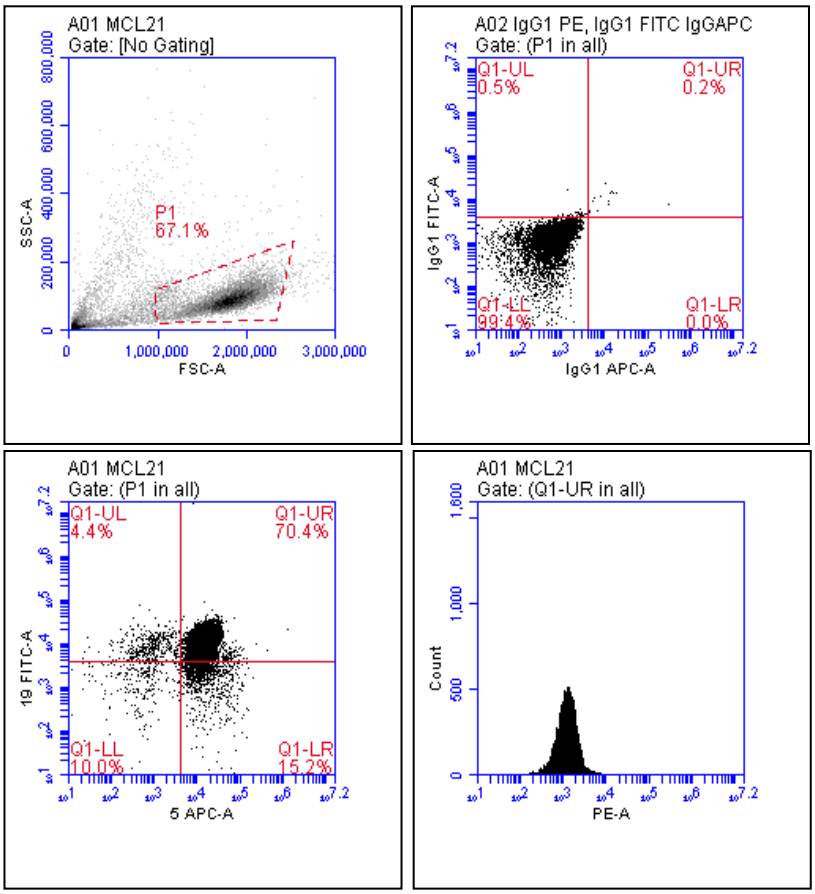

Figure 2-5. An example of the plots obtained by FACS analysis used to calculate the median fluorescent intensity for each adhesion molecule. Firstly, a forward / side scatter plot was obtained and a gate placed on the population of cells containing viable lymphocytes (top left). The CD5 / CD19 positive cells within this gate were identified according to their fluorescence compared with the isotype control (top right and bottom left). The median fluorescence intensity of the corresponding surface marker (labelled with PE fluorescein) was derived from this population.

2.11 Statistical Analysis

Data from flow cytometry experiments were analysed using Accuri CFlow Plus (*BD Biosciences*); *Microsoft Excel*™ and *GraphPad Prism*™ (version 5) software. Apoptosis was assessed according to annexin-V positivity; proliferation was assessed according to the percentage of cells which were positive for or Ki-67 compared with negative isotype control within the population of CD5 / 19 positive lymphocytes. The proportion of cells expressing surface adhesion markers was determined by calculation the median fluorescence intensity ratio (MFIR) = median fluorescence of adhesion antibody / median fluorescence of isotype control (presented in arbitrary units (a.u.)). Where a series of data is presented together, the mean value of the median fluorescence intensity together with the standard error of the mean is presented. Paired Wilcoxon signed rank tests were used to compare the mean and to derive p values, in which a two-tailed p value is displayed.

3. CHAPTER 3. Can a tractable *ex vivo* culture be developed to support and model the growth of mantle cell lymphoma?

Introduction

3.1 Mature B-lymphocytes survive, grow and proliferate within a marrow or lymph node microenvironment where essential signals are provided by specific accessory cells. These signals control essential aspects of behaviour, and there is evidence that accessory cells are required for extended survival/proliferation of MCL *in vitro*.[12,27,39,67,89] There is also growing evidence that the tumour micro-environment confers resistance to MCL cells by offering protection from immunochemotherapy.[38,39,67]

It was hypothesised, therefore, that an appropriately designed culture system would allow evaluation of MCL biology and cell interactions, and permit study of responses to drugs within an environment relevant to that encountered *in vivo*.

This chapter describes the development and testing of a system to model MCL growth *in vitro,* focussing particularly on the proposed role of accessory cells that express relevant receptors, and on the use of soluble factors recognised to alter the of survival and growth of other mature B-cell neoplasms. The *ex vivo* growth and survival characteristics of 15 distinct cases of primary MCL was therefore assessed when cultured in isolation or with murine and human fibroblast support testing also the role of fibroblast-expressed CD40 ligand (CD40-L). The soluble factors interleukin 4 (IL4) and toll-like receptor 9 ligand (TLRL-9) were also examined for their effect on MCL growth.

The CD40 ligand is a member of the tumour necrosis factor (TNF) superfamily. It is expressed primarily by activated T cells and engages with the CD40 receptor on B-cells. It provides a major secondary signal to B-cells which stimulates survival and proliferation through the upregulation of major transcription factors. It also has the ability to rescue B cells from apoptosis by the induction of BCL pro-survival proteins.[45,49,90,91] Although CD40L has recognised effects in other B-lymphoproliferative disorders – promoting their survival or proliferation[48,91,92], the molecule has not been widely studied in MCL and the existing evidence of its effect is conflicting[47,49].

IL-4 is a pleiotropic cytokine which regulates T-cell and B-cell responses, including proliferation, survival and gene expression.[57] It is produced by T-cells, mast cells and bone marrow stromal cells. A combination of CD40-ligand and IL-4 (also secreted by activated Th2 cells) is known to stimulate B cell proliferation *in vitro,* and these molecules have been demonstrated to synergise in driving clonal expansion in normal B-cells and proliferative responses in MCL cells.[49,63] In addition to stimulating proliferative responses, IL-4 has been shown to inhibit apoptosis and maintain cell viability in B-cells, including their malignant counterparts by the upregulation of BCL-2 expression.[60,61]

TLR-9 is expressed on antigen-naïve B-cells, including MCL cells and can recognise T-cell independent antigens, such as lipopolysaccharide (LPS), which are intrinsically mitogenic.[51] Through activation of TLR-9, T-cell independent antigens can initiate a cascade of intracellular events in B-cells, including phosphorylation of cytoplasmic tyrosine kinases resulting in enhanced proliferation and differentiation. There is also evidence that the addition of TLR-9-L with CD40-L stimulation acts synergistically to enhance proliferation and differentiation.[52,55,56]

These observations provide the rationale for the use of IL-4 and TLR9-L in combination with CD40-ligand as a model for stimulating proliferation and survival in primary MCL cells *ex vivo*.

3.2 Summary of Experimental Methods

This chapter employs the culture of stromal cells *ex vivo*, their co-culture with primary MCL cells, and analysis of their survival and proliferation using flow cytometry. The detailed methods are described in Materials and Methods (section 2.8). The antibodies and soluble factors employed are shown in Table 3-1.

Model systems: In brief, two distinct murine fibroblast monolayers, one transfected with the CD40 ligand gene (labelled CD40L-T) and the other, non-transfected (CD40L-NT), were cultured in wells of standard, 24 well plates until 70-80% confluent by visual inspection. Monolayers were then irradiated (15Gy single fraction) to prevent them overgrowing the primary MCL cells. Cell suspensions of primary MCL cells from individual subjects were prepared in complete RPMI media using a density of $4x10^6$/mL. Following washing of the fibroblast layer, 1mL of the PBMC suspension was seeded onto the monolayers in the 24 well plates. In experiments examining the role of IL-4 and TLR9-L as stimulants of survival and proliferation, humanised Interleukin 4 (50ng/mL) or Toll-like-receptor-9 ligand (ODN 2006) (3uM) were added to selected wells along with a DMSO vehicle control. A control ODN experiment was performed previously to ensure oligonucleotides per se did not initiate apoptosis. The co-cultures were then maintained in RPMI medium in humidified, CO_2-enriched conditions at 37^oC for up to 8 days. Cells were inspected and harvested at defined time points and analysed for rates of apoptosis and proliferation.

For experiments involving human bone marrow fibroblasts, separate standard 24 well plates were seeded with human marrow cells or CD40-L transfected murine stroma. The human bone marrow stroma were obtained from a patient with Waldenströms macroglobulinaemia, separated using ficoll-paque then cultured in in 25cm^2 flasks until a sufficiently confluent layer was achieved. The murine stromal layers were irradiated to prevent overgrowth of the primary MCL cells as previously described. The human stromal layer was not irradiated because growth rates observed were much slower and overgrowth of the MCL cells was not anticipated over the time period of the experiment.

Cell assessments: Cell survival and proliferation rates were assessed by flow cytometry using annexin-V as a marker of apoptosis and Ki-67 as a marker of proliferation. Aliquots of 100µL of cell suspension were used for annexin-V assay (approximately 4x10^5 cells) and 200µL of cell suspension (approximately 8x10^5 cells) were used for the Ki-67 assay (a larger volume to account for increased cell loss during the fixation and permeabilisation steps). The cells were co-labelled with fluorescein-conjugated anti-CD5 and -CD19 monoclonal antibodies before addition of annexin-V and before fixation and permeabilisation for the Ki-67 assay. Primary MCL cells were distinguished from fibroblast cells in flow cytometry by their forward and side-scatter characteristics and by their co-expression of CD5 and CD19, characteristic cell surface markers of MCL cells, not expressed on murine or human fibroblasts. All antibodies were anti-human and used with corresponding isotype controls at a concentration of 10µL per test. For annexin V staining, 5µL of annexin-V FITC /100µl cell suspension was used.

Alongside flow-cytometry, the culture plates were visually inspected by light-microscopy for morphological changes after 24 hours and subsequently every 48 hours

of co-culture. Images were taken using a DM IL LED phase-contrast light microscope and CCD grayscale camera (Leica DFC3000 G) and processed using LAS AF Version: 2.6.3 software (*Leica Microsystems*). A further assessment employed cytospin morphological assessment: the primary MCL PBMCs during co-culture, 200µL samples of the cell suspension from selected cases was spun onto a standard microscope slide using a cytofuge, air-dried for 12 hours before being fixed with 4% paraformaldehyde/PBS and stained with modified Wright's stain for light microscopic examination (Materials and Methods section 2.9).

Data analysis: Data were analysed using Accuri CFlow Plus (BD Biosciences); Microsoft Excel™ and GraphPad Prism™ Version 5 software. The tests employed are described in the figure legend of the individual experiments.

Description	Ref/cat no	Source	Fluoro-chrome	µL / test
CD19 mouse anti-human IgG1k	555412	BD Biosciences	FITC	10
CD19 mouse anti-human IgG1k	555413	BD Biosciences	PE	10
CD19 mouse anti-human IgG1k	555415	BD Biosciences	APC	10
CD5 mouse anti-human IgG1k	555355	BD Biosciences	APC	10
CD5 mouse anti-human IgG1k	555353	BD Biosciences	PE	10
CD3 mouse anti-human IgG2ak	555342	BD Biosciences	APC	10
Ki-67 mouse anti-human IgG1k	556026	BD Biosciences	FITC	10
Mouse anti-human IgG1k isotype control	556026	BD Biosciences	FITC	10
Mouse anti-human IgG1k isotype control	559320	BD Biosciences	PE	10
Mouse anti-human IgG1k isotype control	555751	BD Biosciences	APC	10
Mouse anti-human IgG2aκ isotype Control	555574	BD Biosciences	PE	10
ODN 2006 (ODN 7909) Class B CpG oligonucleotide; a human TLR9 ligand	tlrl-2006-1	InvivoGen	n/a	3uM
Recombinant Human IL-4	AD-200-04	PeproTech	n/a	50ng/mL

Table 3-1 Monoclonal antibodies and cell stimulants. Monoclonal antibodies employed to label and assay primary MCL cells for apoptosis and proliferation experiments. FITC - fluorescein isothiocyanate; PE - phycoerythrin; APC –allophycocyanin.

3.3 Clinical and biological features of primary MCL cases

The clinical and biological features of the cases used in this chapter are summarised in Table 3-2. Fourteen of the subjects had peripheral blood mononuclear cells (PBMCs) sampled at single time-points in their disease history, either before treatment or at relapse. One of the subjects, (MCL11), underwent blood sampling at diagnosis (before any treatment) and at first relapse after immunochemotherapy, whilst on second-line treatment with a BTK-inhibitor. Because MCL cells are known to evolve new mutations at relapse, cells from subject MCL11 were tested and presented separately, as a clinically distinct sample (labelled MCL12).[93]

Although the biological features of each case are uniform in terms of the diagnostic hallmarks (t(11;14) translocation and cyclin D1 overexpression), the cases showed significant clinical heterogeneity between subjects, which is a well-known feature of the disease. For example, subject MCL07 was diagnosed with MCL nearly 15 years ago after an incidental finding of a peripheral leucocytosis (WCC $15x10^9$/L). However there were no clinical symptoms or evidence of bulky lymphadenopathy at diagnosis and therefore the subject was merely observed at routine appointments. This pattern of observation has continued for nearly 15 years without the requirement for therapy and remains the case at the point of writing.

In contrast, subject MCL08 presented with lymphadenopathy and constitutional symptoms at diagnosis. This required immediate therapy, but the individual subsequently relapsed after a relatively short remission (less than 2 years). After a second line of therapy with ibrutinib, (a BTK inhibitor), his disease again relapsed with a rapidly rising white cell count ($200x10^9$/L) and progressive lymphadenopathy. It was at this point that his cells were harvested and cryopreserved and unfortunately no

further treatment was successful and the patient died shortly afterwards. Both cases harboured the single t(11;14) translocation resulting in over-expression of cyclin-D1.

The clinical variation exemplified in these two cases allows MCL cases to broadly be divided into indolent and aggressive forms of the disease. For the purpose of this study, aggressive disease is defined as requiring treatment at or shortly after diagnosis; whereas indolent disease is defined as present but causing no clinically significant problems to the patient and not requiring treatment for 2 years from diagnosis. Where appropriate the samples used in this chapter have been subdivided in this way for the purpose of presentation and data analysis.

Case	Age, gender	Molecular data	Immuno-phenotype	Clinical phenotype	Prior Treatment	Indolent or Aggressive*
MCL01	66 f	t(11;14)+	CD5/19+	Stage IV; WCC $300x10^9/L$	None	Aggressive
MCL02	68 m	(t11;14)+ cyclin D1	CD5/19+	Stage IV WCC $234x10^9/L$	Immunochemotherapy, and BTK-inhibitor	Aggressive
MCL03	74 m	cyclin D1	CD5/19+	Stage IV WCC $30x10^9/L$	None	Aggressive
MCL04	65 f	(t11;14)+	CD19+	Leukaemic, MCL WCC $280x10^9/L$	None	Indolent
MCL05	63 f	t(11;14)+	CD5/19+	Leukaemic MCL, splenomegaly	None	Aggressive
MCL06	64 f	t(11;14)+	CD5/19+	Stage IV WCC $30x10^9/L$	None – but refractory to treatment	Aggressive
MCL07	65 m	t(11;14)+ cyclin D1+	CD19+	Leukaemic MCL WCC $30x10^9/L$	None	Indolent
MCL08	56 m	t(11;14)+	CD5/19+	Stage IV WCC $200x10^9/L$	Immunochemotherapy, and BTK-inhibitor	Aggressive
MCL09	70 m	cyclin D1+	CD5/19+	Stage IV WCC $190x10^9/L$	Immunochemotherapy	Aggressive
MCL10	54 m	t(11;14)+ cyclin D1+	CD5/19+	Stage IV WCC variable†	Immunochemotherapy	Aggressive
MCL11	60 f	cyclin D1+	CD5/19+	Stage IV	Immunochemotherapy	Aggressive
MCL12	62 f	cyclin D1+	CD5/19+	Stage IV WCC $250x10^9/L$	Immunochemotherapy and BTK-inhibitor	Aggressive
MCL13	64 m	cyclin D1; t(11;14)	CD5/19+	Low volume disease WCC $152x10^9/L$	None	Indolent
MCL14	62 m	cyclin D1; t(11;14)	CD5/19+	Localised low volume	Local radiotherapy to eye	Indolent

				disease		
MCL15	70 f	cyclin D1; t(11;14)	CD5/19+	Stage III	None	Aggressive

Table 3-2 Primary MCL Subject Clinical and Biological Characteristics. MCL subject demographics, diagnostic molecular data, immunophenotyping of PBMCs and clinical disease summary of 12 cases of MCL examined in this chapter.

The variation of clinical features observed between cases was also apparent when cases were observed by light microscopy. The cellular growth patterns of two selected cases (MCL07, an indolent case, and MCL08, an aggressive case) are demonstrated in Figure 3-1. Cells from subject MCL08, a proliferative and aggressive case of MCL, form clusters after four days of culture on CD40-ligand transfected murine fibroblasts compared with little obvious evidence of cluster formation in the CD40-ligand negative environment. Cells from subject MCL07, an indolent case, fail to demonstrate any obvious cluster formation in the same environment over the same time period.

It is interesting to note that an increase in proliferation was noted in the cells from MCL08, whereas no significant proliferation was observed in any environment for cells from subject MCL07 (see Table 3-4). These different behaviours not only support the concept of different responses to the stromal environment between clinically distinct cases of MCL, but also support the subsequent study of different adhesion properties of MCL reported in Chapter 4.

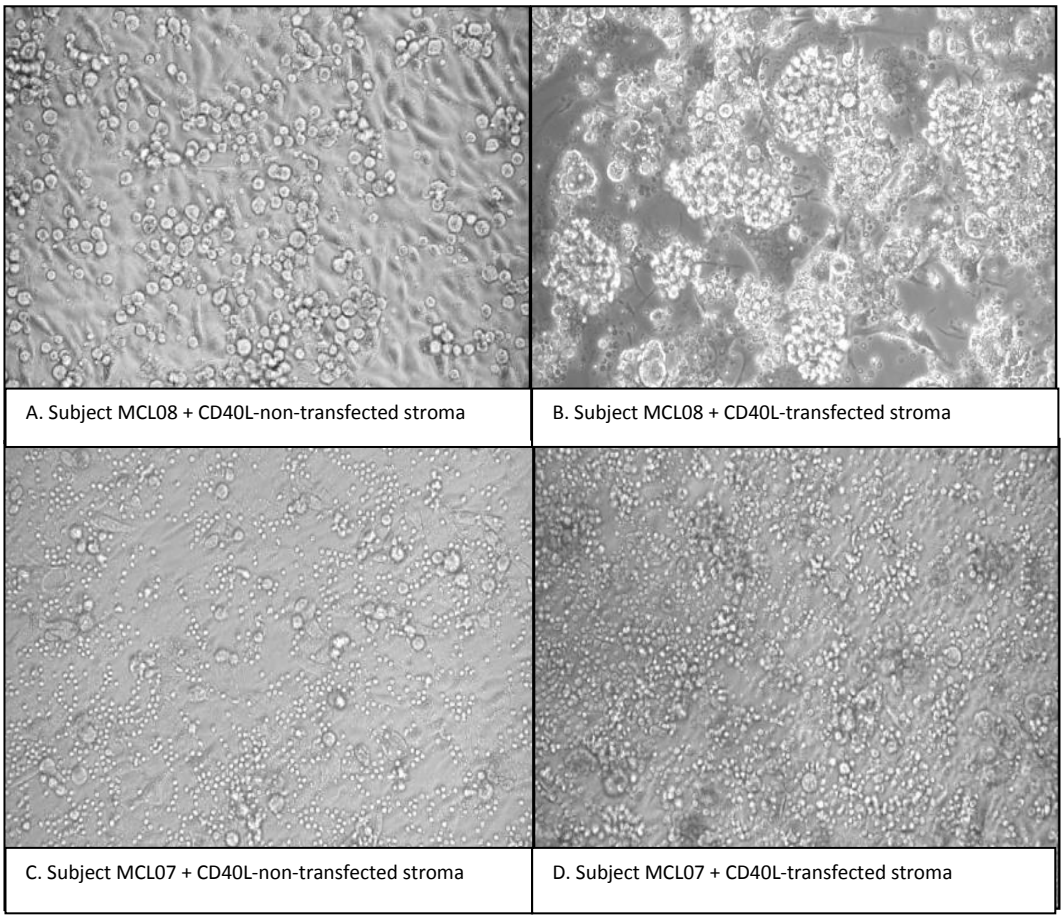

Figure 3.1 Serial Light-Microscopy Images of Primary MCL Cells on Fibroblast Monolayers After 4 Days of Culture. Subjects MCL07 (indolent) and MCL08 (aggressive) PBMCs co-cultured with CD40-L transfected murine fibroblasts for 4 days. Cells from MCL08 demonstrate no evidence of cluster formation in the CD40-L non-transfected microenvironment (A) compared with obvious cluster formation on the CD40-ligand transfected stromal cell layer (B). Cells from MCL07 (indolent case) demonstrate no clear cluster formation in either microenvironment (C & D). (PBMCs seeded in complete RPMI at $4x10^6$/mL and cultured for 4 days on CD40-ligand non-transfected (CD40L-NT) murine fibroblasts (left) versus CD40L-transfected stroma (right) (Mag x20, objective lens).

3.4 Primary MCL cells demonstrate increased survival when cultured *ex vivo* with CD40L-T stromal cell support compared with CD40L-NT stroma or media alone

To establish the effects of stromal cell support on cell survival, four cases of primary MCL were seeded into wells in culture media alone or with murine fibroblast cells, either CD40L-NT or CD40L-T. Wells were sampled and analysed for rates of apoptosis after 24 hours and 3 days. Marked heterogeneity was observed, however cells co-cultured on a murine stromal layer transfected with CD40L had the best overall survival. Similar rates of apoptosis were observed in cells cultured in media alone or on a CD40L-NT stromal layer suggesting that accessory cell support in the absence of CD40L offers no significant survival advantage over the culture of cells in media alone (Figure 3-2).

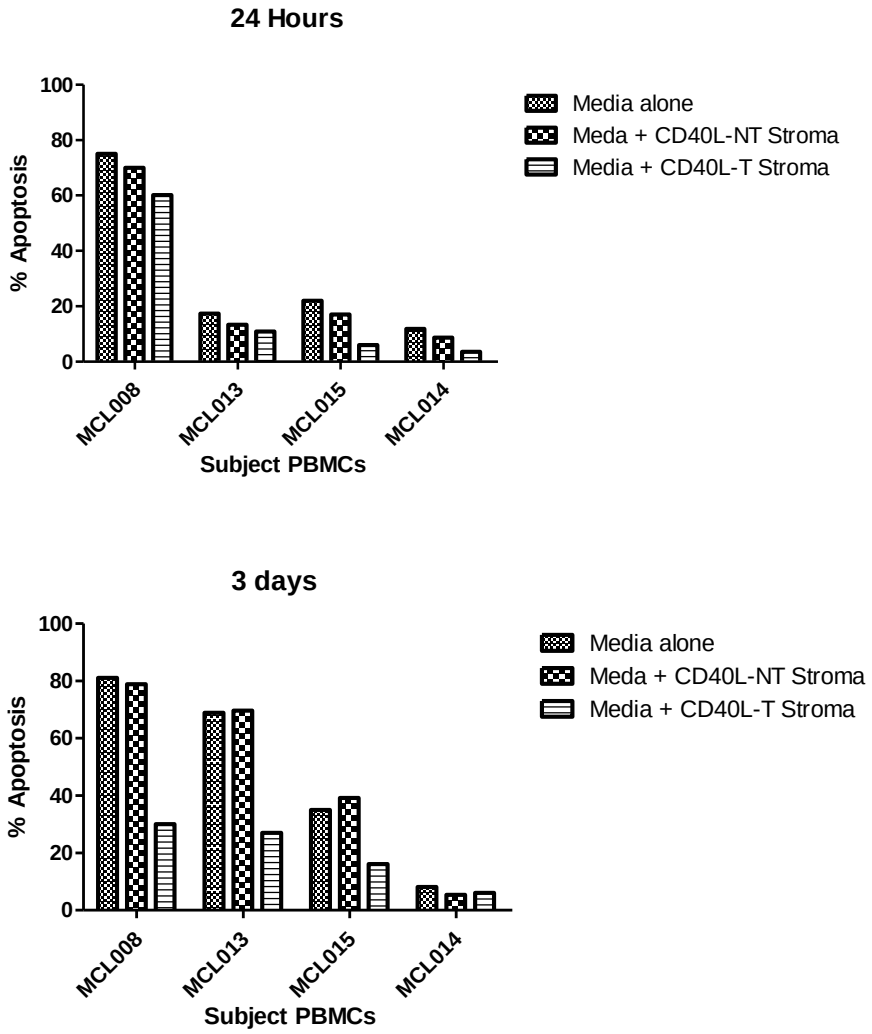

Figure 3.2 Survival of primary MCL is sustained when cultured with CD40-ligand transfected fibroblasts when compared to non-transfected fibroblasts or media alone. Rates of apoptosis are shown for the four cases as a mean value at two time points demonstrating a protection from apoptosis in the presence of CD40L.

Since media alone and CD40-NT did not differ in observed survival rates, subsequent co-culture experiments compared CD40-L-transfected murine fibroblasts as a supportive layer with CD40-ligand non-transfected cells employed as the most relevant control.

3.5 Biological characterisation of primary MCL cells cultured *ex vivo* with or without CD40L, TLR9-L or IL4 stimulation

Building on the observation that MCL cells survive best when cultured with a stromal cell supportive layer *ex vivo*, primary MCL cells from 12 subjects were tested for survival and proliferation after co-culture on two different murine fibroblast monolayers, one transfected with the CD40L gene and the other non-transfected.

The culture system was assessed for rates of apoptosis and proliferation using annexin-V and Ki-67-positivity by flow cytometry. After 8 days of culture, the contents of each well was removed and divided into aliquots for quantification of the surviving and proliferative fractions by annexin-V and Ki-67 FACS assays as previously described. The rate of apoptosis and proliferation for each individual primary MCL case within the different microenvironment is presented in Tables 3-3 and 3-4, and for apoptosis shown graphically in Figure 3-3 (the mean apoptosis percentage for all 12 cases displayed in red). The mean proliferation and apoptosis rates derived from all the cases after culture with CD40L-T and CD40L-NT stroma, together with IL-4 and TLR9-L stimulation are compared in Figure 3.4.

Case	Time Zero	CD40L-NT	CD40L-NT + IL-4	CD40L-NT + TLR9-L	CD40L-T	CD40L-T + IL-4	CD40L-T + TLR9-L
MCL01	6	3.3	2.8	23	6.1	3.8	9.1
MCL02	4.2	11.8	12.8	41.7	8.0	11.0	22.7
MCL03	5.6	3.1	3.4	6.0	4.1	2.3	2.2
MCL04	37.6	10.6	3.2	14.9	3.6	0.4	2.1
MCL05	19.7	1.9	3.7	2.3	7.3	5.1	9.4
MCL06	5.1	9.8	10	43.7	15.2	15.4	27
MCL07	8.7	1.6	2.9	1.1	3.4	4.5	13.7
MCL08	36	27.4	2.6	51.9	4.4	14.1	18.7
MCL09	5	75.6	71.8	81	48.1	19.5	33.7
MCL10	13.6	90.3	87.1	90.6	33.3	30	42.1
MCL11	3.1	82.7	68.8	79.2	36.2	22	49.2
MCL12	4.0	84.9	87.7	91.4	27.6	15.5	46.5
Mean	**12.4**	**33.6**	**29.7**	**43.9**	**16.4**	**11.7**	**23**

Table 3-3 Survival of primary MCL PBMCs after 8 days co-culture on a stromal layer. Percentage of apoptotic MCL PBMCs from 12 cases of primary MCL before and after 8 days of co-culture in different microenvironments as determined by annexin V positivity by flow cytometry. Cells were co-cultured with murine fibroblastsCD40L-T; or CD40L-NT after the addition of 3µM TLR9-L or 50ng/mL of recombinant IL-4 as indicated.

Case	CD40L-NT	CD40L-NT + IL-4	CD40L-NT + TLR9-L	CD40L-T	CD40L-T + IL-4	CD40L-T + TLR9-L
MCL01	3.6	1.2	8.4	6.8	9	12.1
MCL02	9.2	14.8	17.4	60	40.1	44.2
MCL03	0.3	0.2	0.3	1.5	1.8	1.7
MCL04	0.9	1.4	4.9	11	7.5	7.5
MCL05	0.8	0.7	1.8	4.3	5.1	6.2
MCL06	1.4	1.1	0.6	1.5	2.2	1.3
MCL07	0.6	0.7	0.8	16.2	19.3	15.3
MCL08	4.9	1.9	failed	34	29	38.2
MCL09	0.3	0.8	0.7	0.2	0.6	0.2
MCL10	4.9	5.4	6.3	1.7	1.3	1.2
MCL11	0.1	0.2	0.3	0.6	0.6	0.4
MCL12	0.3	1.2	0.9	0.8	0.9	1.4
Mean	**2.26**	**2.47**	**3.85**	**11.55**	**9.78**	**10.81**

Table 3-4 Proliferation of primary MCL PBMCs after 8 days co-culture. Percentage of proliferating MCL PBMCs from 12 cases of primary MCL before and after 8 days of co-culture in different microenvironments as determined by Ki-67 expression determined by flow cytometry. Cells were co-cultured with murine fibroblasts CD40-T or CD40-NT with or without 3μM TLR9-L or 50ng/mL of IL-4 as indicated.

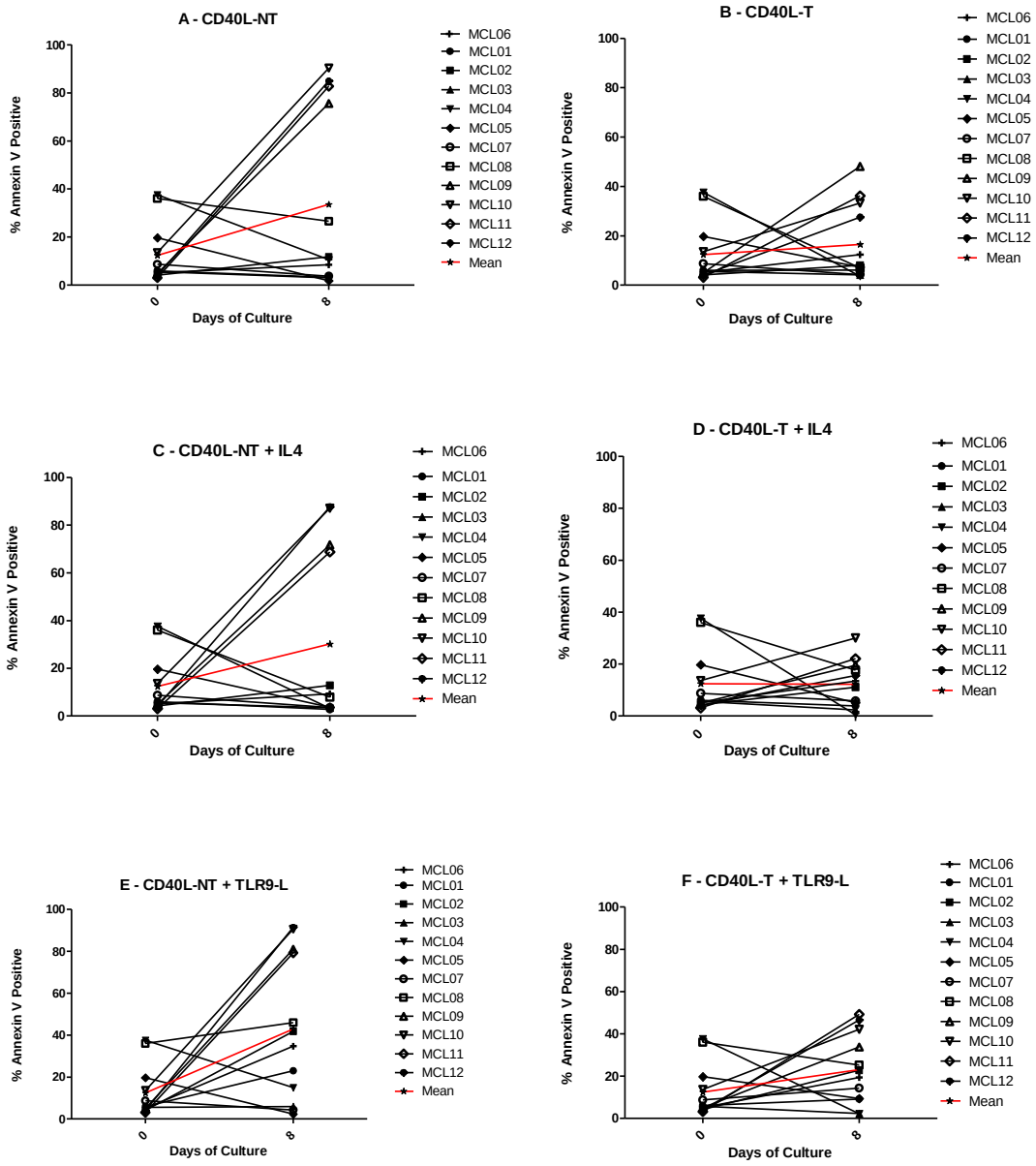

Figure 3.3 Rates of apoptosis for each primary MCL case before and after 8 days co-culture with murine fibroblasts without CD40L (CD40L-NT) and with CD40L (CD40L-T). In addition to CD40-ligand stimulation (B), cells shown in D also received 50ng/mL human recombinant IL-4 and cells shown in F also received 3µM TLR9-L at time 0. Percentage of apoptotic cells determined by annexin-V positivity by flow cytometry is presented (mean values are shown in red).

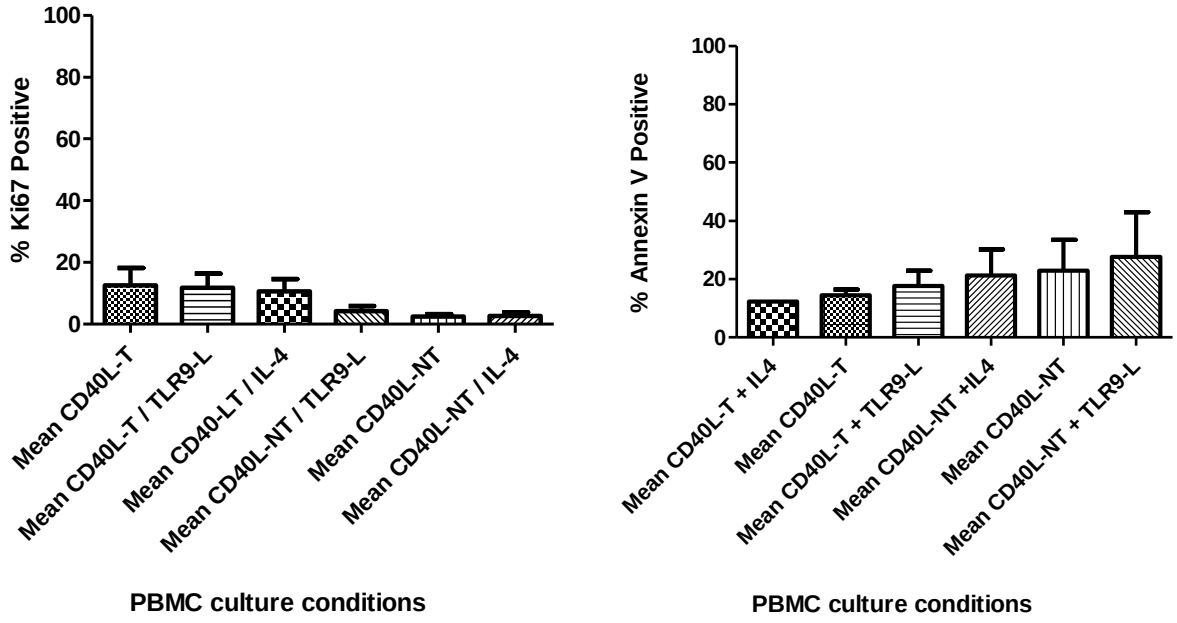

Figure 3.4 A summary of proliferation (left) and apoptosis (right) of primary MCL PBMCs co-cultured in different micro-environments. Mean percentage of Ki67-positive MCL PBMCs and mean percentage of annexin-V positive MCL PBMCs (determined by FACS) from 12 cases of MCL after 8 days co-culture with murine fibroblasts (CD40L-transfected (CD40T) vs CD40-non-transfected (CD40-NT) with 5µL DMSO; after addition of 50ng/mL human recombinant IL-4 or 3µM Toll-like receptor 9 ligand (TLR9-L). (Mean + standard error displayed).

3.5.1 Primary MCL cells exhibit heterogeneity in their ability to survive and proliferate *ex vivo*.

There is striking variability of primary MCL cells from different cases to survive *ex vivo* (Table 3.3). Some cases show high levels of apoptosis and a clear survival benefit with CD40L (for example MCL09) whereas in other cases (for example MCL03) there is very little apoptosis with or without CD40L. Further, survival at time zero is not predictive of survival after 8 days. Proliferation of MCL in culture is disappointingly low and again the response is heterogeneous (Table 3.4). Overall though, both survival and proliferation appear to be optimised by the presence of CD40L (mean apoptosis CD40L-NT 33.6% vs CD40L-T 16.4% ; mean proliferation CD40L-NT 2.26% vs CD40L-T

11.55%). TLR9 -L appears to enhance apoptosis possibly more so in the absence of CD40L (Figure 3.4). Data for TLR9-L negative control shows no difference to DMSO vehicle control (data not shown). The effects of IL4 are less clear. There is a suggestion that IL-4 may promote survival with a reduction in mean apoptosis by 4% (CD40L-NT) and 5% (CD40L-T). The individual effects of CD40L, IL4 and TLR9-L on both apoptosis and proliferation are studied in more detail below.

3.5.2 CD40-ligand significantly reduces apoptosis and enhances proliferation of MCL cells when cultured *ex vivo*

The effect of CD40L on cell survival and proliferation was analysed in more detail (Figure 3.5). The effect of CD40L when analysed collectively with or without IL4 or TLR-9-L markedly enhances survival ($p=0.0007$) and proliferation ($p=0.0001$). This significance is also demonstrated when only CD40L is assessed. Where apoptosis rates in cases cultured in the absence of CD40L were less than 5% it was deemed best to exclude these from analysis since additional benefit of the CD40L would be difficult to detect within case-case and experimental variability.

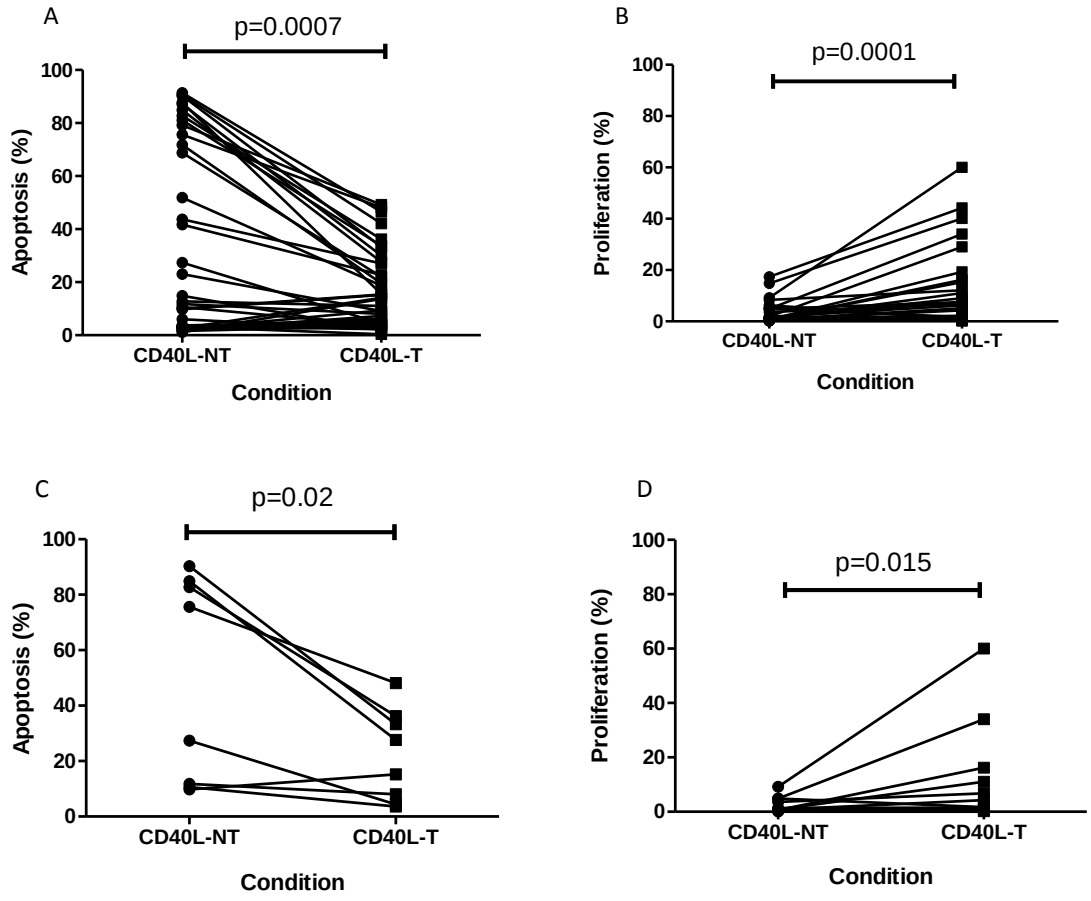

Figure 3.5 CD40-ligand reduces apoptosis and enhances proliferation of MCL cells when cultured *ex vivo*. Paired Wilcoxon signed rank test comparing mean rates of apoptosis (A & C) and proliferation (B & D) for 12 cases of primary MCL cells cultured *ex vivo* with CD40-ligand non-transfected murine fibroblasts (CD40L-NT) and CD40-ligand transfected murine fibroblasts (CD40-L-T). Panels A & B: all cases; Panels C & D: case set restricted to CD40L-T vs CD40L-NT.

The results were subsequently analysed to see if there was any link between proliferation and survival. The results (Figure 3.6) clearly show that in the absence of CD40L there is no correlation between proliferation and survival (R^2=0), the cases highlighted in red are the indolent MCL cases, however, when CD40L is present, the proliferative effect and protection from apoptosis are linked responses (R^2=0.79). Therefore it is a response to CD40L rather than an intrinsic biological phenomenon of linked proliferation and apoptosis.

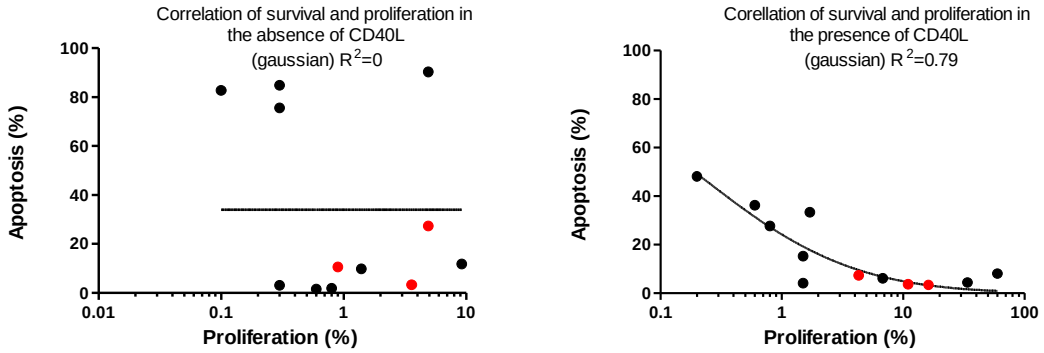

Figure 3.6 In the presence of CD40-ligand, changes to proliferation and apoptosis are linked. These plots demonstrate a positive correlation between lower rates of survival and increased rates of proliferation amongst primary MCL cells cultured in the presence of CD40-L transfected murine fibroblasts. There is no correlation in absence of CD40L.

3.5.3 Human interleukin-4 stimulation has a significant pro-survival effect but no significant effect on proliferation of primary MCL PBMCs cultured *ex vivo*

A pooled analysis of the effect of IL-4 on survival and apoptosis for all 12 cases of MCL cultured *ex vivo* is shown (Figure 3.7). Overall, IL-4 appears to lead to an improvement in survival as determined by reduced rates of annexin-V positivity (mean apoptosis without IL-4 25% vs 20.9% with IL-4 p=0.037). However, IL-4 does not significantly affect proliferation as determined by Ki-67 positivity after 8 days of culture (mean proliferation 6.9% without IL-4 vs 6.1% with IL-4 p=ns). However, when the effect of IL-4 was considered according to the presence or absence of CD40L, no significant effect on either survival or proliferation of primary MCL cells was evident (Figure 3.8). These findings suggest that the effects of IL-4 on MCL in this culture system are not marked.

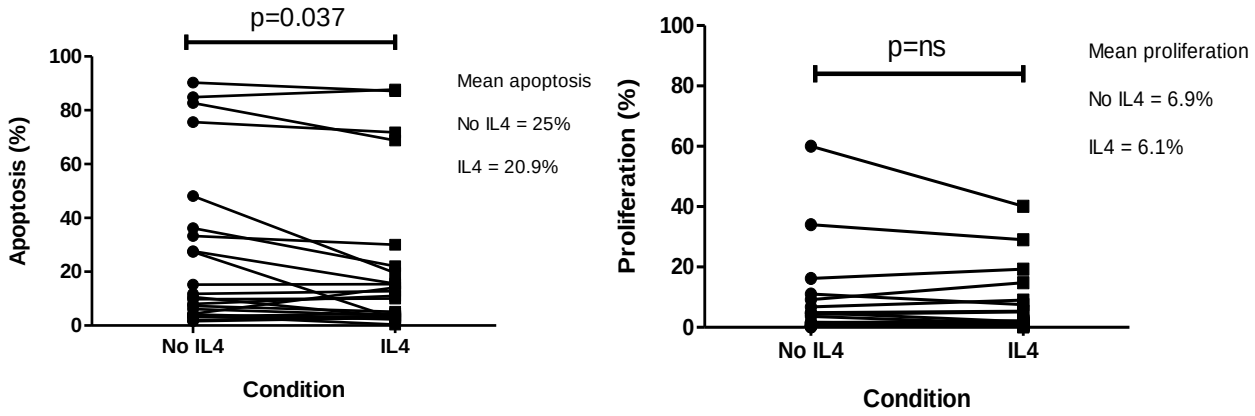

Figure 3.7 IL-4 reduces rate of apoptosis of *ex vivo* cultured MCL PBMCs but has no effect on proliferation. Paired Wilcoxon signed rank test comparing mean rates of apoptosis and proliferation determined by annexin-V and Ki-67 positivity respectively (assessed by flow-cytometry). Samples were subject to stimulation with 50ng/mL of recombinant human IL-4 at baseline and cultured on murine fibroblast monolayers in RPMI media for 8 days. Results are pooled for the presence or absence of CD40L.

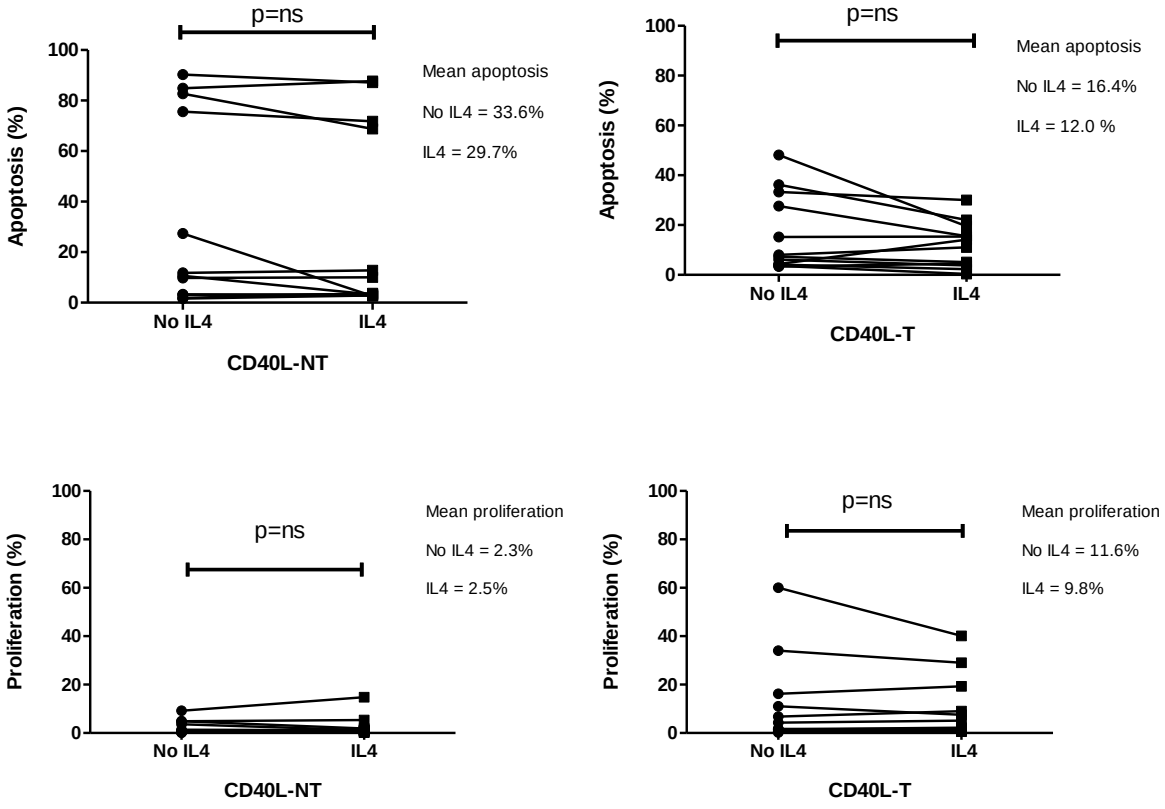

Figure 3.8 A subset analysis of the addition of interleukin-4 (IL-4) to primary MCL cells cultured with or without CD40-ligand demonstrates no significant change in survival or proliferation. Paired Wilcoxon signed rank test comparing mean rates of apoptosis and proliferation determined by annexin-V and Ki-67 positivity respectively (assessed by flow-cytometry). Samples were subject to stimulation with 50ng/mL IL-4 at baseline and cultured on murine fibroblast monolayers in RPMI media for 8 days

3.5.4 Toll-Like Receptor-9 Ligand appears to impair survival of MCL PBMCs but has no effect on proliferation in *ex vivo* culture

A pooled analysis of survival and proliferation of all 12 cases of primary MCL cells cultured with or without TLR-stimulation at baseline is displayed in Figure 3.9 with a subset analysis of the effects of TLR stimulation according to the presence or absence of CD40-L shown in Figure 3.10.

In the pooled analysis, no significant effect on proliferation could be demonstrated in the presence of TLR9-L (Mean proliferation 7% without TLR9-L vs 7.5% with TLR9-L, p=ns). However there was evidence of a significant reduction in survival in the presence of TLR9-L (mean apoptosis 25% without TLR9-L, 33.5% with TLR9-L, p=0.0016) (Figure 3.9). When the effects of TLR9-L stimulation was sub-stratified according to the presence or absence of CD40L, survival is significantly reduced in both microenvironments and there appears to be more of an effect in the absence of CD40L, (mean apoptosis 33.6% without TLR9-L vs 43.9% with TLR9-L in the absence of CD40L (p=0.012); 16.4% without TLR9-L vs 23% with TLR9-L in the presence of CD40L (p=0.043)). Although proliferation in the absence of CD40L is enhanced with TLR9-L (mean proliferation without TLR9-L 2%; with TLR9-L 3.9% p=0.02), proliferation rates are notably low. Proliferation is not affected byTLR9-ligation in the presence of CD40-L (Figure 3.10).

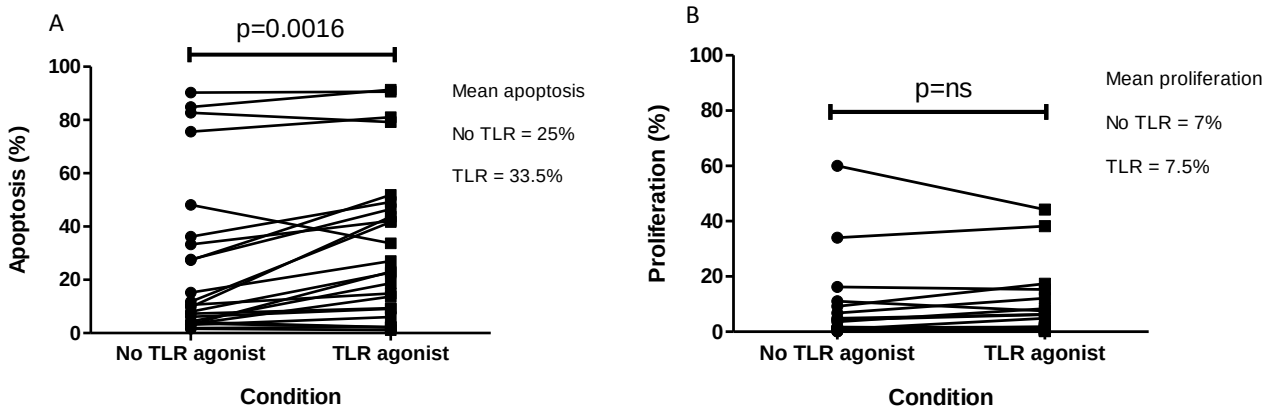

Figure 3.9 TLR9L increases rates of apoptosis in *ex vivo* cultured primary MCL cells but has no effect on proliferation Paired Wilcoxon signed rank test comparing mean rates of apoptosis (A) and proliferation (B) determined by annexin-V and Ki-67 positivity respectively (assessed by flow-cytometry). Samples were subject to stimulation with 3uM TLR-9-L at baseline and cultured on murine fibroblast monolayers in RPMI media for 8 days.

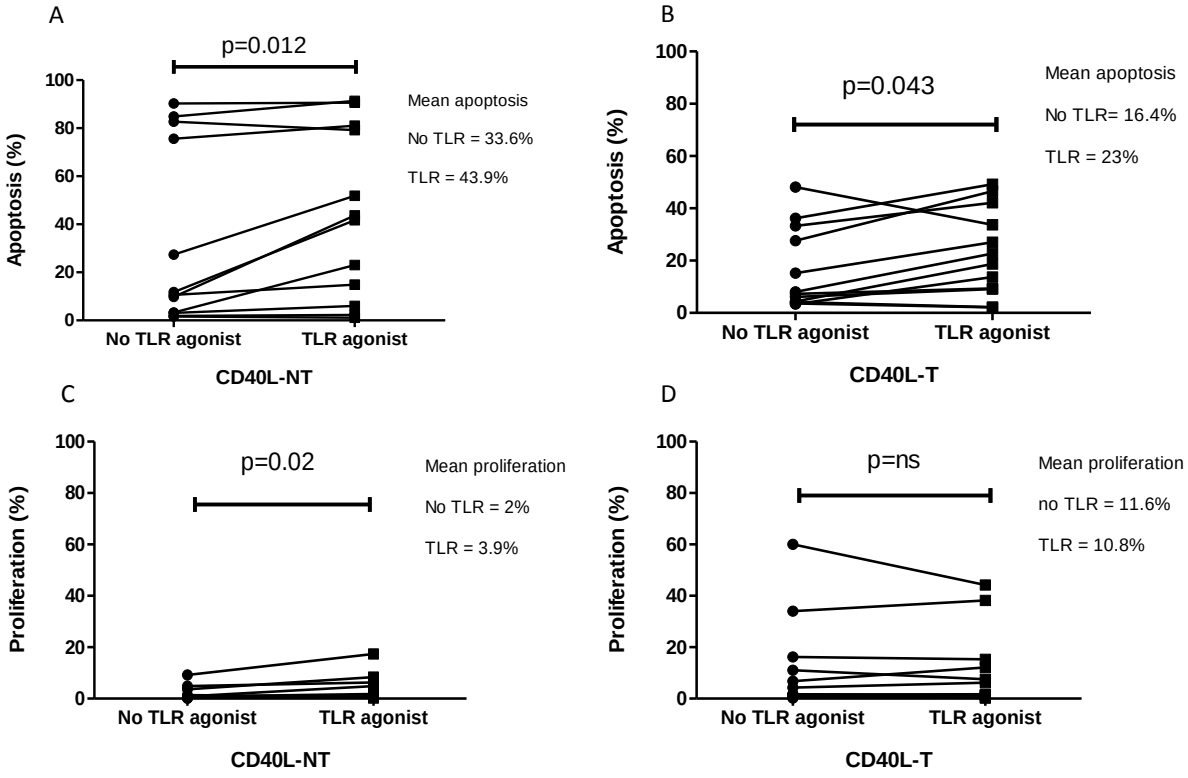

Figure 3.10 TLR9L significantly increases the rate of apoptosis in primary MCL cells with a greater effect on cells cultured in the absence of CD40-ligand. TLR9 stimulation appears to have no significant effect on proliferation. Paired Wilcoxon signed rank test comparing mean rates of apoptosis (A & B) and proliferation (C & D) determined by annexin-V and Ki-67 positivity respectively (assessed by flow-cytometry). Samples were subject to stimulation with 3μM TLR9-L at baseline and cultured on murine fibroblast monolayers in RPMI media for 8 days. A & C: CD40L-non-transfected stroma; B & D: CD40L-transfected stroma.

3.6 Subset Analysis of Survival and Proliferation of MCL Cells in *ex vivo* Culture According to the Clinical Phenotype of the MCL Subject

The variation observed in the clinical features of subjects with MCL is one of the disease's characteristic features. Most subjects have significant constitutional symptoms and / or rapidly progressing lymphadenopathy, requiring treatment at or soon after diagnosis, whereas a minority can display an indolent, slowly progressing phenotype justifying a prolonged period of watchful waiting before treatment.[94]

Although there is marked heterogeneity between cases, these subtypes of MCL can be broadly identified allowing a clinical and biological comparison. There is no universally accepted definition of these subtypes, but a useful definition of aggressive disease is that requiring treatment at or shortly after diagnosis; whereas indolent disease can be defined as present but causing no clinically significant problems to the patient and not requiring treatment for 2 years or more from diagnosis. The subject samples used in these experiments have been divided in this way, then analysed according to their survival and proliferation profiles *ex vivo*.

The mean apoptotic and proliferating fractions of the cultured PBMCs according to clinical phenotype in both the CD40L positive and negative stromal environment are displayed in Figures 3.11 and 3.12.

3.6.1 Rates of apoptosis are intrinsically higher in the proliferative subset and significantly reduced in the presence of CD40-Ligand. Apoptosis rates are low in the indolent MCL cases and unaffected by the presence of CD40-Ligand

More proliferative forms of MCL have a variable, but higher intrinsic rate of apoptosis than the indolent cases (mean percentage of apoptotic cells = 44% vs 4.6% respectively). In the presence of CD40L this is significantly reduced in the aggressive forms (21%, p=<0.001). Indolent cases have a relatively low rate of apoptosis (mean = 4.6%), which is unaffected by the presence of CD40L (mean =5.5%, p=n.s.) (Figure 3.11).

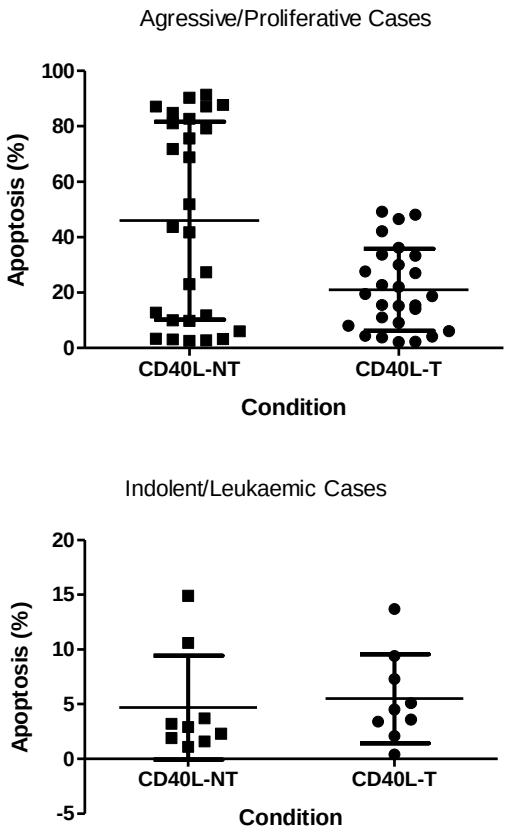

Figure 3.11 Comparison of effect of CD40-ligand on survival of primary MCL cells from clinically aggressive versus indolent disease cases. The MCL cells have been co-cultured on murine fibroblasts for 8 days prior to harvest and assay for Annexin V positivity by flow cytometry. Scatter dot plots showing percentage apoptotic cells in each environment with mean and standard deviation. A Wilcoxon t-test (paired signed rank) was used to derive p values. The fibroblasts were CD40-L non-transfected (CD40L-NT) or transfected (CD40L-T). More proliferative forms of MCL have a variable, but higher intrinsic rate of apoptosis than the indolent cases (mean = 44%). In the presence of CD40L this is significantly reduced (21%) $p<0.001$. Indolent cases have a relatively low rate of apoptosis (mean = 4.6%), this is unaffected by the presence of CD40L (mean =5.5%) (p=n.s.)

3.6.2 Rates of proliferation are significantly increased by CD40-L in MCL cells from both indolent and aggressive forms of MCL

With respect to proliferation, CD40-L significantly increases proliferation in both indolent and aggressive cases. The mean proliferation rates for indolent and aggressive cases without CD40L were 1.4% and 3% respectively, increased to 11% (p=0.009) and 10% (p=0.006) respectively in the presence of CD40L (Figure 3.12).

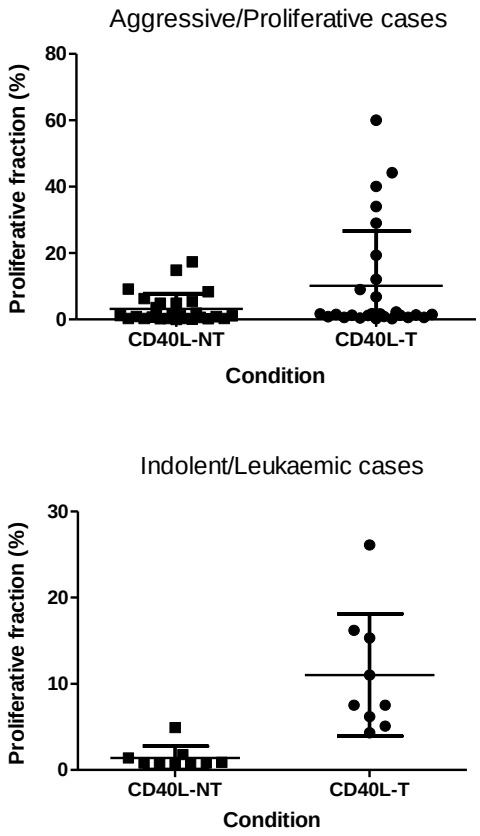

Figure 3.12 Comparison of effect of CD40L on proliferation of primary MCL cells from clinically aggressive versus indolent cases of MCL. MCL cells were co-cultured on murine fibroblasts for 8 days prior to harvest and assay for Ki-67 positivity by flow cytometry. The fibroblasts were CD40-L non-transfected (CD40L-NT) or transfected (CD40L-T). Scatter dot plots showing percentage Ki-67 positive cells in each environment with mean and standard deviation. A Wilcoxon t-test (paired signed rank) was used to derive p values. CD40L significantly increases proliferation in both indolent and aggressive cases. The mean proliferation rates for indolent and aggressive cases without CD40L were 1.4% and 3% respectively, increased to 11% (p=0.009) and 10% (p=0.006) respectively in the presence of CD40L.

3.7 Culture of Primary MCL PBMCs on Human versus Murine Stroma

From the data obtained hitherto, it appears that survival and proliferation of primary MCL PBMCs was enhanced when cells were cultured with CD40L-T murine stroma compared with CD40L-NT and no stromal support. The addition of the cytokine IL-4 also appeared to improve MCL cell survival during *ex vivo* culture. The next step was to assess the effect of human bone marrow stroma on survival and proliferation and to establish whether or not this is a superior system for the culture of MCL PBMCs *ex vivo*. In addition, an attempt was made to establish whether or not the addition of IL-4 exerts any effect on the human bone-marrow culture system.

Primary MCL PBMCs from subjects MCL02 and MCL07 were selected for culture based on previous data suggesting that MCL02 cells demonstrate increased proliferation reflecting a more aggressive clinical phenotype and MCL07 cells demonstrate low rates of apoptosis and proliferation reflecting a more indolent clinical phenotype. The effects of culture on human stroma were compared with culture on CD40L-T murine stroma with and without the addition of IL-4.

Confluent monolayers of human and CD40-L fibroblasts were grown in separate standard 24 well plates before being seeded with MCL cells and cultured for 4 days before being assessed for apoptosis and proliferation as previously described. Rates of apoptosis and proliferation after 4 days of co-culture with and without IL-4 stimulation at baseline are shown in Figure 3.13.

The rate of apoptosis observed after 4 days of culture did not differ between human and murine stromal co-culture (mean apoptosis 6.75% at baseline and 3.75% versus 2.65% in CD40L-T murine and human stromal culture respectively). No differences were observed with IL-4 stimulation.

The proliferation rates observed in the cells from the indolent subject (MCL07) were consistently low in all microenvironments (mean 4.3%). In the cells from the more proliferative case, (MCL02), the rate of proliferation after 4 days co-culture appeared higher in the human stromal culture in the presence of IL-4 (77.8%) compared with human stroma without IL-4 (55%) or CD40L-T murine stroma with or without IL-4 (51% and 50.6% respectively) (Figure 3.13). Due to the low number of samples, statistical comparison was not possible.

Thus from initial observations human stroma seems to be as effective as murine CD40L-T stroma at enhancing survival and promoting proliferation with some early results showing a greater proliferation with the combination of human stroma with IL4 Numbers however are small and need further analysis with a larger case set.

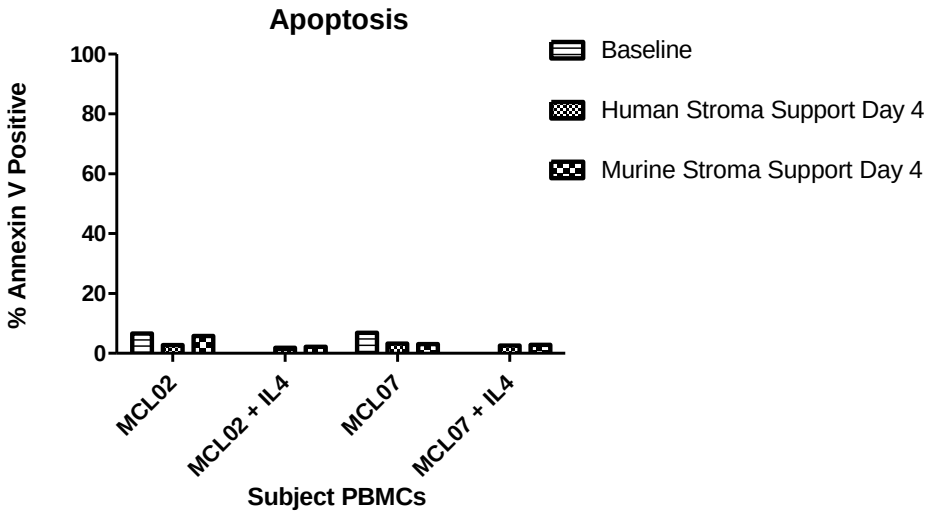

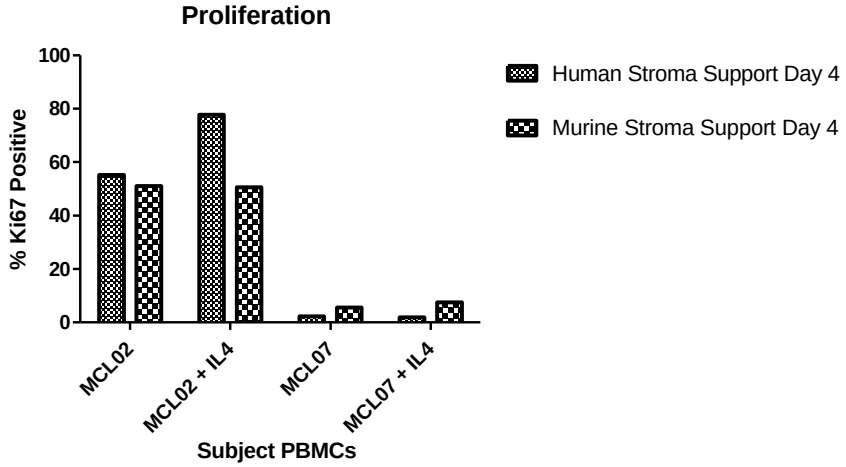

Figure 3.13 Human stroma increases proliferation rates of primary MCL cells in combination with IL-4 Stimulation. MCL cells from 2 subjects (MCL02, a clinically aggressive case and MCL07, a clinically indolent case) were cultured on human and CD40-T murine stroma for 4 days with and without interleukin 4 stimulation at baseline. Survival and proliferation was measured on CD5/19 labelled PBMCs using annexin-V and Ki-67 positivity by FACS.

3.8 The Morphological Effects of Culturing MCL Cells *Ex vivo* on Murine Stroma

In order to further characterise the microscopic features of primary MCL cells after 8 days co-culture with murine fibroblasts, cell suspension samples from four cases were removed and spun onto glass slides for fixation and staining with haematoxylin and eosin to examine cellular morphology.

3.8.1 Light Microscopy Reveals Clustering in some cases of Primary MCL cells after co-culture with murine fibroblasts

When clusters of cells containing 10 or more lymphoma cells in contact with each other were counted, a tendency towards cluster formation could be observed in the CD40-Ligand positive culture conditions. Light microscopy images of cells from subject MCL06 (aggressive MCL phenotype) which have been harvested after 8 days co-culture with murine stroma and spun onto glass slides before fixation and staining are displayed in Figure 3.14. Cell clustering can be observed in the cells from the CD40L-T environment.

The mean number of cell clusters of more than 10 cells per cluster observed in each culture environment is displayed in Figure 3.15. A Wilcoxon non-parametric t-test has been applied demonstrating the tendency towards cluster formation in the CD40-L positive environment that is not statistically significant (p=0.065). No significant pattern is observed with IL-4 or TLR9-L although the numbers of cases examined was small.

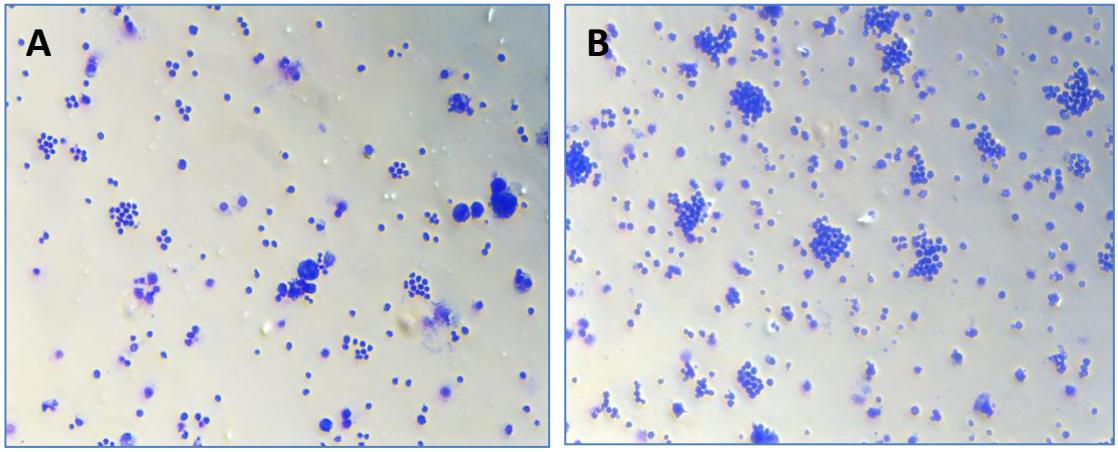

Figure 3.14 Primary MCL cells from subject MCL06 demonstrate a tendency towards cluster formation in the presence of CD40 ligand. Primary MCL PBMCs were co-cultured for 8 days with murine fibroblasts (CD40L-non-transfected (A) and CD40L-transfected (B)). Cells were harvested and spun onto glass slides before being fixed and stained with modified Wright's stain. Clusters of cells were defined as 10 cells in direct contact with each other determined by light microscopic examination (Mag 10x).

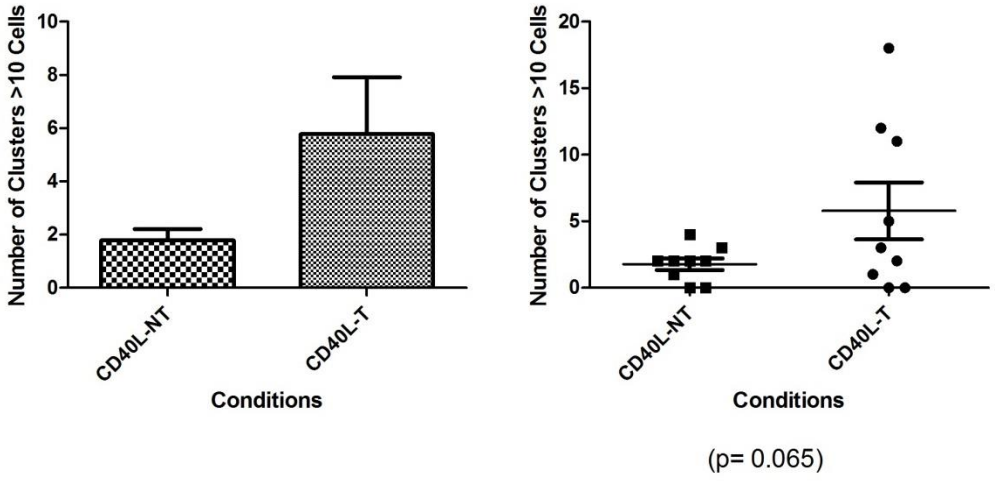

Figure 3.15 CD40L and cell cluster formation of primary MCL cells. Primary MCL PBMCs were co-cultured for 8 days with murine fibroblasts CD40L-NT or CD40L-T. Cells were harvested and spun onto glass slides then fixed and stained with modified Wrights stain. A cluster of cells were defined as 10 cells in direct contact with each other determined by light-microscopy (a Wilcoxon t-test was used to derive p value).

3.9 Discussion

The data obtained and presented has revealed several notable observations concerning the behaviour of primary MCL cells during *ex vivo* culture, and adds to the limited body of work in this area.

It is clear from work with primary cells that there is marked variation between primary MCL cells from different subjects in their ability to survive *ex vivo*. Marked genetic heterogeneity between MCL cases is well described in the literature, with an accumulation of mutations in addition to the hallmark t(11;14) translocation being observed. Secondary chromosome alterations targeting genes involved in cell cycle control, DNA damage responses and cell survival pathways are frequently observed in aggressive MCL cases which may be responsible for the marked variation observed between cases in these experiments.[5,7,93,95]

A clinical correlation is that cells from subject MCL08 which demonstrate high levels of apoptosis, were obtained at the point of relapsed disease, with rapid clinical progression despite the use of a BTK-inhibitor, compared to the relatively low levels of apoptosis observed in 3 other cases, 2 of which were from subjects with indolent disease and one which was previously untreated.

It is important to note that many patients with MCL do not demonstrate a peripheral lymphocytosis which means that this study has a particular selection bias for cases with a leukaemic presentation. Although this bias is unavoidable for this particular study it is important to bear in mind when considering these data in the general context of MCL.

Studies suggest a pro-survival and protective effect of stromal cells on malignant B-lymphocytes, probably due in part to stromal cell secretion of pro-survival cytokines

such as IL-6, IL-8 and vascular endothelial growth factor.[30,96,97] The survival and proliferative advantage conferred by activation of the CD40 synapse, normally provided by FT_H cells *in-vivo,* is well described in both normal and malignant B-cells[44,49,63,90,98]. Furthermore the *ex vivo* culture of CLL cells, a closely related lymphoproliferative disorder to MCL, show dependence on CD40L[92], although CLL cells can survive when cultured at high density suggesting a role in for CLL homotypic interactions.[99] Given this we analysed the effects of stroma and CD40L on the survival and proliferation of MCL cells.

Marked heterogeneity was observed, however cells co-cultured on a murine stromal layer transfected with CD40L had the best overall survival. Interestingly similar rates of apoptosis were observed in cells cultured in media alone or on a CD40L-NT stromal layer suggesting that accessory cell support in the absence of CD40L offers no significant survival advantage over the culture of cells in media alone (Figure 3.2). Survival though was only assessed for a short period given the concerns over viability and only a limited number of cases were analysed, but there is a suggestion that in some cases, culture in media alone is adequate for cell survival and would be similar to that observed in the *ex vivo* culture of CLL cells.

The analysis of a further 12 cases of MCL is a significant number of cases given the availability of MCL cases with peripheral lymphocytosis. This further analysis confirmed the significance of CD40L on enhancing survival and promoting proliferation. Indeed in the presence of CD40L survival and proliferation appear linked; cells which are actively proliferating have a low rate of apoptosis whereby cells which are not proliferating have a reduced survival. Thus strengthening the significance of CD40L in the *ex vivo* culture of MCL cells.

When the cases were analysed based on our clinical phenotypic description it was clear that the indolent cases, those which could be considered most like CLL, have very low apoptotic rates and show little benefit of the addition of CD40L. The proliferative /aggressive cases however have much higher intrinsic rates of apoptosis, not surprising maybe, but in these cases CD40L significantly reduces apoptosis. One possible explanation for the association between higher rates of apoptosis in the proliferative cases is the accumulation of additional mutations affecting cell survival in cells from subjects with particularly aggressive disease. Additional mutations affecting survival pathways are well described in association with blastoid MCL.[5,95]

For proliferation, indolent and proliferative/aggressive cases appear to respond similarly to the effect of CD40L, equally promoting proliferation, perhaps indicating a continued dependence on external signalling through the CD40 synapse for cell division in MCL.

In addition to the effect of CD40L, the presence of IL-4 appears to significantly enhance survival of primary MCL cells *ex vivo* and is consistent with other reports in the literature which suggest a protective effect of IL-4 on B lymphocytes, probably due to the activation of multiple intracellular pathways, including the upregulation of pro-survival BCL-2 protein transcription.[60,61] This is, however, an extrapolation from other B-cell lymphomas. However, no obvious associative effect could be demonstrated according to the presence of CD40L to either proliferation or survival. This is interesting as other studies have demonstrated an augmented effect of IL-4 and CD40L on proliferation in primary MCL cells.[49]

The effects of TLR9-L on the *ex vivo* culture of MCL cells demonstrated some interesting results. The presence of TLR9-L appeared to significantly impair survival of

primary MCL cells during *ex vivo* culture in both CD40-L positive and negative environments, with a greater effect observed in the CD40L-NT microenvironment, suggesting that CD40L can in some way protect the cells against TLR9 effects. With respect to proliferation of primary MCLs *ex vivo*, TLR9-L appears to significantly improve proliferation in the CD40L-negative environment (although the effect is small) and is an observation in contrast to other published studies of the effects of TLR-9-L which has been shown to have a synergistic effect with CD40L on proliferation.[52,55,56] However on pooled analysis no significant effect on proliferation could be demonstrated.

A comparison of human stroma to murine CD40L –T stroma was assessed as it was anticipated that human stroma might better support the *ex vivo* culture of MCL cells. Although preliminary and over a short culture period (due to technical difficulties) survival does not appear to be altered by culture with human stroma compared with CD40L positive murine stroma. However, in the cells from the more proliferative, clinically aggressive case, (MCL02), proliferation rates appear to be higher in the human-stroma cultured cells when IL-4 is added (Figure 3.13). Repeating this experiment with more primary MCL cases, assessing CD40L expression in the human stroma and culturing over a longer time period may help to establish if this is a significant pattern.

Given the results seen with CD40L microscopic examination was performed to determine whether any changes in morphology could be seen. Microscopic examination of MCL cells in *ex vivo* culture revealed a non-significant tendency towards cell clustering in the CD40L-T microenvironment. It is already established that cell to cell contact is a requirement for survival and proliferation in other related

haematological malignancies, such as CLL.[100] Therefore cell clustering could potentially be a microscopic indicator of increased survival and proliferation although further work is need with greater numbers to establish the significance of this observation in MCL.

Overall this chapter has shown that CD40L- T murine stromal cells are able to support the survival and proliferation of MCL cells *ex vivo* with a suggestion that cellular behaviour following CD40L is affected with cluster formation implying an additional role for adhesion. This 2D model of the microenvironment seems to have a greater support on aggressive proliferative cases. Not surprisingly there is marked heterogeneity between cases. The low proliferative nature of these cases was disappointing, surprising and requires further development but the tools and findings in this chapter suggest that these drugs may potentially be assessed in *ex vivo* culture models.

4. CHAPTER 4 –Cellular Adhesion Molecule Expression of MCL Cells

4.1 Introduction

Classical mantle cell lymphoma usually presents with generalised adenopathies, often there is also bone marrow and gastro-intestinal tract involvement.[4,101] A purely leukaemic presentation is relatively uncommon, but up to 52% of cases have a lymphocyte count ≥5 x 10^9/L and one case series of 48 patients circulating mantle cells were found in 92% when analysed by flow-cytometry, including 17% of cases with no morphological involvement detected.[102] Several studies have also identified a distinct subtype of MCL with leukaemic, non-nodal disease often associated with splenomegaly.[103,104] From a clinical perspective, it has been suggested that cases with a non-nodal phenotype characterised by leukaemic involvement and splenomegaly with minimal lymphadenopathies have a more indolent course.[10,103,104]

The pathobiology of the leukaemic subtype and the reasons for its more indolent clinical course remain unclear. Several studies have revealed distinct genetic and molecular patterns, but a single unifying pattern is yet to be identified. Lower rates of unmutated IgVH genes have been observed in some leukaemic case series, indicating experience of the germinal centre.[103,105,106] Other studies have shown leukaemic MCL cases to have a distinct genetic signature from nodal cases with patterns such as 8p21.3 deletion and gain of 8q24.1 at the MYC locus.[10] Others have demonstrated down modulation of genes involved in cell projection through actin cytoskeleton organisation and cell adhesion / tumour invasion molecule expression, suggesting that leukaemic MCL cells lack tumour invasion properties that might contribute to the absence of nodal involvement and to a less aggressive clinical course.[107] Other

investigators have identified a subset of patients with indolent disease and a low signature of *SOX11*, *HDGFRP3* and *DBN1* genes.[9]

Whatever the reason for differences in invasive MCL subtypes, it is logical that the persistence of disease and early relapses characteristic of nodal MCL indicate that neoplastic cells *in vivo* must be partly protected from the effect of immunochemotherapy by their tissue microenvironment. One of the reasons for this relative resistance to therapy could be the ability of MCL cells to enter and colonise extra-nodal sites, such as the bone marrow where the microenvironment has proven protective effects.[4] *In vitro* studies have demonstrated that adhesion to cultured stromal cell layers can protect malignant B cells from apoptosis induced by chemotherapy. Equally, blockade of the BCR, which down-regulates expression of receptors such as CD184 (CXCR4), which promotes entry of MCL cells to bone marrow and nodal stromal cells, has been shown to reverses these protective effects.[28,30,67]

In vivo, evidence of a role of cellular adhesion in MCL comes from observations of the effects of BCR blockade within clinical trials. Peripheral blood lymphocytosis is a characteristic feature of therapy with the BTK-inhibitor ibrutinib, which blocks the BCR receptor pathway downstream of the surface receptor. Patients receiving ibrutinib experience a transient increase in peripheral absolute lymphocyte counts which, in the phase II study of ibrutinib for relapsed MCL, peaked at a median of 4 weeks of treatment and gradually decreases over subsequent months.[64] This was associated with a reduction in the expression of the chemokine receptor molecule, CD184, and a fall in the plasma chemokines, CCL22, CCL4 and CXCL14.[65]

This rise in lymphocytes in the blood appears to be particularly marked in patients with disease involving the bone marrow, particularly those with ≥30% marrow involvement.[66]

Therefore it is hypothesised that expression of CAMs and chemokine receptors, such as CD184, play an important role in protecting MCL cells from therapy by maintaining malignant cells within the relative sanctuary of sites such as the bone marrow, leading to residual disease and early relapse after treatment. Therefore mobilisation of MCL cells away from sites of protection from chemotherapy or immune-surveillance could represent a therapeutic target.

However, the expression of CAMs by primary MCL cells is not well characterised in the literature, particularly in relation to the effect of stromal-cell co-culture and the effects of drugs. This chapter aims to characterise the surface adhesion molecules profile of a series of primary MCL cases both on MCL cells from the peripheral blood and bone marrow with the aim of identifying any common adhesion receptors or patterns of receptor expression which may be candidates for future study.

A more detailed review of the CAMs involved in B-NHL is given in the introductory chapter (1.3). Briefly, CAMs are groups of ligands and receptors involved particularly in cell homing and migration. Their expression on the cell surface is dynamic and dependent on external signals such as cytokine release. This process of dynamic expression allows the cells of the normal immune system to circulate freely as non-adherent cells in the blood and lymph, patrolling the body for infectious organisms and congregate as adherent cells in lymphoid organs as well as crossing endothelial and basement membrane barriers to aggregate at sites of infection. A brief overview of

the CAMs considered important in B-NHL and analysed in primary MCL cells in this chapter is displayed in Table 4-1.

Adhesion Molecule	Description	Ligand
CD11a	An integrin alpha L chain which combines with the beta 2 chain (CD18) to form the integrin lymphocyte function associated antigen, LFA-1. Expressed on all leukocytes. Involved in leukocyte extravasation, antigen presentation and T-lymphocyte alloantigen-induced proliferation.[75] Reportedly expressed on MCL and marginal zone NHL cells (MZL) more than CLL and thought to facilitate lymph node adhesion to FDCs via ICAM1-3.[76]	ICAM 1(CD54) ICAM2(CD102) ICAM3 (CD50)
CD11c	CD11c combines with integrin beta 2 subunit (CD18) to form Mac-1, expressed mainly on myeloid lineage cells and involved in phagocytosis of infectious agents; transendothelial migration of phagocytes and activation of neutrophils and monocytes. High rates of splenic involvement in CLL patients are associated with strong CD11c expression. Also over expressed in hairy cell leukaemia (HCL) and splenic marginal zone lymphoma, but conflicting results in the literature with predominantly low level expression in MCL, even splenic MCL.[82]	ICAM1 Fibrinogen Factor X iC3b denatured proteins
CD49d	The integrin alpha-4 subunit (CD49d) combines with B1 subunit (CD29) to form VLA-4. VLA-4 (CD49d/CD29) is expressed on resting lymphocytes and monocytes and functions as both a matrix and cell receptor. As a matrix receptor it binds to fibronectin at a different site than that recognised by VLA-5 (CD49e). As a cell receptor, it binds to VCAM-1, a member of the immunoglobulin superfamily. VCAM-1 is induced by inflammatory mediators on endothelium. CD49d is reportedly expressed on MCL and MZL cells more than CLL and thought to facilitate lymph node adhesion to FDCs via VCAM-1.[76]	Fibronectin VCAM-1
CD49e (VLA-5)	A fibronectin receptor, integrin alpha-5 combines with beta 1 to form CD49e which binds the extracellular matrix protein fibronectin.	Fibronectin
CD54 (ICAM-1)	A member of the immunoglobulin superfamily, normally with a lower expression in peripheral blood compared with lymph node mononuclear cells. Lower expression has been demonstrated to correlate with leukaemic / disseminated disease, bone marrow and extranodal involvement in some papers.[77–79]	CD11a
CD58 (LFA-3)	A member of the immunoglobulin superfamily expressed on antigen presenting cells (APCs), particularly macrophages, which binds to LFA-2 on T cells and reinforces adhesion between T cells and APCs.[80] It is expressed on haematopoietic and non-haematopoietic cells and overexpressed in acute lymphoblastic leukaemia.[81]	LFA-2
CD62L (L-selectin)	A single chain transmembrane protein found in granulocytes, monocytes and most lymphocytes. Low affinity binding facilitates the capture, rolling and slow-rolling steps of leukocyte recruitment to the region of inflammation which in turn is followed by firm adhesion and transmigration. Low expression has been demonstrated in MCL, CLL and MZL.[76]	Blood vessel endothelium
CD183 (CXCR3)	A G-protein-coupled transmembrane receptor expressed primarily on activated T lymphocytes and Natural Killer (NK) cells, preferentially on Th1 T-cells. It binds to CXCL-9, -10 and -11 through which it is able to elicit influx of intracellular calcium and activate phosphoinositide 3-kinase as well as mitogen-activated protein kinase (MAPK). CXC ligands are IFN-induced and produced locally in the tissues.	CXCL9, 10 and 11
CD184 (CXCR4)	High level expression of CD184 has been demonstrated on primary MCLs. It is down-regulated by BTK-inhibition.[65] Stromal cells in secondary lymphoid tissues constitutively express its corresponding chemokine CXCL12, providing guidance for B cell positioning within distinct nodal compartments. CXCL12 has been demonstrated to induce actin polymerisation in MCL cells and induce a chemotactic response which can be inhibited by blocking the receptor CD184, indicating an important role in migration and localisation.[33]	CXCL12
CD185 (CXCR5)	A G-protein-coupled transmembrane receptor. High level expression has been demonstrated on primary MCLs together with CD184 and VLA-4 whereas expression of CD183 and CD62L is largely negative in some reports.[28] It is thought to be used by MCL cells to disseminate by interaction, trafficking and homing to secondary lymphoid tissues via ligands CXCL12 and CXCL13. The MCL cell line, Granta 519, displays low levels of CD184 and is negative for CD185 (possibly due to Epstein Barr virus-infection causing down-regulation). Ligands for CD184, 5 and VLA-4 may trigger the pseudoemperipolesis phenomenon.[33]	CXCL12, 13

Table 4-1. A summary of the adhesion molecules and their respective ligands which have been proven to be expressed in MCL and other B-NHL subtypes and which will be characterised in this chapter.[76,78,82]

Summary of Experimental Methods

A clinical and biological summary of the MCL subjects is included in Table 4-2.

4.2 Fluorescence associated cell sorting (FACS) was used to profile the expression of a series of CAMs on a panel of cases of primary MCL. Peripheral blood mononuclear cells or marrow mononuclear cells were harvested from consenting subjects with MCL and ficoll-separated from blood and plasma as previously described (Methods 2.7). A panel of ten cellular adhesion molecules were chosen to study in these subjects (see Table 4-3) These molecules were chosen based on previously published data on the relevant surface adhesion molecules in B-NHL and more specifically, previously published profiles of primary MCL surface adhesion molecules.[33,74,108–111]

For each case, mononuclear cells were resuspended in warmed, complete RPMI medium and the cell density was adjusted to $1x10^6$/100µL in accordance with the recommendations of the manufacturers of the monoclonal antibodies used for flow cytometry. Ten microlitres of FITC- or APC-conjugated mouse anti-human CD5 and CD19 mononuclear antibody were added to 12 labelled, 1.5mL Eppendorf tubes. To the first 10 tubes, 10µL of PE-conjugated, mouse anti-human monoclonal antibody specific to individual cellular adhesion molecules was added. To two tubes, 10µL of appropriate isotype control antibodies were added and one tube was labelled as an unstained control with no antibodies. A list of the monoclonal antibodies used is shown in Table 4-3. To each labelled tube, 100µL of cell suspension was added and the tubes were gently vortexed to mix before being incubated at room temperature in the dark for 20 minutes. Three hundred microlitres of staining buffer (0.5% BSA in PBS) was added to each tube before analysis by FACS.

Within the chapter the expression of CAMs was analysed after co-culture with CD40L-T or CD40L-NT murine stromal cells. In these experiments MCL PBMCs were suspended in complete RPMI medium and seeded at a density of $5x10^6$ cells per mL on confluent monolayers of CD40L -T and CD40L-NT murine stromal cells (pre-irradiated with 15Gy) and incubated (5% CO_2, 37^oC) for 6 days. 100µL samples were removed at baseline, 24 hours, 3 days and 6 days, incubated with PE-conjugated mouse-anti-human monoclonal antibodies against the target CAMs or corresponding isotype control before analysis by flow cytometry.

The expression level of CAM or other molecules was assessed on primary MCL cells following treatment with the BTK inhibitor ibrutinib when co-cultured on human bone marrow stroma. For these experiments human stromal cells derived under ethical permission from aspirated bone marrow sample, excess to clinical need were ficoll-separated from blood and plasma and cultured in $25cm^2$ vented flasks in modified IMDM long-term culture medium until reaching confluence as described in the materials and methods chapter (2.7.3). The monolayer was then loosened by trypsinisation, washed and resuspended in modified IMDM before seeding wells of a standard 24 well plate. Once confluence had been achieved, the wells were washed and seeded with primary MCL cells in complete RPMI medium and seeded at a density of $5x10^6$ cells per mL before being returned to the incubator. After 24 hours culture, cells were treated with 100nm ibrutinib (*Selleckchem*, Houston, Texas, USA), control wells were treated with the same volume of DMSO vehicle control. The MCL cell suspension was sampled at baseline, 24 and 56 hours, co-labelled for CD5 / 19 and the target CAM antibody (or respective isotype control) and assayed for fluorescence by flow cytometry.

4.2.1 Deriving the Fluorescent Intensity Ratios

An Accuri C6 flow cytometer and Accuri CFlow Plus software (*BD Biosciences*) was used for analysis. Wherever possible, 10,000 events were collected per tube to obtain the median fluorescence intensity (FI) value for each CAM of the population of CD5/CD19 positive mononuclear cells (MCL cells) within the lymphocyte gate as defined by the forward / side scatter plot. The median FI value was used instead of the mean because the distribution of peaks for the fluorescence intensity were not always evenly distributed, thus skewing the mean value. The median was therefore deemed to be a more reliable estimate of fluorescent intensity. In accordance with other published data on CAMs in MCL, the median fluorescence intensity ratio (MFIR) was calculated by dividing the mean fluorescence intensity of the analysed marker by the median fluorescence intensity of the respective isotype control (in arbitrary units).[33]

Case	Age, gender	Molecular data	Immuno-phenotype	Clinical phenotype	Prior Treatment	Indolent / aggressive disease
MCL04	**65 f**	**(t11;14)+**	**CD19+**	**Leukaemic, MCL; WCC 280x109/L**	**None**	**Indolent**
MCL07	**65 m**	**t(11;14)+ cyclin D1+**	**CD19+**	**Leukaemic MCL; WCC 30x109/L**	**None**	**Indolent**
MCL13	**64 m**	**cyclin D1; t(11;14)**	**CD5/19+**	**Leukaemic; WCC 152x109/L**	**None**	**Indolent**
MCL14	**62 m**	**cyclin D1; t(11;14)**	**CD5/19+**	**Leukaemic; Stage II**	**Local radiotherapy to eye**	**Indolent**
MCL01	**66 f**	**t(11;14)+**	**CD5/19+**	**Stage IV, nodal; WCC 300x109/L**	**None**	**Aggressive**
MCL02	**68 m**	**(t11;14)+ cyclin D1**	**CD5/19+**	**Stage IV, nodal; WCC 234x109/L**	**Immunochemotherapy and BTK-inhibitor**	**Aggressive**
MCL03	**74 m**	**cyclin D1**	**CD5/19+**	**Stage IV WCC $30x10^9$/L**	**None**	**Aggressive**
MCL11	**60 f**	**cyclin D1+**	**CD5/19+**	**Stage IV, nodal**	**Immunochemotherapy**	**Aggressive**
MCL15	**70 f**	**cyclin D1; t(11;14)**	**CD5/19+**	**Stage III, nodal**	**None**	**Aggressive**
MCL16	**70 f**	**cyclin D1; t(11;14)**	**CD5/19+**	**Stage IV, nodal**	**None**	**Aggressive**
MCL17	**74 m**	**cyclin D1; t(11;14)**	**CD5/19+**	**Stage IV, nodal**	**Immunochemotherapy**	**Aggressive**
MCL18	**91 m**	**cyclin D1; t(11;14)**	**CD5/19+**	**Stage IV, nodal**	**Immunochemotherapy**	**Aggressive**
MCL19	**71 m**	**cyclin D1; t(11;14)**	**CD5/19+**	**stage IV, nodal**	**Immunochemotherapy**	**Aggressive**

MCL20	**63 m**	**cyclin D1; t(11;14)**	**CD5/19+**	**stage III, nodal**	**Immunochemotherapy**	**Aggressive**
MCL21	**70 m**	**cyclin D1; t(11;14)**	**CD5/19+**	**stage III, nodal**	**Immunochemotherapy**	**Aggressive**
MCL22	**60 m**	**cyclin D1; t(11;14)**	**CD5/19+**	**stage IV, nodal**	**Multiple lines including BTK-inhibitor**	**Aggressive**
MCL23	**60 m**	**cyclin D1; t(11;14)**	**CD5/19+**	**stage IV, nodal**	**Allogeneic Stem cell transplant**	**Aggressive**
MCL24	**77 f**	**cyclin D1; t(11;14)**	**CD5/19+**	**stage III, nodal**	**None**	**Aggressive**
MCL10	**54 m**	**cyclin D1; t(11;14)**	**CD5/19+**	**stage IV; nodal**	**Immunochemotherapy**	**Aggressive**

Table 4-2 Primary MCL Subjects' Clinical and Biological Characteristics. MCL subject demographics, diagnostic molecular data, immunophenotyping of PBMCs and clinical disease summary of cases of MCL from which PBMCs and / or bone marrow MCL cells were obtained for use in adhesion profile experiments.

Description	Cat. No.	Source	Fluoro-chrome	µL / test
CD19 mouse anti-human IgG1k	555412	BD Biosciences	FITC	10
CD5 mouse anti-human IgG1k	555355	BD Biosciences	APC	10
CD3 mouse anti-human IgG2ak	555342	BD Biosciences	APC	10
CD11c mouse anti-human IgG1k	555392	BD Biosciences	PE	10
CD62L (L-selectin) mouse anti-human IgG1k	555544	BD Biosciences	PE	10
CD49d (Integrin α4 chain) mouse anti-human IgG1k	555503	BD Biosciences	PE	10
CD49e (Integrin α5 chain) mouse anti-human IgG1k	555617	BD Biosciences	PE	10
CD11a (LFA 1α; ITGAL) mouse anti-human IgG1k	555384	BD Biosciences	PE	10
CD58 (LFA-3) mouse anti-human IgG2ak	555921	BD Biosciences	PE	10
CD54 (ICAM-1) mouse anti-human IgG1k	555511	BD Biosciences	PE	10
CD183 (CXCR3) mouse anti-human IgG1k	557185	BD Biosciences	PE	10
CD184 (CXCR4) mouse anti-human IgG2ak	555974	BD Biosciences	PE	10
CD185 (CXCR5) mouse anti-human IgG2b	FAB190P-100	R & D Systems	PE	10
Mouse anti-human IgG1k isotype control	556026	BD Biosciences	FITC	10
Mouse anti-human IgG1k isotype control	559320	BD Biosciences	PE	10
Mouse anti-human IgG1k isotype control	555751	BD Biosciences	APC	10
Mouse anti-human IgG2aκ isotype Control	555574	BD Biosciences	PE	10

Table 4-3 Fluorescein-conjugated human monoclonal antibodies employed in labelling and adhesion experiments including isotype controls. FITC - fluorescein isothiocyanate; PE - phycoerythrin; APC –allophycocyanin

4.3

Baseline expression of cellular adhesion molecules on MCL cells

The expression profile of a panel of 10 cellular adhesion molecules was assessed on the neoplastic lymphocytes taken from peripheral blood of 17 MCL cases (Table 4-4). A further assessment of adhesion molecule expression of the neoplastic lymphocytes taken from bone marrow was performed in 4 MCL cases (Table 4-5), in three cases

peripheral blood, marrow samples were matched. Patient MCL10 had no peripheral lymphocytosis at the time of marrow sampling and is therefore unmatched.

These data show the wide variation in adhesion molecule expression between cases. The mean values of the pooled median fluorescence intensity ratios for both peripheral blood and bone marrow primary MCL cells are shown in Figure 4-1. The highest expressions of CAMs are CD11a, CD49d and CD54 with low level expression observed in the rest of the panel. Comparison of the CAM expression on the bone marrow neoplastic lymphocytes shows a greater expression of integrin molecules, particularly CD11a and not surprisingly CD54 and CD183 (CXCR3). Comparison of the overall expression of adhesion molecules (mean expression for each molecule in all cases) between peripheral blood MCL cells and bone marrow cells showed a significant difference (Wilcoxon matched-pairs signed rank test p=0.0098) (Figure 4-2). However as the number of paired samples were only 3, so the comparison of each individual adhesion molecule between blood and marrow was deemed unsuitable for statistical comparison.

Further analysis of the adhesion molecule expression depending on the clinical and biological features of the cases was assessed and divided into leukaemic (indolent) or nodal (aggressive) disease. The nodal cases are denoted in Table 4-4 shaded red, and the leukaemic cases shaded green for ease of interpretation. The mean values of the pooled median fluorescence intensity ratios are shown in Figure 4-3. Cells from subjects with nodal disease appear to demonstrate a higher expression of CD11a compared with cells from leukaemic MCL cases and when the mean median fluorescence intensity ratio for each adhesion molecules was compared for leukaemic or nodal cases (Figure 4-4) there was a significant difference in the expression profiles

(Wilcoxon matched-pairs signed rank test p=0.002). However, when nodal and leukaemic MCL fluorescence intensity was compared for each adhesion molecule using a Mann Whitney test, no significant difference was observed (Table 4-6); this may reflect the low number of leukaemic cases.

Subject	CD11a	CD11c	CD49d	CD49e	CD54	CD58	CD62L	CD183	CD184	CD185
MCL01	3.7	2.6	11.7	2.7	5.4	0.8	1.9	4.4	2.4	3.3
MCL02	5.4	3.0	6.4	2.9	9.0	0.9	1.9	5.2	4.2	14.4
MCL24	39.2	3.6	23.3	4.4	6.6	2.2	4.9	25.2	1.1	2.6
MCL17	225.0	12.8	40.9	58.0	23.5	31.3	8.9	32.7	5.7	0.2
MCL15	22.4	4.0	21.1	3.9	8.0	3.1	6.7	6.4	3.3	10.7
MCL16	16.7	3.7	15.5	3.7	13.2	1.7	3.2	6.4	11.0	6.4
MCL18	3.4	2.4	6.2	2.2	11.5	2.2	2.1	4.3	2.4	10.3
MCL19	152.4	2.6	19.6	5.6	5.3	6.3	1.5	4.2	0.5	1.0
MCL20	14.8	3.5	17.0	3.6	24.5	2.3	14.8	4.9	3.0	9.2
MCL11	10.0	3.7	10.5	4.4	17.3	2.0	3.5	7.2	4.4	10.4
MCL21	11.4	2.6	11.0	3.3	13.4	1.3	1.2	6.3	1.6	2.2
MCL22	131.0	3.1	17.3	3.0	15.4	2.5	14.1	7.9	0.4	1.1
MCL23	5.0	3.5	12.8	3.8	7.1	1.5	2.1	5.1	7.5	3.5
MCL13	4.1	2.8	8.1	2.9	6.4	1.2	2.3	5.1	6.1	3.4
MCL14	58.2	3.2	14.2	4.5	6.3	1.8	5.0	4.8	0.9	1.1
MCL07	20.4	3.6	19.3	4.2	6.7	2.9	3.5	6.4	1.9	6.0
MCL04	6.7	3.8	5.8	3.7	6.3	1.4	2.1	5.0	1.4	4.1
Mean	42.9	3.8	15.3	6.9	10.9	3.8	4.7	8.3	3.4	5.3

Table 4-4 The median fluorescence intensity ratios (analysed marker/isotype control) for 10 adhesion molecules of peripheral blood MCL cells from 17 subjects. Nodal cases shaded red, Leukaemic (indolent) cases are shaded green. (Units are arbitrary).

Subject	CD11a	CD11c	CD49d	CD49e	CD54	CD58	CD62L	CD183	CD184	CD185
MCL10	3.9	2.2	2.7	2.5	8.0	1.1	7.0	1.4	2.0	1.2
MCL17	310.8	14.7	67.6	60.0	34.8	29.2	13.0	25.4	6.4	0.6
MCL21	20.4	1.2	15.0	27.9	7.2	3.0	1.4	24.6	1.1	7.2
MCL18	3.7	2.7	6.8	2.9	11.0	2.4	2.1	4.3	2.0	9.5
Mean	84.7	5.2	23.0	23.3	15.3	8.9	5.9	13.9	2.9	4.6

Table 4-5 The median fluorescence intensity ratios (analysed marker/isotype control) for 10 adhesion molecules of bone marrow MCL cells from 4 subjects. All are nodal (aggressive) cases (shaded red). (Units are arbitrary).

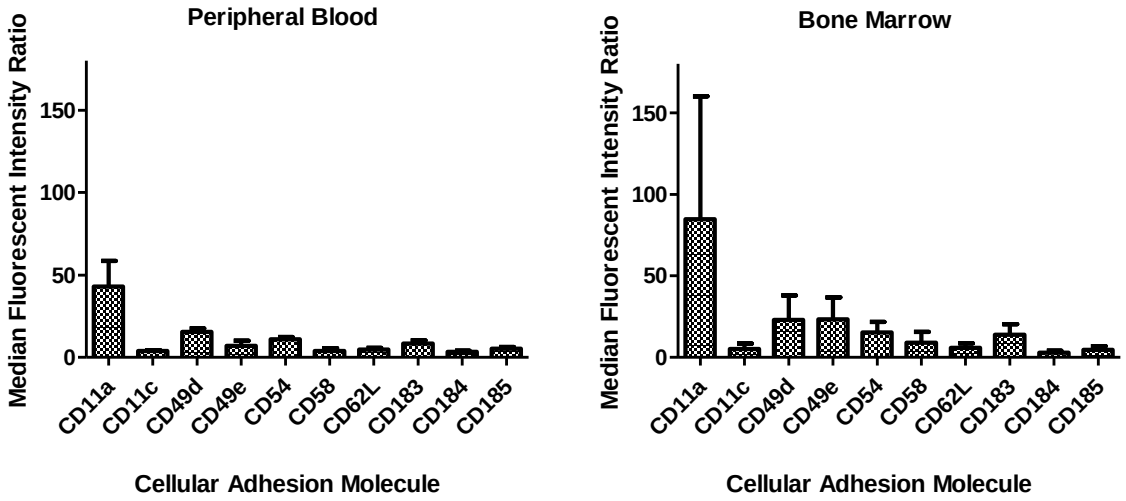

Figure 4.1. Comparison of adhesion marker expression on MCL lymphocytes taken from blood and bone marrow. The mean (bars indicate standard error of the mean) of the pooled median fluorescence intensity ratios for each analysed cellular adhesion molecular marker is displayed for 17 cases of primary MCL peripheral blood mononulear cells (left) and 4 cases of bone marrow MCL cells ().

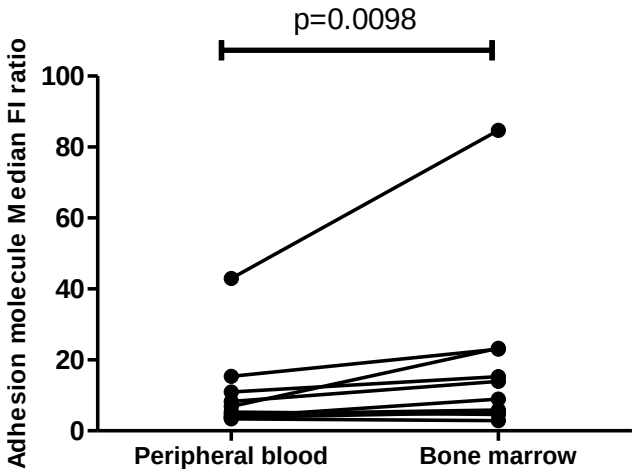

Figure 4.2 Comparison of adhesion molecule profile on MCL cells from peripheral blood vs bone marrow. The mean median FI ratio for all adhesion molecules for either neoplastic cells in peripheral blood or bone marrow are compared using a Wilcoxon matched-pairs signed rank test and shows significance (p=0.0098).

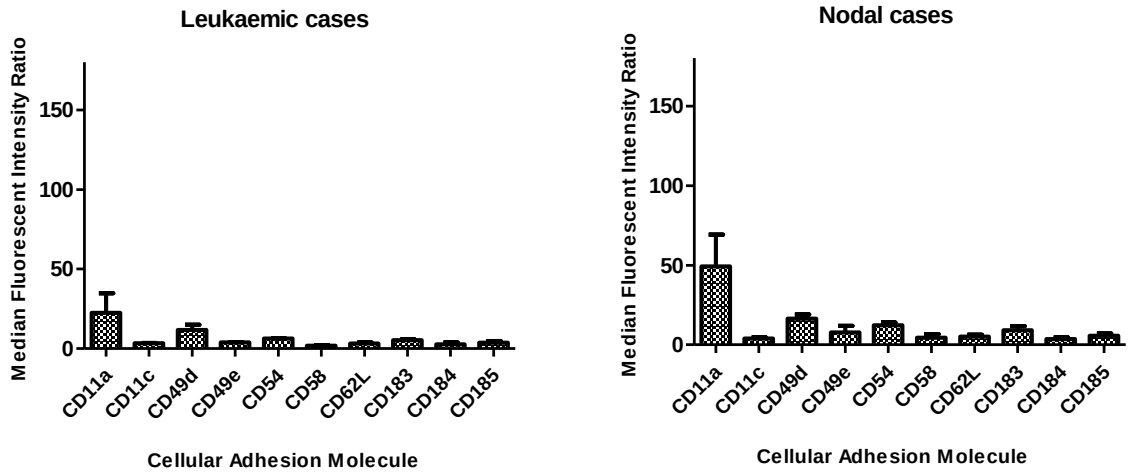

Figure 4.3 Assessment of adhesion marker expression on peripheral blood MCL lymphocytes based on clinical phenotype. The mean (with SEM) of the pooled median fluorescence intensity ratios for each analysed cellular adhesion molecular marker is displayed for 17 cases of primary MCL peripheral blood mononuclear cells subdivided according to leukaemic (left) or nodal (right) clinical phenotype.

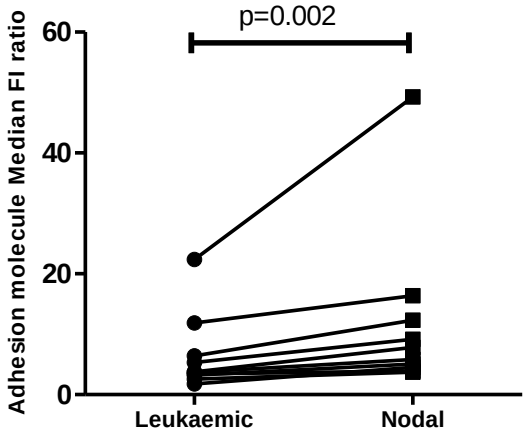

Figure 4.4 Comparison of adhesion molecule profile on leukaemic vs nodal cases of MCL. The mean median FI ratios for all adhesion molecules considered together from either leukaemic or nodal cases. All were higher on nodal cases with a significant difference (Wilcoxon matched-pairs signed rank test).

Nodal vs Leukaemic cases										
Column A	CD11a (N)	CD11c (N)	CD49d (N)	CD49e (N)	CD54 (N)	CD58 (N)	CD62L (N)	CD183 (N)	CD184 (N)	CD185 (N)
vs	vs	vs	vs	vs	vs	vs	vs	vs	vs	vs
Column B	CD11a (L)	CD11c (L)	CD49d (L)	CD49e (L)	CD54 (L)	CD58 (L)	CD62L (L)	CD183 (L)	CD184 (L)	CD185 (L)
Mann Whitney test										
P value	0.8651	0.6919	0.3358	0.7771	0.0617	0.5335	0.9549	0.6104	0.5335	0.6919
Exact or approximate P value?	**Gaussian Approximation**									
P value summary	ns	ns	ns	ns	ns	ns	ns	ns	ns	ns
Are medians signif. different? (P < 0.05)	No	No	No	No	No	No	No	No	No	No
One- or two-tailed P value?	**Two-tailed**									
Sum of ranks in column A,B	119 , 34	113 , 40	126 , 27	114 , 39	134 , 19	123 , 30	116 , 37	122 , 31	123 , 30	121 , 32
Mann-Whitney U	24	22	17	23	9	20	25	21	20	22

Table 4-6 Comparison of expression of cellular adhesion molecules between nodal and leukaemic cases of MCL: No significant differences between expressions of individual adhesion molecules were observed between the two groups (Two-tailed Mann Whitney test).

4.4 The expression of surface adhesion molecules after co-culture of with stromal cells

Having obtained a profile of the baseline expression of CAMs in primary MCL cells, it was considered important to explore the effect of the MCL microenvironment on surface adhesion molecule expression. Therefore an experiment was designed in which MCL PBMCs from 4 subjects (3 subjects with a nodal and aggressive clinical phenotype (MCL03, MCL08 and MCL23) and 1 subject with a leukaemic and indolent clinical phenotype (MCL04) were co-cultured with murine stromal cells for 6 days with surface adhesion molecular profiling at set points within the time period. Both CD40L-transfected and –non-transfected stromal cells were used to compare the effect of CD40L.

When analysed over time, the only cellular adhesion molecules that changed were CD184 which showed a pattern of rising expression with CD40L-T and NT stroma during culture, but more significantly on CD40L-NT; and CD54 which increased in expression over 3 days in the MCL cases co-cultures on CD40L-T stroma (Figure 4-5). When adhesion molecule expression of cases was compared between CD40L-T and CD40L-NT stroma both CD184 and CD54 show significance (Figure 4-6). The mean expression of CD184 when analysed over all time points is significantly lower in the presence of CD40L (paired Wilcoxon signed rank sum p=0.0137) and CD54 significantly higher (paired Wilcoxon signed rank sum p=0.0005).

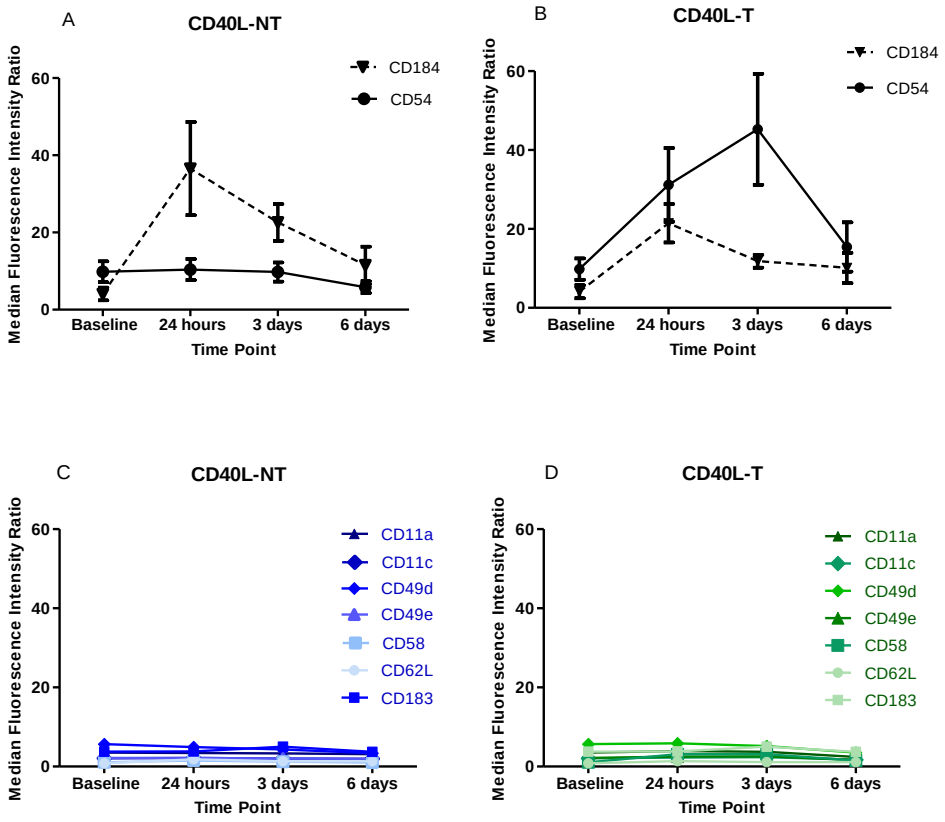

Figure 4.5 Patterns of expression of cellular adhesion molecules co-cultured on CD40L-T and CD40L-NT stroma. CD184 expression was upregulated after 24 hours by co-culture with stromal cells showing reducing expression over prolonged culture (A and B). CD54 upregulation requires the presence of CD40-L (B). All other adhesion markers show no change in expression levels over time when cultured on either CD40L-NT (C) or CD40L-T (D) stroma. Primary MCL peripheral blood mononuclear cells co-cultured on CD40-L-NT (A,C) and CD40L-T (B,D) stroma for 6 days. Cultures were sampled and analysed for expression of CAMs at baseline, 24 hours, 3 days and 6 days. The mean (with SEM) of the pooled median fluorescence intensity ratios from 4 patients for each analysed cellular adhesion molecular marker is displayed.

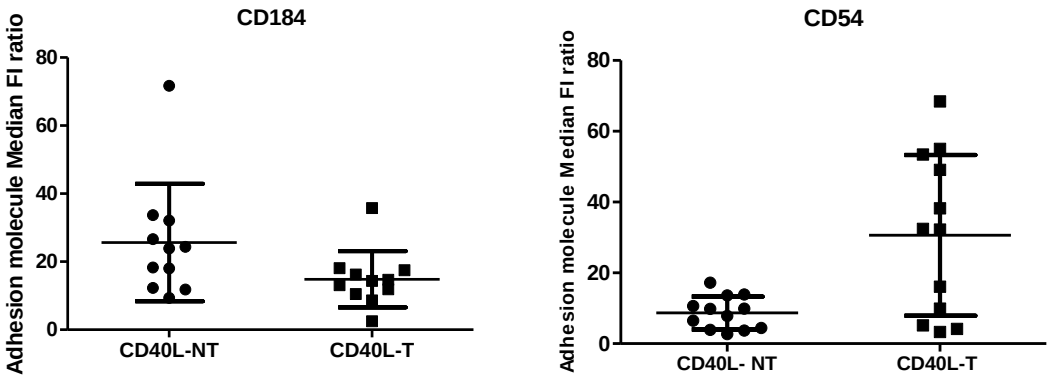

Figure 4.6 Comparison of adhesion molecule expression in the presence of CD40L. Expression of both CD184 (CXCR4) and CD54 differ significantly in the presence of CD40L. CD184 MFIR (pooled mean from 4 patients) is significantly lower at all time points in the presence of CD40L (paired Wilcoxon signed rank sum p=0.0137) and CD54 significantly higher (paired Wilcoxon signed rank sum p=0.0005).

4.5 The effect of BTK-inhibition on cellular adhesion molecules

Ibrutinib is an orally active small molecule which binds irreversibly to the cysteine residue (C481) at the activating phosphorylation site of Bruton's tyrosine kinase (BTK), leading to irreversible inactivation and disruption of the signalling pathway from the BCR to the nucleus.[112,113] The BCR pathway plays a crucial role in cell division, differentiation, homing and survival and is constitutively activated in MCL cells.[114,115] Inhibiting cell signaling via the BCR not only impairs proliferation and attenuates cell survival, but also impairs the ability of MCL cells to home to and remain in their normal protective niche in lymphoid tissue or bone-marrow.[66]

As the pattern of adhesion molecule expression had not previously been studied in detail in MCL we undertook a comparison of adhesion molecule expression on neoplastic lymphocytes from a nodal and leukaemia MCL case when co-cultured on human stroma and following *in-vitro* treatment with ibrutinib. In this part of the study, primary MCL cells from subject MCL15 (leukaemic) and MCL02 (nodal) were cultured on human stromal cells and treated after 24 hours with 100nm ibrutinib. The adhesion molecule profile of the MCL cells was assessed by flow cytometry, as before, at baseline, 24 hours and 56 hours with and without treatment with ibrutinib (Figure 4-7).

There is baseline variation in the adhesion molecule profile between cases. After 24 hours the profiles are similar but with prolonged co-culture on a stromal layer the leukaemic case shows increased expression of CD62L (L-selectin) and CD184 (CXCR4) compared to the nodal case. Although ibrutinib treatment results in very little change in the expression profile there is a trend in fact for the expression levels to increase in the leukaemic case compared with the nodal case which, changes may be more apparent with a longer ibrutinib treatment period. Numbers of cases in this

experiment are too low, for statistical comparison but it is of interest that there are differences detected between leukaemic, indolent cases and nodal, aggressive cases which could be correlated clinically and deserves further investigation.

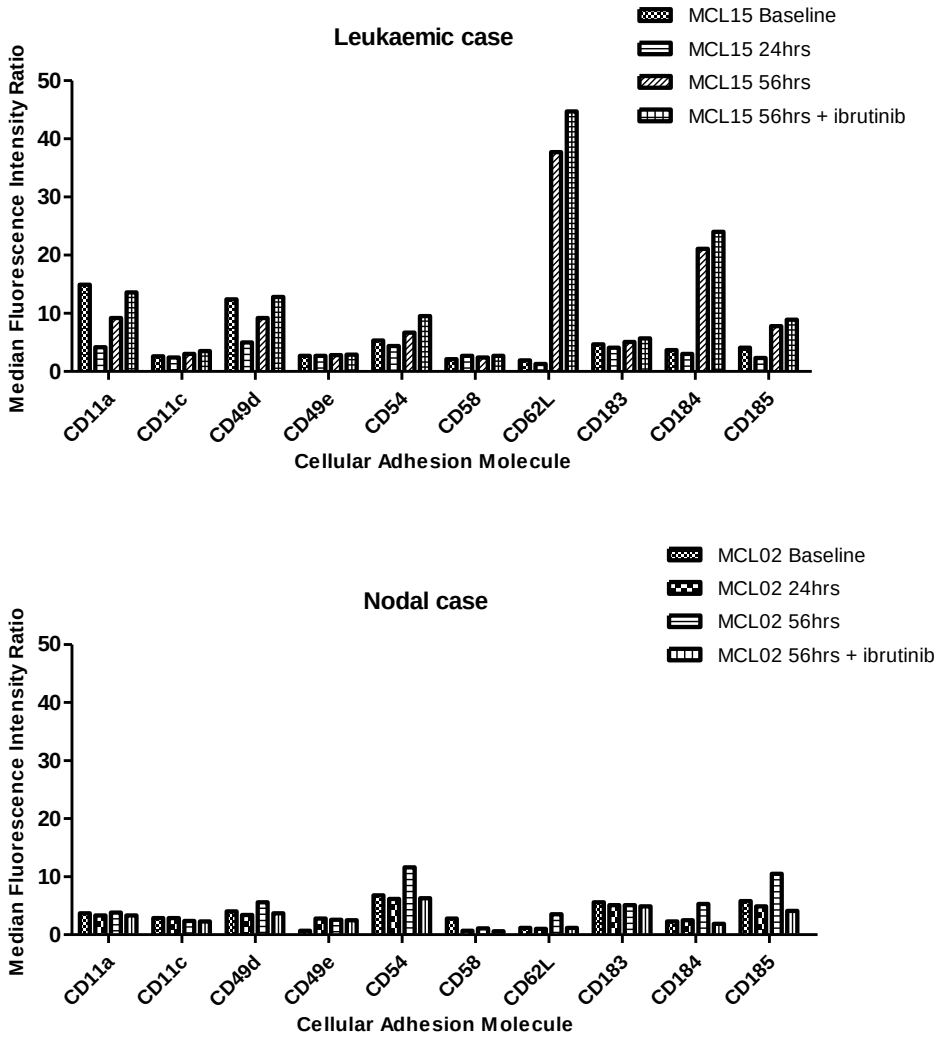

Figure 4.7 Co-culture of primary MCL cells with human stromal cell support. Expression profiles between cases show variation with a marked elevation of expression of CD62L and CD184 seen with prolonged culture in the leukaemia case. The expression profile changes little with ibrutinib treatment. Human primary MCL cells were cultured on human bone marrow stromal cells for 56 hours with the addition of 100nM of ibrutinib after 24 hours. Cultures were sampled at baseline, 24 hours and 56 hours for analysis of cellular adhesion molecule expression by flow cytometry.

4.6 Discussion

The profile of CAMs on PBMCs has been performed in a large number (17) of MCL patients including both aggressive (nodal) and indolent (leukaemic) cases with a comparison with bone marrow where possible. This is a unique and extensive profile of CAMs based on the known literature. It has demonstrated extensive inter-patient variability in the expression profile of CAMs.

In this series, the most highly expressed CAMs in peripheral blood are CD11a, CD49d and CD54 which is consistent with previously published case series of adhesion molecule profiles of B-cell non-Hodgkin's lymphomas in the leukemic phase, although the panel of markers assessed differed slightly.[76] In this published study, significantly greater expression of CD49d was observed than that seen in CLL samples with no significant differences in expression of CD11a or CD54.

CD11a, which is highly expressed in this series, forms the alpha L chain of integrin molecule LFA-1 and is universally expressed on leucocytes. It is involved in extravasation, antigen presentation and T-lymphocyte alloantigen-induced proliferation.[75] It is also thought to facilitate lymphocyte adhesion to FDCs via ICAMs (including CD54) within the lymph node.[76] Variations in expression are well recognised in NHL subtypes.[110] Low level expression of CD11a has been demonstrated in CLL whereas higher levels are described in its nodal counterpart, small lymphocytic lymphoma (SLL) and other predominantly nodal diseases such as diffuse large B-cell lymphoma (DLBCL).[116]

CD49d is the α4 subunit of the integrin heterodimer α4β1 (VLA-4) and is expressed on resting lymphocytes and monocytes and functions as both a matrix and cellular receptor. As a matrix receptor it binds to fibronectin. As a cellular receptor, it binds to

VCAM-1, a member of the immunoglobulin superfamily. VCAM-1 is induced by inflammatory mediators on endothelium. Together with CD11a, CD49d is thought to facilitate lymph node adhesion to follicular dendritic cells (FDCs) via VCAM-1.[76,108,109] Interestingly CD49d can differentiate indolent and aggressive subgroups in CLL,[117] however no significant difference can be seen by clinical phenotype in this case series.

CD54 (ICAM-1) is a member of the immunoglobulin superfamily and expressed on APCs. It is involved in reinforcing adhesion between T-cells and APCs [80] . Expression on fibroblasts can be regulated by CD40L.[118]

One of the aims of this study was to identify differences in expression of CAMs between blood and marrow MCL cells. However, the bone marrow sample acquisition was low (4) and therefore comparison in the expression of individual markers showed no statistical differences. However when the profiles were pooled and analysed they were statistical different. In particular there was higher expression of CD11a, CD54 and, not surprisingly, CD183 (CXCR3) in the bone marrow MCL cells. Further study of marrow adhesion molecule expression is therefore warranted. This is a particularly important correlation to study, given the relative sanctuary which MCL cells enjoy in the bone marrow.

Comparison of CAM expression between leukaemic (indolent) and nodal (aggressive) MCL cells also highlighted important differences which could be explored in further studies. Although no individual marker differed between groups, again perhaps because of the low number of indolent cases, the pooled profiles between the groups differed significantly. Again CD11a and CD54 were noticeably higher in the nodal cases. This may be significant in that CD11a is thought to facilitate lymph node adhesion via

ICAMs 1-3 and could be important in maintaining a nodal distribution of MCL cells in this subgroup.

If these differences were confirmed when analysed in a greater number of samples, it could be explored as a biomarker to predict need for treatment.

The observation in Chapter 3 that cells from subjects with more proliferative, nodal disease appear to form clusters when cultured ex-vivo (Figures 3.1, 3.14 and 3.25) may relate to the increased expression of CD11a and CD54 which may be required for homotypic cellular adhesion and cluster formation in MCL.

The assessment of CD40L on the CAM expression profile was analysed in 4 cases of MCL. This showed that the pattern of CXCR4 expression, the receptor ligand for the chemokine CXCL12 found in the microenvironment, was similar between CD40L-T and NT microenvironments. Expression of CXCR4 rose acutely in both conditions after 24 hours of culture. However when compared at all time points, the level of CXCR4 expression was significantly higher in cells cultured with the CD40L-NT stroma. Expression of CD54, however, was significantly higher on CD40L-transfected stroma demonstrating a dependency on CD40L. No other adhesion molecules differed significantly either over time or with CD40L.

Stromal cells in secondary lymphoid tissues constitutively express chemokines such as CXCL12 and 13, the corresponding ligands for CD184, providing guidance for B cell positioning within distinct nodal compartments. CXCL12 and 13 have been demonstrated to induce actin polymerisation in MCL cells and induce a chemotactic response which can be inhibited by blocking the receptor CD184, indicating an important role in migration and localisation.[33] High level expression of CD184 has been demonstrated on primary MCLs in other published studies together with a down-

regulation with ibrutinib exposure.[65] Interestingly, the pooled median fluorescence intensity ratio for CD184 is higher for the nodal cases (17.4) than the leukaemic case (14.7) after co-culture with stroma, suggesting a dependence on CD184 in nodal cases within the microenvironment.

There is an associative link between interference of CAM expression and BCR blockade with ibrutinib in MCL cells. *In vivo*, ibrutinib treatment is associated with a reduction in the expression of CD184, CD38 and Ki-67 as well as a significant reduction in plasma chemokines CCL22, CCL4 and CXCL13.[65] This shift in CAM expression manifests itself clinically as a rapid reduction in tissue burden in association with a marked peripheral lymphocytosis, which is dependent on continuous administration of the drug.[66,112,119–121] *In vitro*, blockade of the BCR signal of primary MCL cells with ibrutinib impairs adhesion to stromal cell layers and reverses the protective effect of stromal cells on MCL cells.[67] It has also been demonstrated that direct blockade of CD184 and VLA-4 with receptor-specific antibodies impairs adhesion to stroma and cell survival in MCLs *ex vivo*.[33] In CLL, a direct link between blockade of the BCR by ibrutinib and interference of cellular adhesion has been demonstrated in mouse models. Ibrutinib treatment has been demonstrated to impair CD184 receptor surface expression but not expression of CD185 or CD49d on CLL cells.[122]

However, the study of adhesion molecule expression in MCL cells following treatment with ibrutinib has not been studied in detail particularly in cells cultured in an *in vitro* model of microenvironment and was the rationale behind the treatment of MCL cells cultured on human stroma.

In these experiments the culture of MCL cells on human stroma produced some interesting and intriguing results. In the leukaemic case there was a marked rise in the

expression of CD62L (L-selectin) and CD184 after 56 hours of culture compared to the nodal case co-cultured on human stroma.

The effects CD62L is a single chain transmembrane protein found in granulocytes, monocytes and most lymphocytes. Low affinity binding by CD62L facilitates the capture, rolling and slow-rolling steps of leukocyte recruitment which in turn is followed by firm adhesion and transmigration. Low expression has been demonstrated in MCL, CLL and MZL in other studies.[76] It is therefore interesting that expression appears upregulated in the cells from the leukaemic MCL case cultured on human stroma but not on murine stroma.

The effects of ibrutinib are subtle. There is a possible trend to increased expression of CAMs in the leukaemic case over the nodal case which could help explain some differences in biology between groups and further study is warranted.

This thesis chapter has characterised the adhesion molecule profile of circulating MCL cells and shown it to be different to MCL cells from bone marrow and between clinical subgroups of indolent and aggressive lymphoma. The profile is dynamic and changes with changes within the microenvironment. Further studies to characterise these changes in more detail particularly following BCR-targeted treatment would help in understanding differences in MCL biology and mechanisms to improve treatment responses.

5. CHAPTER 5 - Developing a 3-Dimensional Module for the Study of Mantle Cell Lymphoma

5.1 Introduction

The aim of these experiments was to develop a three dimensional model for the study of MCL *ex vivo*. This was a novel concept and therefore this chapter mainly describes the steps involved in trying to develop this model, rather than on data obtained from a 3-dimensional (3-D) model. The chapter is divided into a discussion of the relevance of 3-D models for the study of cell biology; a brief overview of the models already in development and the justification for the choice of model for this work followed by the sequential experiments performed in order to explore and optimise this model for the study of MCL, predominantly using primary MCL cells.

5.1.1 Why Development of a 3-Dimensional Model for Cell Biology is Important

Mantle cell lymphoma cells normally reside within the supportive 3-D structures of the lymph-node or bone marrow. Within these structures, survival and proliferation of malignant cells is heavily influenced by stromal cells and other components of the tissue micro-environment (Figure 5-1).[29] This relationship with the tissue microenvironment has been extensively studied in CLL and this knowledge has helped to establish a reproducible in vitro tissue model that mimics the *in vivo* microenvironment of the disease.[27] In comparison, few studies have been performed in MCL and there is a real need for well-defined tissue models to form the basis for studying how different microenvironmental factors influence the biology and behaviour of the cells. In the era of targeted molecular therapies such as BTK-inhibitors, which are known to disrupt the relationship between malignant cells and

their extra-cellular environment, the need for a model to study this relationship is of particular importance.

A large amount of data and subsequent understanding of cellular interactions in tumour biology has been gained from 2-dimensional (2-D) cell culture methods. However, it is generally recognised that the hard, flat, plastic or glass surface commonly used for cell culture is not representative of the complex 3-D microenvironment found in living organisms. Indeed many of the functional structures studied in 2-D cell biology have specifically developed in the cell to allow it to proliferate, differentiate, interact with and migrate through the 3-D tissue microenvironment biochemical cues may be lost under 2d conditions.[123] In studies of cancer cells, growing cells within 3-D models has demonstrated significant differences in preservation of morphology[124,125], triggers of proliferation[126], differentiation of stem cells[127], protein expression and sensitivity to therapy[128] and cellular metabolism[129] when compared with 2-D culture.

While attempts have been made to develop models with the 3-D characteristics of the bone marrow microenvironment in other diseases[130,131], there is little or no published data on 3-D culture models in MCL. Given the differences in cellular behaviour demonstrated in other malignancies in 2-D and 3-D models, it would seem logical to attempt to design and establish a 3-D model in vitro for the further study of MCL.

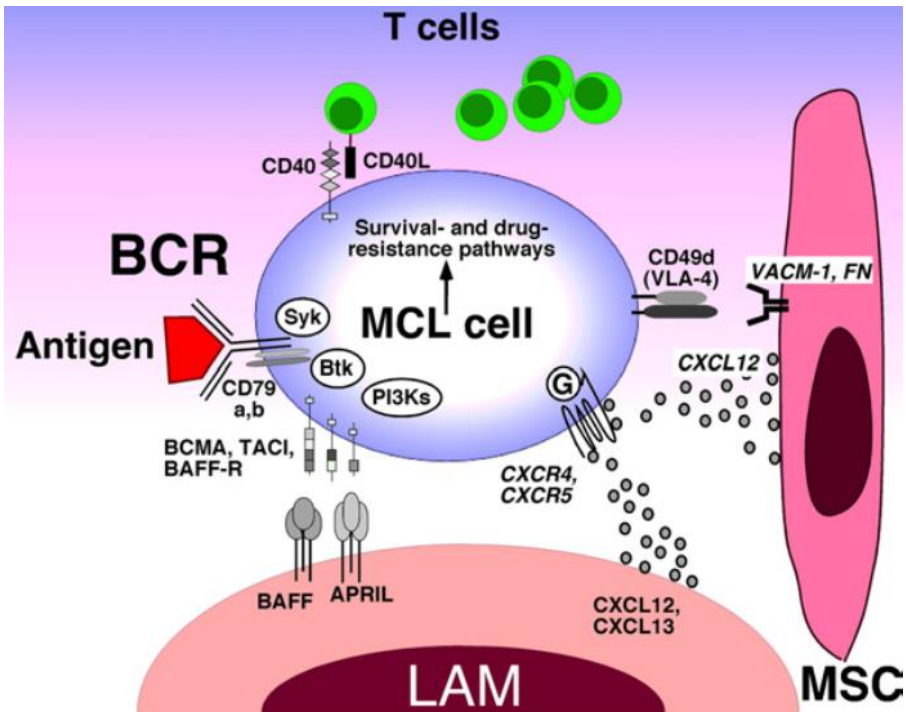

Figure 5.1 MCL microenvironment. The diagram (adapted from[29]) reflects the important cellular, soluble and molecular interactions known to be important in the interaction between MCL lymphocytes and the tissue microenvironment. The chemoattractant chemokines CXCL12 and CXCL13 secreted by stromal cells such as mesenchymal stromal cells (MSC) and lymphoma-associated macrophages (LAM) attract MCL lymphocytes via G-protein coupled receptors CXCR4 and CXCR5. Adhesion molecules such as VLA-4 are important in binding to the extracellular matrix and stromal cells within the microenvironment. Complex intracellular signaling pathways following stimulation via the BCR, chemokine receptors, TLR or CD40 L are also involved in the proliferation and survival of MCL with the microenvironment.

5.1.2 An Overview of 3 Dimensional Models in Current Cellular Research

A 3-D model form MCL would need to be able to accommodate the complex structure of the bone marrow, which can be subdivided into cellular constituents and extracellular matrix (ECM). The cellular components are subdivided into haematopoeitic cells and stromal cells including fibroblasts, adipocytes, macrophages and osteoblasts.[132] The ECM is formed predominantly by collagens (predominantly type 1), glycoproteins such as fibronectin and laminin and proteoglycans such as heparin sulphate.[133] These structural components also form a reservoir for cytokines, chemokines and growth factors. Collectively, the bone marrow microenvironment contains complex cellular, structural and chemical factors which interplay in

maintaining homeostasis. Additional factors such as matrix stiffness and flow rates of interstitial fluid play important roles in tumorigenesis.[134,135]

Numerous 3-D models have been established for the study of various tissue types, and these, together with the rationale for selecting a model for experimentation with primary MCL cells are briefly described below.[123,136]

5.1.2.1 Organotypic Explant Culture

Organotypic explant culture is a model in which dissected organ slices are placed on a porous substrate, supported by a rigid mesh and cultured at the air/liquid-growth-medium interface. This preserves the architecture and cellular differentiation of the original tissue and is particularly useful in studying brain physiology.[137] However, initiation of this model requires solid tissue samples and is therefore not applicable to liquid bone marrow or peripheral blood samples obtained in this project and are therefore discussed no further.

5.1.2.2 Spheroid Formation using the Hanging Drop Method

In the spheroid model, large cellular spheroids are formed by aggregation of tumour cells from a suspension, either within a "hanging drop" of liquid media or within a flask of medium which rotates to prevent adhesion.[138] Suspended cells cluster and aggregate and can re-establish contact-dependent interactions.

This is a relatively simple method which does not require an external scaffold for aggregation. Bone marrow fibroblast spheroids have been cultured in 3-D models using the hanging-drop method predominantly for the study of tissue engineering and chondrogeneisis.[139] Drawbacks of this method in the context of this project may include difficulties in preventing contamination during routine examination of the

droplets by microscopy; the relative fragility of the culture droplets during the handling process and the requirement for specialist equipment to incubate and roll flasks simultaneously. However, this method in its application to a MCL model is explored briefly at the end of this chapter (5.4).

5.1.2.3 The Use of Microporous Membranes

Three-dimensional epithelial structures can also be grown on microporous membranes by culturing immortalised epithelial cells as polarised monolayers on microporous membranes. This method is particularly suited to cells from epithelial organs such as glandular breast or kidney tissue which form acinus or tubular structures respectively.[140] However, an epithelial-like model is probably not a suitable choice as a 3-D model in the study of lymphoma cells due to histological differences in the architecture of the lymphoma microenvironment.

5.1.2.4 Biological Scaffolds

A potentially suitable method for the study of MCL employs the use of a ready-made biological scaffold which mimics the lymph node or bone marrow architecture onto which stromal and lymphoma cells can potentially adhere and ultimately colonise within a suitable culture medium. Various materials have been explored in producing a scaffold which has the necessary qualities, such as thermo-reversible collagen-containing hydrogels, fibrous scaffolds derived from methoxy-copolymers and alginate sponge matrices.[141–143]

5.1.2.5 Macroporous Alginate Scaffold as a Candidate Model for 3-Dimensional Culture

One readily available and relatively inexpensive model for studying 3-D cell culture is the alginate macroporous scaffold model. Alginates are polysaccharides consisting of

linear linked residues of β-D-mannuronic acid (M) and its C5-epimer α-L-glucuronic acid (G). The molecular structure contains blocks of consecutive (-GGG- or –MMM-) or alternating G or M monomers (–MGMG-). Cells do not have receptors that recognise alginates and therefore commercially available alginates can be considered inert. Alginate matrices are available in hydrogel form, as beads or as macroporous scaffolds.

Macroporous scaffolds have the advantage of allowing larger cellular constructs because the mass transfer of nutrients and waste products is enhanced by a larger pore size than in hydrogel models and have been used as a model for 3-d cell culture in both human and animal cell experiments.[144,145]

A challenge with the macroporous scaffold approach is cell seeding efficiency and cellular distribution as the pores are often either too big to retain cells or too small to admit them. However, a variety of cell-seeding approaches have been used to overcome this including cell seeding devices, bioreactors, centrifugal force and vacuum.[146]

5.1.2.6 Thermo-reversible collagen-containing hydrogels (Matrigel)

Matrigel is a soluble extracellular matrix system comprised of gelatinous protein mixtures secreted by Engelbreth-Holm-Swarm (EHS) mouse sarcoma cells which resemble the extracellular matrix found in many tissue types.[142] It contains a sterile extract of basement membrane proteins derived from the EHS tumour which forms a gel at 37^{o}C and supports cell morphogenesis, differentiation and tumour growth. It is stored as a frozen solution, is thawed at 4^{o}C and gels at 24-37^{o}C in 30 minutes. It does not redissolve readily on cooling. Cells are generally plated on top of the gel but can be mixed with the matrix prior to gelling. Many cell lines and primary cells do not proliferate but differentiate when exposed to Matrigel and the morphology often

reflects a more differentiated phenotype. Matrigel, like other basement membranes represent a rich source of angiogenic and growth factors which can be used by tumour and other cell types. Laminin-1, collagen IV and other matrix proteins can contribute to growth-promoting signals and may affect the expression of adhesion molecules.[147]

Because of the potential effects on expression of surface markers by growth factors and matrix proteins within the gel and because of the potential difficulties in cell retrieval and analysis of expression of surface markers which can be encountered with Matrigel[148], this method may not be suitable for the culture and assessment of MCL primary cells *ex vivo.*

5.1.2.7 AlgiMatrix® Bioscaffold

AlgiMatrix® (*Gibco*) is an animal origin-free bioscaffold that facilitates three-dimensional cell culture. AlgiMatrix® is based on ionically gelled and dried alginate scaffolds, available as sterile discs in standard culture well plates. The matrix itself returns to a hydrogel substance on rehydration and can be stained and microscopically evaluated or dissolved for retrieval of cells.

Each bioscaffold is an individual alginate sponge with a pore size of 50 – 200 microns. A concentrated cell suspension is absorbed by the dry sterile disc as it is applied to the top surface and the cells are subsequently trapped inside the scaffold.

5.1.3 Justification for Selecting AlgiMatrix for this Project

This system has several qualities that make it a suitable for testing in the context of this project:

- it is a chemically defined animal-origin free material therefore limiting interaction and cross reactivity of antigens with MCL or stromal cells;

- after re-constitution with firming buffer and cell suspension, its translucency allows relatively easy visualisation of cells by light-microscopy;
- it may also be possible to dissolve the bioscaffold non-enzymatically without disrupting cell spheroids, clusters or other 3D structures using an enzyme-free dissolving buffer in order to retrieve the cells for viability assays and other experiments;
- it is possible to retrieve the sponge from the standard well plate after a period of cell culture for fixation, dehydration and paraffin embedding prior to staining and microscopic examination of cellular colonisation;
- although the sponges are packaged in a single standard 24 well plate, individual sponges can be removed from the original plate under sterile conditions and placed into a second plate allowing multiple sequential experiments.

Therefore a series of experiments using AlgiMatrix® discs were designed.

5.1 General AlgiMatrix® culture, fixation and staining

Below is a description of the reagents and equipment used in the development of a 3-D model for MCL culture.

5.1.4 Reagents and equipment

AlgiMatrix system

AlgiMatrix® disc culture system (*Gibco*);

AlgiMatrix® firming buffer (*Gibco*)

AlgiMatrix® dissolving buffer (*Gibco*)

General suspension media

RPMI Media + glutamax (*Gibco*) containing 10% FCS (heat inactivated, qualified grade) (*Fisher Scientific)*, and 1% Streptomycin/penicillin (*Sigma*)

Modified IMDM culture medium containing 10% FCS, 10% horse serum, 1% pen/strep and $5x10^{-7}$ M hydrocortisone

Fixation

100nM barium chloride solution (in distilled H_2O)

Neutral buffered formalin (NBF) (*Genta Medical*);

Paraffin Wax, Granular, (ACROS Organics™).

Staining

Harris Haematoxylin (supplied by *Fisher Scientific* at working concentration)

1% hydrochloric acid alcohol (*Fisher Scientific*)

Eosin-Y working solution (*Fisher Scientific*) 20% in ethanol.

Mounting media (*Histomount*).

Cell lines

Murine stromal cells: CD40-ligand-transfected (CD40L-T) (kind gift from Professor M Dyer, Leicester, UK)

Granta-519 (G519) human mantle cell lymphoma cell line (Deutsche Sammlung von Mikroorganismen and Zelkulturen GmbH (DSMZ) (Braunschweig, Germany))

Equipment

Embedding cassette (*Sigma-Aldrich*)

Tissue processor (*Sakura TISSUE-TEK VIP E300*)

Tissue embedder (*Leica Biosystems EG1150*)

Cold plate (*Leica Biosystems EG1150 C*)

Manual rotary microtome *(Mircom Heidelberg HM 320)*

DM IL LED phase-contrast light microscope (*Leica Microsystems*)

CCD grayscale camera (Leica DFC3000 G) (*Leica Microsystems*)

LAS AF Version: 2.6.3 software (*Leica Microsystems*)

5.1.5 AlgiMatrix® disc.

The optimisation of seeding the AlgiMatrix® discs is described in the following sections. The lyophilised AlgiMatrix® sponges require rehydration with cell suspension media, firming using the AlgiMatrix® firming buffer and seeding with a cellular suspension at an optimal cellular concentration. Following the manufacturers recommendations an initial seeding concentration of $1x10^6$ cells/mL was used.[149] Cells were suspended in RPMI media with glutamax (*Gibco*) containing 10% FCS (heat inactivated, qualified grade, (*Fisher Scientific)*, and 1% streptomycin/penicillin (*Sigma*). Individual AlgiMatrix® sponges (*Gibco*) were transferred from the manufacturer's plate to a sterile 24 well flat-bottomed plate (*Fisher Scientific*) in a laminar flow hood. The lyophilised sponge was initially rehydrated with 500µl media then once all bubbles had dispersed a further 500µl of media was slowly pipetted onto the top of the sponge. The percentage of firming buffer and cell concentration is described in more detail in the following experiments.

The sponge was inspected by light microscopy on a daily basis and twice weekly media changes were performed by gently moving the matrix to one side of the well with a 200µL pipette tip whilst aspirating the spent culture medium from the other side of the well, being careful to avoid aspirating or damaging the sponge. The spent media was then replaced with 500µL of warmed suspension media and the plate returned to the incubator.

5.1.1 Disc Fixation, Paraffin Embedding and Sectioning

5.1.1.1 Fixation methods

In order to visualise colonisation of the AlgiMatrix® system, the sponges were examined by phase-contrast light microscopy (Figure 5-2). However, only limited views of the outer parts of the sponge were possible with this method. In order to

visualise the inner parts of the matrix, the sponges required fixation and sectioning. Because the sponge was soft and friable once rehydrated, sectioning could only be performed after fixation and paraffin embedding.

Fixation of tissues is necessary to inhibit decay or autolysis of tissues in order to preserve samples for future study. It can be achieved by cross-linking agents, e.g. PFH, which is effective at preserving cell structure but can obstruct antibody binding, therefore antigen retrieval techniques are sometimes required. Fixation is achieved by immersion of the specimen in a 4% paraformaldehyde (PFH) solution.

Neutral buffered formalin (NBF) was used to fix the AlgiMatrix® sponges in this project. Neutral buffered formalin is equivalent to 4% PFH in a buffered solution plus a preservative (methanol) which prevents the conversion of formaldehyde to formic acid. Because of this preservative, NBF has a shelf life of several months compared with 4% PFH which must be made fresh.

The AlgiMatrix® manufacturer suggests that fixation, paraffin embedding and sectioning is feasible,[149] however because this part of the method required development, it is described in detail below.

5.1.5.1 Establishing an optimal fixation time

Fixation times vary depending on tissue thickness: if specimens are very large, longer is required for the fixative to penetrate the inner portion of the sample. Under-fixation can lead to edge staining (strong-staining at the edge but none in the middle) whereas over fixation can mask any epitopes being studied. A guideline for fixation time is one hour of fixation for every 0.5mm of specimen thickness.[72] As the alginate discs measured approximately 3-4mm thick once rehydrated, a fixation time of at least 6

hours was initially considered necessary. However the optimal time for fixation remained to be established.

In the initial experiments, after 6 days of culture, the sponge was transferred to a fresh well in the 24 well plate. To fix the cells, 500µL of 4% NBF solution was added to the well for overnight (12 hour) fixation. However, after twelve hours, the tissue was friable and broke up, even with careful handling.

Because there were no calcified or fibrous components in the tissue, a shorter fixation time of 2 hours was tested. A 2 hour fixation appeared to be adequate in terms of balance between maintaining the integrity of the tissue and allowing adequate fixation to prevent degradation of the sections over time. However, because no antigen labelling was performed in these experiments, further work is required in establishing the optimal time for fixation for epitope preservation. For the purposes of paraffin embedding and haematoxylin and eosin staining, a 2 hour fixation time was employed in this research. After fixation, the disc was transferred to the tissue processor for dehydration and paraffin infiltration.

5.1.2 Paraffin Infiltration

Before paraffin infiltration can take place, the fixed specimen must be dehydrated through a series of graded ethanol baths to displace water. The infiltrated tissue can then be embedded in wax blocks where it can remain stable for many years. Commercial paraffin wax is commonly used for infiltration, usually a mixture of straight chain or n-alkanes with a carbon length of 20 to 40 atoms. Melting temperature for histological use is usually between 56 – 58^{o}C.

After tissue fixation, the disc was transferred to a labelled embedding cassette and placed into the tissue processor. A standardised dehydration and embedding protocol

was used throughout the project (See Appendix 4).

After paraffin embedding, the disc was removed from the cassette and the lid of the cassette discarded. The cassette was transferred to a pre-heated tissue embedder. A small amount of molten paraffin was poured into a metal mould from the paraffin reservoir. The tissue was transferred into the mould using warmed forceps. The mould was transferred to the cold plate where the paraffin solidified in a thin layer holding the disc in position. The cassette, minus the lid, was then placed on top of the disc in the mould and hot paraffin was added to the mould from the dispenser to cover the face of the plastic cassette. The mould was then transferred to a cold plate and left to solidify for 30 minutes before the block was popped out of the mould and ready for sectioning.

5.1.3 AlgiMatrix® Disc Sectioning

Paraffin blocks are best sectioned cold as sectioning is generally optimal when the specimen and wax are well matched in hardness. Cold wax provides better support to the tissue allowing thinner sections to be taken.

The disc was sectioned using a manual rotary microtome. After removing excess wax, the block was inserted into the clamp in a horizontal orientation. The microtome was set to cut at a section thickness of 10µM. Once the block was correctly orientated and perpendicular to the cutting blade, a ribbon of tissue sections was cut. Using brushes and forceps to handle the cut ribbon of sections, two to three sections were transferred to a water-bath set at 50^{o}C (4-8 degrees below the melting point of the wax).

The sections were then quickly transferred to a frosted glass microscopy slide (*Corning™*) by gently floating the section onto the slide using a brush to guide the

section. The slide was then removed from the water bath, carefully dried and labelled and the wax section was baked onto the surface of the slide ready for staining for 2 minutes using a hotplate.

5.1.4 Staining

Haematoxylin and eosin staining is the most commonly used staining method in histopathology because it gives a good general overview of the structure of tissues. It was selected as the staining method of choice in this project in order to visualise the colonisation of the disc by both fibroblasts and MCL cells as these cells are readily distinguished using this staining method.

Haematoxylin Staining

Haematoxylin is a natural dye. It does not stain tissue well until it is combined with a metallic salt (iron or aluminium). It is used to dye cell nuclei by binding to histones via the metallic salt. In the regressive staining method used in this project, the slides are initially over-stained with haematoxylin by submerging them in the stain for 5-8 minutes. At this stage, the nuclei are stained a deep purple but the next stage renders the stained nuclei dark blue. Achieving a blue nucleus is a two stage process. In the first (differentiation) stage, the slides are placed in an acid alcohol solution which removes excess stain. The second stage involves rinsing the slides in tap water, a step called “blueing”. This is done by running the slide under a gentle stream of alkaline tap water.

Eosin Staining

Eosin is a counterstain used to stain cytoplasm. The pink counterstain also helps to differentiate between nuclei and non-nuclear components in cells. The most commonly used eosin dye is eosin-Y (eosin-Yellowish), derived from fluorescein. The exact mechanism of staining is not fully understood but is thought to be electrostatic.

The slides are usually immersed in eosin for two minutes before being rinsed in tap water. Sections can be inspected at intervals during the staining process to prevent overstaining and a certain amount of overstain can be removed by placing the slides in a container with running water.

5.1.4.1 Haematoxylin and Eosin Staining Protocol

The mounted tissue-sectioned slides (10 micron sections of paraffin-embedded AlgiMatrix® disc) were first heated briefly at 65^{o}C to soften the wax. With appropriate safety precautions, the slides were then immersed twice in xylene for 5 minutes; 95% ethanol for 2 minutes; 70% ethanol for 2 minutes and then washed in distilled water.

The slides were then stained with 1mL of haematoxylin stain with for 5-8 minutes before being run gently under tap water 5 minutes to wash off excess stain. The slides were then immersed in 1% acid alcohol for 30 seconds to regress the haematoxylin stain before "blueing" by immersion in tap water for 5 minutes. The slides were then dipped in 95% ethanol 10 times before staining with eosin-Y working solution for 2 minutes. The slides were then immersed in 95% ethanol twice for 5 minutes; then 100% ethanol twice for 5 minutes before immersion in xylene twice for 5 minutes. Slides were mounted with glass cover slips *(Fisher Scientific*) using mounting media (Histomount) and examined by light microscopy.

5.2 Cellular colonisation

5.2.1 Murine stromal cells

In order to test the ability of murine fibroblasts to colonise the alginate sponge an initial experiment was designed with murine stroma which are abundantly available and known to proliferate well in 2-D culture conditions.

Adherent CD40-ligand-transfected murine stromal cells (kind gift from Professor M Dyer, Leicester, UK), were cultured to 100% confluence in a vented, 75cm^2 plastic flask, maintained in complete 1640 RPMI medium at 100% humidity, 5% CO_2 and 37^{o}C, as previously described (Methods 2.6). A cell suspension at 1 x 10^6 cells/ml was prepared in warmed suspension media (Reagents and equipment 5.2.1) following trypsin digestion (Methods 2.6.2). Individual AlgiMatrix® sponges were rehydrated with 500µl of 10% AlgiMatrix® firming buffer in media and seeded with 500µl of cell suspension (5 x 10^5 cells) as previous described.

As a 2-dimensional control, 10mLs of the same murine stromal cell suspension was transferred to a 25cm^2 vented flask. Both flask and sponge-containing plate were then maintained in an incubator at 5% CO_2, 100% humidity, 37^{o}C.

The flask and sponge were inspected for colonisation by phase-contrast microscopy every 24 hours. After 6 days, the sponge was fixed, embedded in paraffin, sectioned and stained with haematoxylin and eosin for microscopic assessment of colonisation. At first attempt the fixation time chosen was 12 hours, however, this made the disc too fragile and it disintegrated on handling. Therefore the experiment was repeated under the same conditions but with a 2 hour fixation time which preserved disc integrity.

Phase contrast observation highlighted differences in both morphology and proliferation. The observed cells in the 2D system are flat spindle shaped cells compared to the development of small clusters of cells observed in the 3D system (Figure 5-2). However the colonisation of cells appeared markedly reduced in the 3-D culture system in comparison to the 2D system and indeed a significant proportion of the fibroblasts were observed on the well floor rather than in the sponge. Possible

explanations for this were failure of cells to migrate into and adhere to the matrix, suboptimal cellular density or failure of proliferation. Higher cell densities, addition of extracellular matrix proteins or different seeding techniques may be required.

Images from light-microscopy of the stained sections demonstrate suboptimal preservation of the structure following tissue processing (Figure 5-3). Further optimisation of the method to improve the structural integrity of the matrix was required and is described in below.

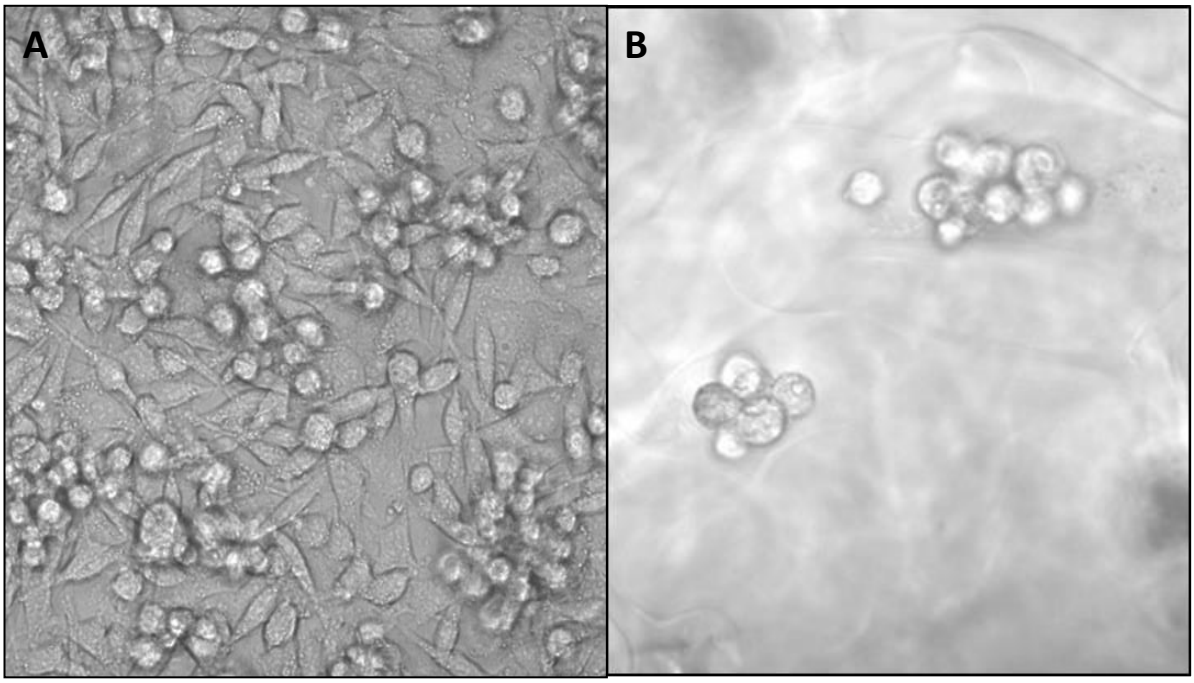

Figure 5.2 Culture of murine stromal cells for 5 days reveals flat spindle-shaped cells in 2-D culture conditions (A) compared with small clusters of spheroidal cells in the 3-D matrix (B). Light microscopy comparison of (A) murine stromal cells grown on the bottom of a 25cm^2 vented flask in complete RPMI medium in comparison with the same cells cultured within an AlgiMatrix® sponge matrix in a 24 well plate in RPMI medium(B). Images taken after 5 days of growth (sponge and flask both seeded at a density of 1x10^6 cells/mL) (both images x40 magnification)

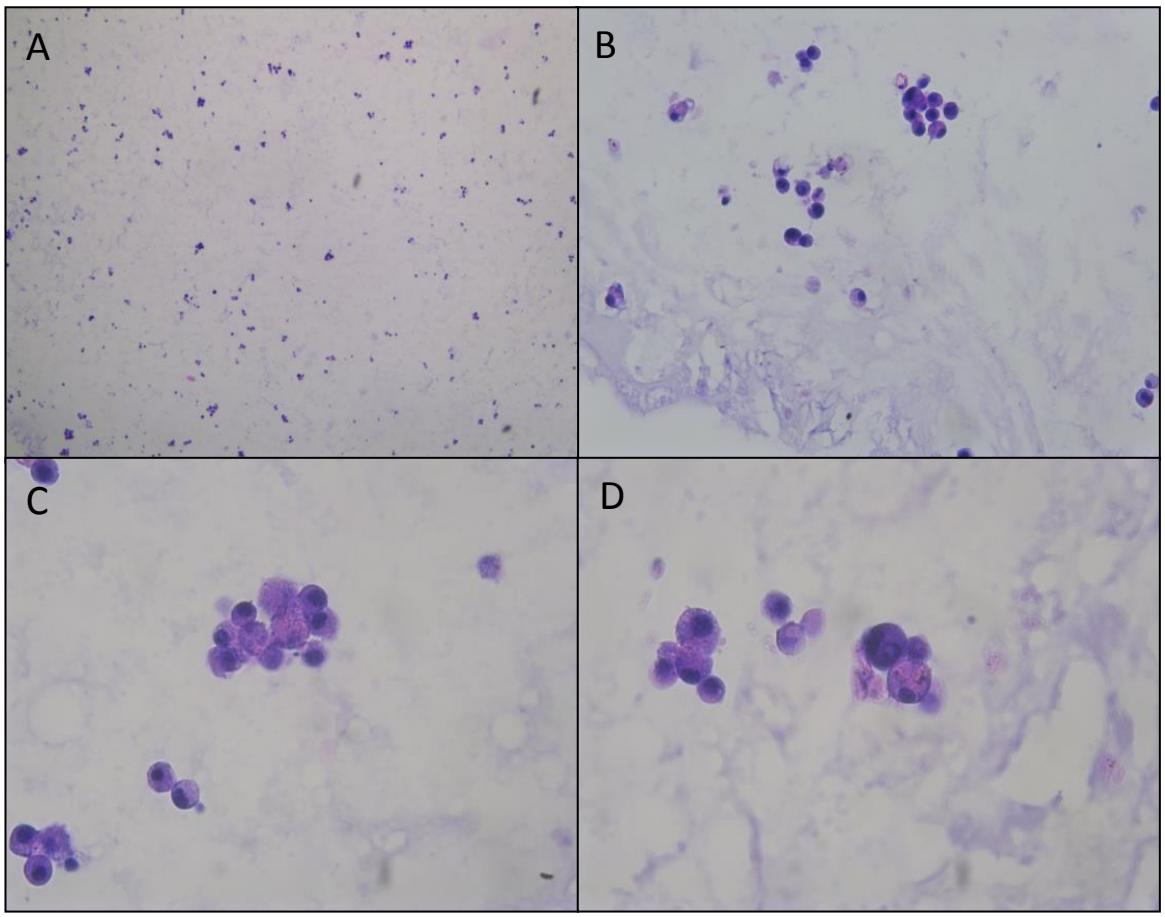

Figure 5.3. Haematoxylin and eosin-stained sections of a 3-dimensional culture of murine fibroblasts using an AlgiMatrix® scaffold. Images demonstrate disintegration of matrix structure during the dehydration and embedding process. The AlgiMatrix® disc was seeded with CD40L-transfected murine bone-marrow stromal cells at a density of $1x10^6$/mL in complete RPMI culture medium with 10% AlgiMatrix® firming buffer. The disc was cultured for 6 days (5% CO_2, 37^{o}C) with media changes every 3 days before being fixed for 2 hours in 4% neutral buffered formalin, embedded in paraffin, sectioned (10 microns) and stained with haematoxylin and eosin. (Magnification: Ax4, Bx10,C x20,D x20)

5.2.2 Seeding the AlgiMatrix® with a MCL cell line

The aim of this chapter was to explore the development of a 3-D model for the study of MCL, in particular, to establish a model that could be used to test the effects of different micro-environmental conditions on the growth and survival of primary MCL cells. However, primary MCL cells obtained from subject donors are a precious resource. Therefore an experiment with a rapidly proliferating and readily available MCL cell line (G519) was conducted.

Building on the observations from the initial murine fibroblast culture, several changes were made to the initial seeding protocol in an attempt to improve proliferation and colonisation of the disc. The AlgiMatrix® disc was not rehydrated with complete RPMI medium containing 10% firming buffer. Instead, a suspension of G519 cells in RPMI culture medium *containing* 10% firming buffer was used to rehydrate and seed the sponge simultaneously. The aim of this modification was to improve colonisation of the disc by absorption of cells with liquid into in the disc during the rehydration process. A two hour fixation time was used prior to paraffin embedding, sectioning and staining. A longer culture period of 21 days was used in order to give the G519 cells more time to form proliferative centres in 3-D.

The basic protocol was as previously described. A 1 ml suspension containing 1 x 10^6 G519 MCL cells was prepared in suspension media containing 10% AlgiMatrix® firming buffer. 500µL of this cell suspension was then seeded onto a lyophilised AlgiMatrix® sponge in a 24 well plate as previously described. Once any bubbles had dispersed, a further 250µL of cell suspension was added to the well (to ensure adequate media and cell numbers for colonisation).

The sponge was incubated at 37^{o}C, 5% CO_2. Culture medium changes were performed every 2-3 days and visual inspection by light-microscopy every 48hrs. The discs were maintained in incubation for a total period of 21 days prior to tissue fixation, paraffin embedding, sectioning and staining.

Microscopic phase contrast examination of the AlgiMatrix® disc demonstrated the formation of spheroid clusters after 21 days of culture but proliferation rates within the matrix appeared slower than expected when compared to cells grown in suspension culture (Figure 5-4) . The main challenge encountered from the prolonged culture was deterioration in disc integrity. The disc was rendered extremely fragile and disintegrated during transfer to the paraffin embedding cassette therefore sectioning was not possible.

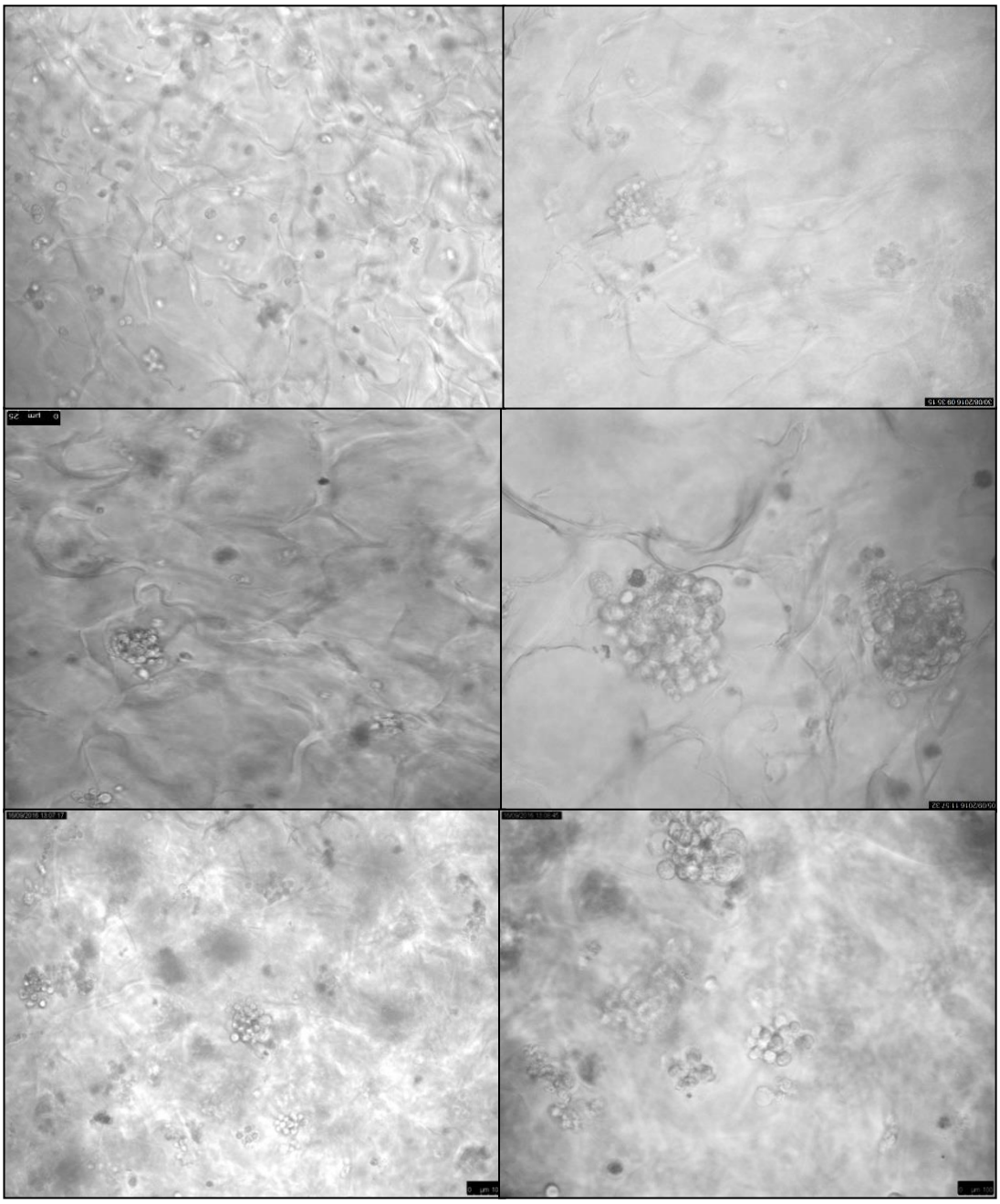

Figure 5.4 Phase Contrast Images of G519 MCL Cells in 3-D Culture on AlgiMatrix®. Granta-519 MCL cells demonstrate formation of spheroid clusters when cultured in an AlgiMatrix® 3-D culture system over 21 days. AlgiMatrix® discs were seeded with G519 MCL cells at a density of $1x10^6$/mL and incubated at 37^oC, 5% CO_2 in complete RPMI medium for 21 days with media changes every 48 hours. Phase-contrast images taken at serial time points in culture: top left - 3 days(mag. x20); top right - 7 days (mag x20), middle row - 12 days (mag x20 left and x40 right); bottom row - 21 days (mag. x 20 left & x40 right).

5.2.1 3D culture using human fibroblast cells

With modification of the methods initially employed, the AlgiMatrix® bioscaffold has demonstrated an ability to support the culture of both murine fibroblasts and G519 MCL cells. It was decided to test this system in respect to the growth of primary human bone marrow cells. Primary human fibroblasts were cultured *in vitro* as a potential stromal support for future primary MCL culture. The following experiment explores the AlgiMatrix® system's ability to support a human fibroblast culture *ex vivo*.

Our ethically approved tissue bank allows the collection and storage of liquid human bone marrow aspirated during the course of a routine investigative bone marrow biopsy from patients with underlying lymphoproliferative disorders. Human bone marrow stromal cells were established as previously described (Methods 2.7). The proliferative capacity of the resultant fibroblasts was variable in line with clinical heterogeneity (Figure 5-5). Upon achievement of a confluent layer of human fibroblasts the cells were washed, trypsinised and resuspended in 1000µL of modified IMDM culture medium containing 10% FCS, 10% horse serum, 1% pen/strep, $5x10^{-7}$ M hydrocortisone and 10% AlgiMatrix® firming buffer. 500µL was then seeded onto a lyophilised AlgiMatrix® disc. Once any bubbles had been dispersed, an additional 500µL of IMDM culture medium without cells was added for nutritional support and to prevent drying out. The disc was incubated at $37^{o}C$, 5% CO_2. Regular examinations by light-microscopy and media changes were performed. After six days of incubation, the disc was fixed for 2 hours in NBF, dehydrated and embedded as previously described (Figure 5-6).

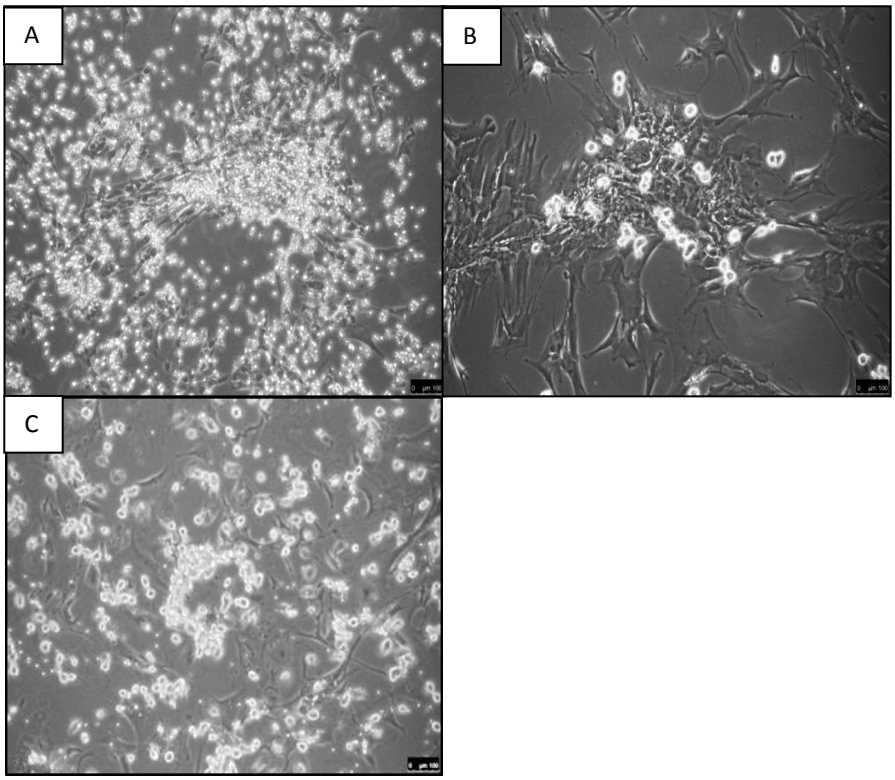

Figure 5.5 Examples of 2-D culture of human bone marrow fibroblasts from 3 different subjects. Phase contrast images of samples taken after 21days (A), 28 days (B) and 35 days (C) (magnification 10x). A 25cm^2 vented flasks was seeded with PBMCs from fresh human bone-marrow (density 5x10^6 cells/mL) in 10mLs of long-term culture medium after ficoll-separation from whole bone marrow aspirate. Cells were maintained at 37^{o}C, 5% CO_2 for 10 days without disturbance and then fed by half-medium separation on days 10, 14, 21, 28 and weekly thereafter.

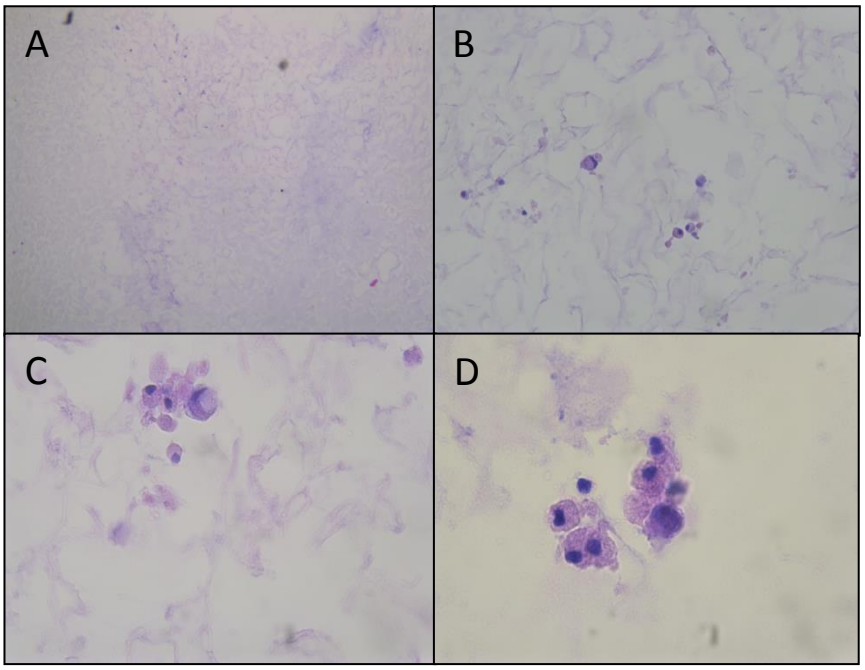

Figure 5.6. Human bone marrow fibroblasts cultured using the 3-D AlgiMatrix® scaffold. A paucity of fibroblasts and diffuse disintegration of the matrix scaffold is demonstrated. Human bone-marrow stromal cells (from a subject with lymphoma but without marrow infiltration) were cultured in 25cm^2 vented flasks to confluence before being removed and resuspended at a density of 1x10^6/mL in complete IMDM culture medium with 10% FCS, 10% horse serum, 1% pen/strep 5x10^{-7} M hydrocortisone and 10% AlgiMatrix® firming buffer. The cell suspension was seeded on to lyophilised alginate sponges (500µL per sponge) in a 24 well plate and then cultured for 6 days (5% CO_2, 37^{o}C) with media changes every 3 days before being fixed for 2 hours in 4% neutral buffered formalin and embedded in paraffin, sectioned (10 microns) and stained with haematoxylin and eosin. (Magnification A x4, B x10, C x20, D x40)

Although colonisation with human bone marrow fibroblasts is apparent within the AlgiMatrix® system (Figure 5-6), cell numbers are poor suggesting the microenvironment is hostile to human stromal cell proliferation. A higher density of cells may be required for successful colonisation. Unfortunately the matrix integrity is again degraded after 6 days culture following the fixation, paraffin embedding and staining process.

5.2.2 3-D Culture of MCL Marrow Buffy Coat

To establish whether the matrix would be suitable model for MCL and in an attempt to address the issue of low cell numbers within the AlgiMatrix® bioscaffold after culture, the entire marrow buffy-coat fraction from a fresh bone marrow sample from a

subject with MCL was used to create the seeding solution applied to the lyophilised disc. It was hypothesised that cells other than fibroblasts, such as T-cells and macrophages may be required for colony formation when using human bone marrow within the 3-D bioscaffold.

The buffy-coat layer was prepared at a cell density of $3.5x10^7$ cells/mL in 500µL of IMDM culture medium with 10% FCS, 10% horse serum, 1% pen/strep, $5x10^{-7}$ M hydrocortisone and 10% AlgiMatrix firming buffer. This cell suspension was then seeded on to a lyophilised AlgiMatrix® disc and maintained at 37^oC, 5% CO_2, 100% humidity for 6 days. A media change was performed on day 3.

After 6 days, media was carefully removed and the disc was fixed for 2 hours in neutral buffered formalin (NBF). The sponge was then dehydrated and embedded in paraffin before sectioning and staining with haematoxylin and eosin (Figure 5-7).

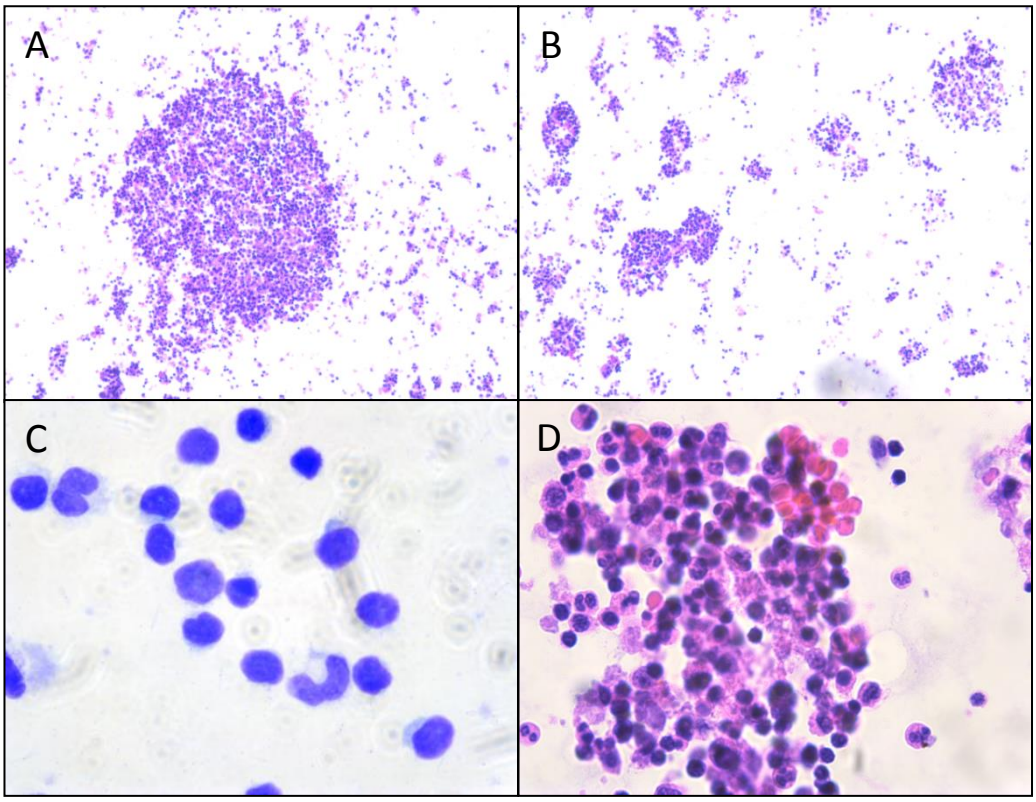

Figure 5.7 Fresh whole marrow buffy-coat cells cultured using the 3-D AlgiMatrix® bioscaffold. Fresh human bone-marrow buffy coat from a patient with MCL with marrow infiltration was washed and resuspended at a density of $3.5x10^{7}$/mL in complete IMDM culture medium with 10% FCS, 10% horse serum, 1% pen/strep, $5x10^{-7}$ M hydrocortisone and 10% AlgiMatrix firming buffer. The cell suspension was seeded on to lyophilised alginate sponges (500µL per sponge) in a 24 well plate and maintained for 6 days in 5% CO_2, at 37^{o}C with a media change every 3 days before fixation for 2 hours in 4% neutral buffered formalin and embedded in paraffin, sectioned (10 microns) and stained with haematoxylin and eosin. (Magnification: A x4,B x4,C x40,D x40)

Whereas in previous experiments, scant clusters of fibroblasts were observed throughout the disc, when a higher density of cells was used including the whole buffy coat from ficoll separation, multiple aggregates of bone marrow cells were observed throughout the disc after 6 days of culture (Figure 5-7). The matrix integrity continues to show evidence of significant deterioration after 6 days culture after fixation, paraffin embedding and staining process.

5.1.6 Improving the structural integrity of the AlgiMatrix® culture system using barium chloride

An obstacle encountered in the development of a 3-D culture model using the AlgiMatrix® system was the disintegration of the disc after cell culture and during handling for the fixation, dehydration and paraffin embedding steps. This appeared to be a particular problem with culture periods longer than a week.

The AlgiMatrix® disc is composed of 1, 4 linked β-D mannuronic acid (M) and α-L-glucuronic acid (G) residues which form a mesh by cross-linking with divalent ions such as calcium. Alginates have a high affinity for alkaline earth metals and 3-D structures can be formed in the presence of most divalent cations. In the AlgiMatrix® system, calcium is the cross-linking ion of choice and this can be dissolved by treatment with chelating agents for divalent ions such as EDTA. However alginates have different affinities for divalent cations. Barium has the highest affinity and forms the strongest cross-linkages.[150] With the aim of making the AlgiMatrix® disc more durable throughout the dehydration and paraffin embedding process, the disc was immersed in a 100mMolar solution of barium chloride to reinforce the matrix cross-linkages prior to fixation and paraffin embedding.

CD40 ligand-transfected murine fibroblasts were cultured in a 75cm^2 vented flasks (5% CO_2, 37^{O}C) in complete RPMI media before being trypsinised, washed and resuspended in complete RPMI culture medium. A cell suspension was prepared in RPMI with 10% AlgiMatrix® firming buffer at cell density of 1x10^7/mL. Two AlgiMatrix® sponges were seeded using 500µL of each suspension and then maintained for 7 days (5% CO_2, 37^{O}C) with media changes every 3 days.

After seven days, the culture medium was removed from the well carefully using a pipette and the solution was replaced with 1000µL of 100mM barium chloride in distilled water for 30 minutes prior to fixation for 2 hours in 4% NBF. The disc was then transferred to an embedding cassette and placed in the tissue processor for dehydration and paraffin embedding. The disc was then cut into 10 micron sections which were mounted and stained with haematoxylin and eosin as previously described.

Immersion in 100mmol barium chloride solution for 30 minutes appears to improve the structural integrity of the disc for the fixation, embedding and sectioning steps (Figure 5-8).

Further work is required to establish whether the use this method of matrix reinforcement with barium chloride prior to fixation in its current form has an effect on antigen expression and binding.

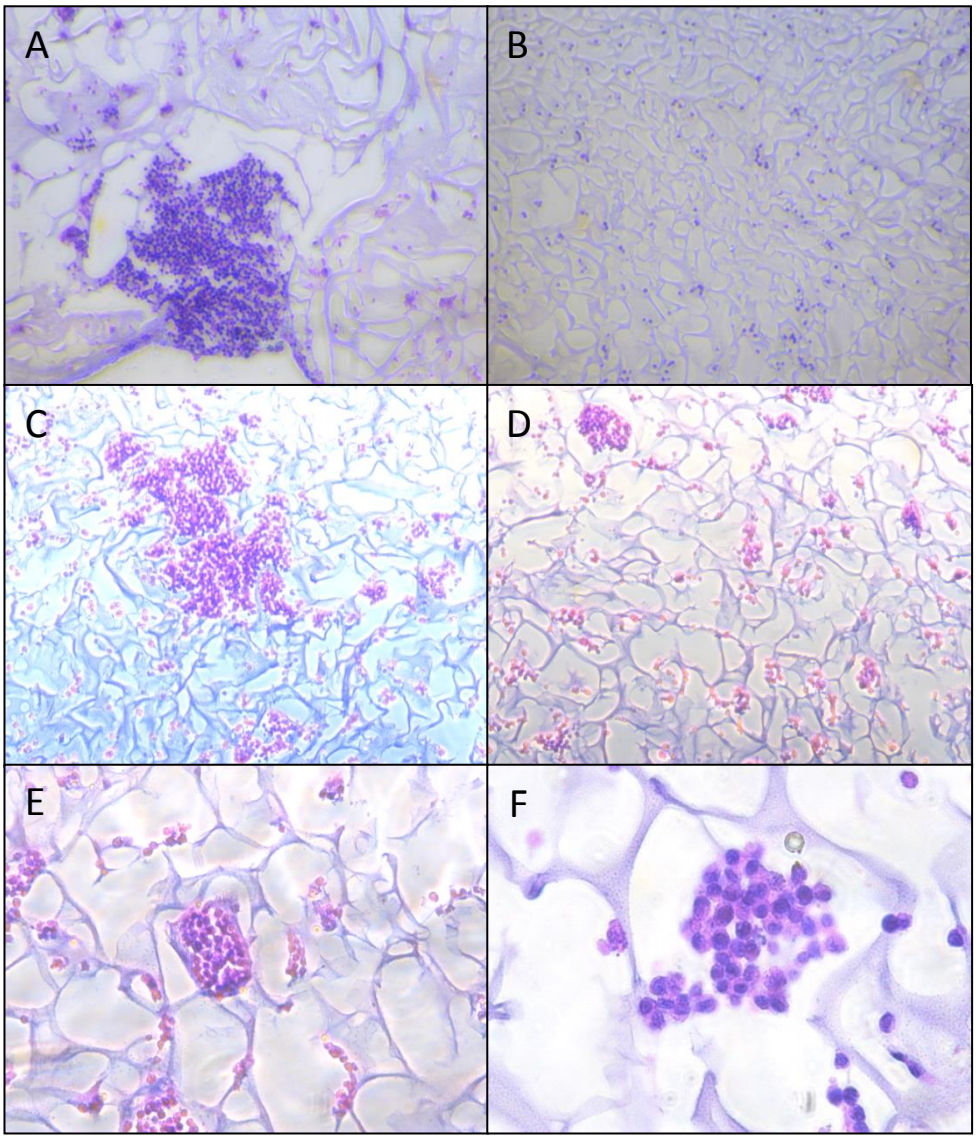

Figure 5.8 Barium chloride fixation of AlgiMatrix disc. Barium Chloride improves cross-linking of 3-Dimensional Alginate Scaffold Prior to Fixation and Preserves Sponge Structure during fixation and paraffin embedding. CD40L-transfected murine bone-marrow stromal cells were seeded onto an AlgiMatrix disc in a standard 24 well culture plate at a density of $1x10^7$/mL. The disc was then maintained at 5% CO_2, 37^oC for 7 days with media change every 3 days. The media was removed and the disc was immersed in a 100mM solution of barium chloride for 30 minutes prior to fixation for 2 hours in 4% neutral buffered formalin, dehydration, embedding in paraffin, sectioning (10 microns) and staining with haematoxylin and eosin. Magnification: A-D x4, E x20, F x40).

5.2.3 Improving Colonisation by increasing the seeding cell density

The AlgiMatrix® manufacturer recommends using a cell suspension with a density of $1x10^6$ cells/mL to seed the disc.[149] However, initial experiments revealed a paucity of stromal and lymphoid cells within the matrix after culture at this cell density.

Explanations for this could include an inability of the cells to penetrate the mesh-work of the matrix or cells falling through the mesh and subsequently colonising the floor of the well. However, on sectioning the disc it is possible to observe small clusters of cells throughout the matrix, suggesting that some cells do penetrate the disc and remain in the mesh.

In order to address this problem and given the better colonisation of the matrix when a higher concentration of cells (marrow buffy coat) was used, an experiment with a series of cell-suspension densities was performed to establish the optimal seeding density.

Three suspensions of CD40 ligand-transfected murine fibroblasts were prepared in RPMI suspension media with 10% AlgiMatrix® firming buffer at cell densities of $5x10^6$/mL, $1x10^7$/mL and $2x10^7$/mL. Three sponges were seeded using 500µL of each suspension and then maintained for 7 days (5% CO_2, 37^{o}C) with media changes every 3 days. After seven days, the culture medium was carefully removed from the well using a pipette and the solution was replaced with 1000uL of 100mM barium chloride for 30 minutes prior to fixation for 2 hours in 4% neutral buffered formalin. The disc was then transferred to an embedding cassette and placed in the tissue processor for dehydration and paraffin embedding. The disc was then cut into 10 micron sections which were mounted and stained with haematoxylin and eosin.

A cell density of 5x106/mL was deemed optimal in terms of colonising the sponge. Seeding densities above this concentration resulted in dense sheets of cells in the peripheries of the sponge with no significant colonisation of the sponge itself (Figure 5-9).

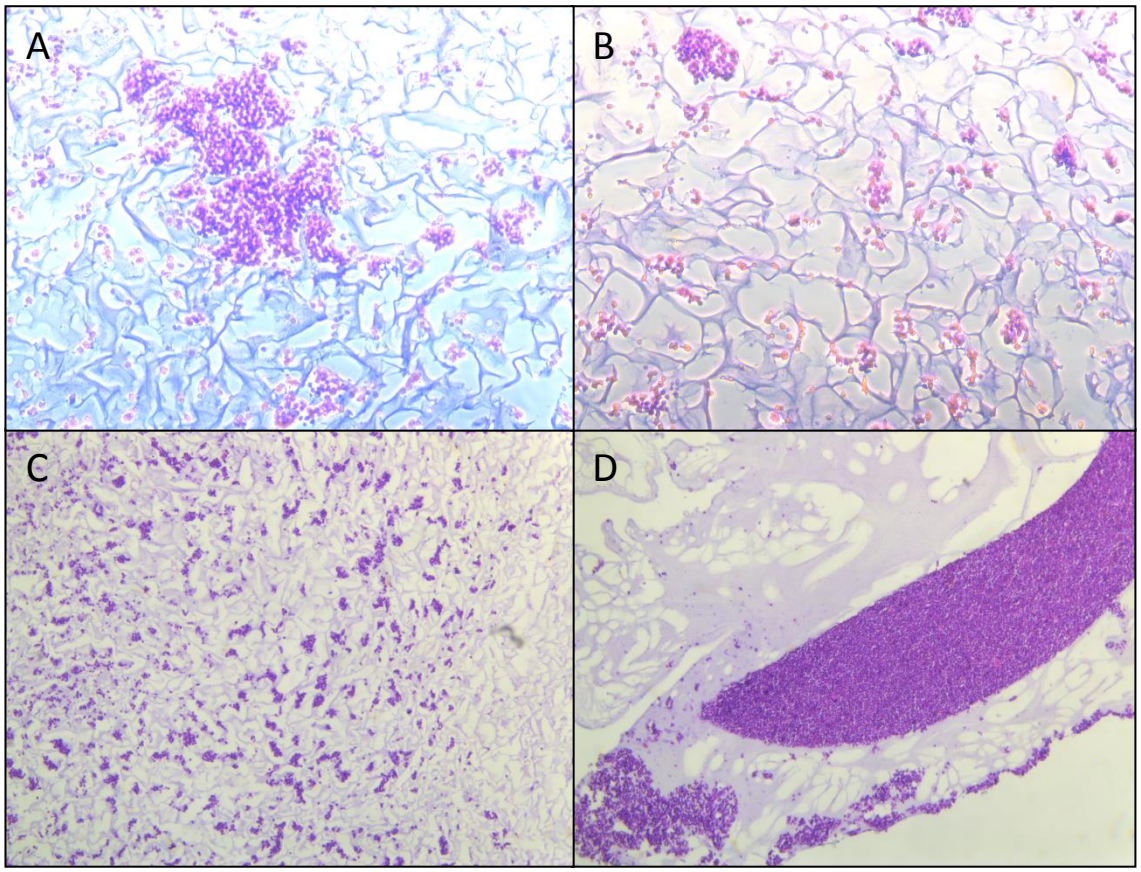

Figure 5.9. Varying the seeding density of stromal cells to improve matrix colonisation. Cell densities above $5x10^6$/mL resulted in dense sheets of cells which did not appear to penetrate the sponge. Three dehydrated alginate sponges were seeded (500µL per sponge) in a 24 well plate at the following cell densities: $5x10^6$/mL $1x10^7$/mL and $2x10^7$/mL. Sponges were then cultured for 7 days (5% CO_2, 37^{o}C) with media change every 3 days before being immersed in 1mM solution of barium chloride for 30 minutes prior to fixation for 2 hours in 4% neutral buffered formalin and embedded in paraffin, sectioned (10 microns) and stained with haematoxylin and eosin. Images A-C: displayed are at a density of $5x10^6$/mL; image D $1x10^7$/mL. (Magnification x4)

5.2.4 Centrifugation to improve distribution of cells through the AlgiMatrix®

Although increasing the density of the cell suspension used to seed the AlgiMatrix® disc appears to improve colonisation of the disc, sectioning reveals the centre of the disc remains largely empty of cells when examined by light microscopy. In an attempt to improve distribution of the cells within the disc, the manufacturer recommends gentle centrifugation of the 24 well-plate holding after seeding.

Two AlgiMatrix® discs were seeded with identical suspensions of human bone marrow fibroblasts from a fresh, ficoll-separated, bone marrow aspirate sample as previously described. The discs were seeded in separate standard 24 well plates. One plate was subjected to gentle centrifugation prior to culture.

Mononuclear cells from a bone marrow aspirate were separated from red cells and plasma by ficoll-separation, washed and resuspended at a density of $5x10^6$/mL in complete IMDM long term culture medium (Dulbecco's Iscove's Modified Dulbecco's Medium (IMDM) containing hydrocortisone ($5x10^{-7}$M); 10% FCS; 10% Horse Serum) containing 10% AlgiMatrix® firming buffer as previously described and subsequently seeded onto two lyophilised AlgiMatrix® discs in separate, standard 24 well plates. One plate was then centrifuged at 500 rpm for 5 minutes prior to incubation. Both plates were then maintained at 5% CO_2, 37^oC for seven days with media changes every 3 days before being fixed for 2 hours in 4% neutral buffered formalin, embedded in paraffin, sectioned (10 microns) and stained with haematoxylin and eosin.

Gentle centrifugation does not appear to enhance distribution throughout the disc. Diffuse colonisation is observed throughout the sections using both centrifuged and uncentrifuged methods with two different patient samples (Figure 5-10).

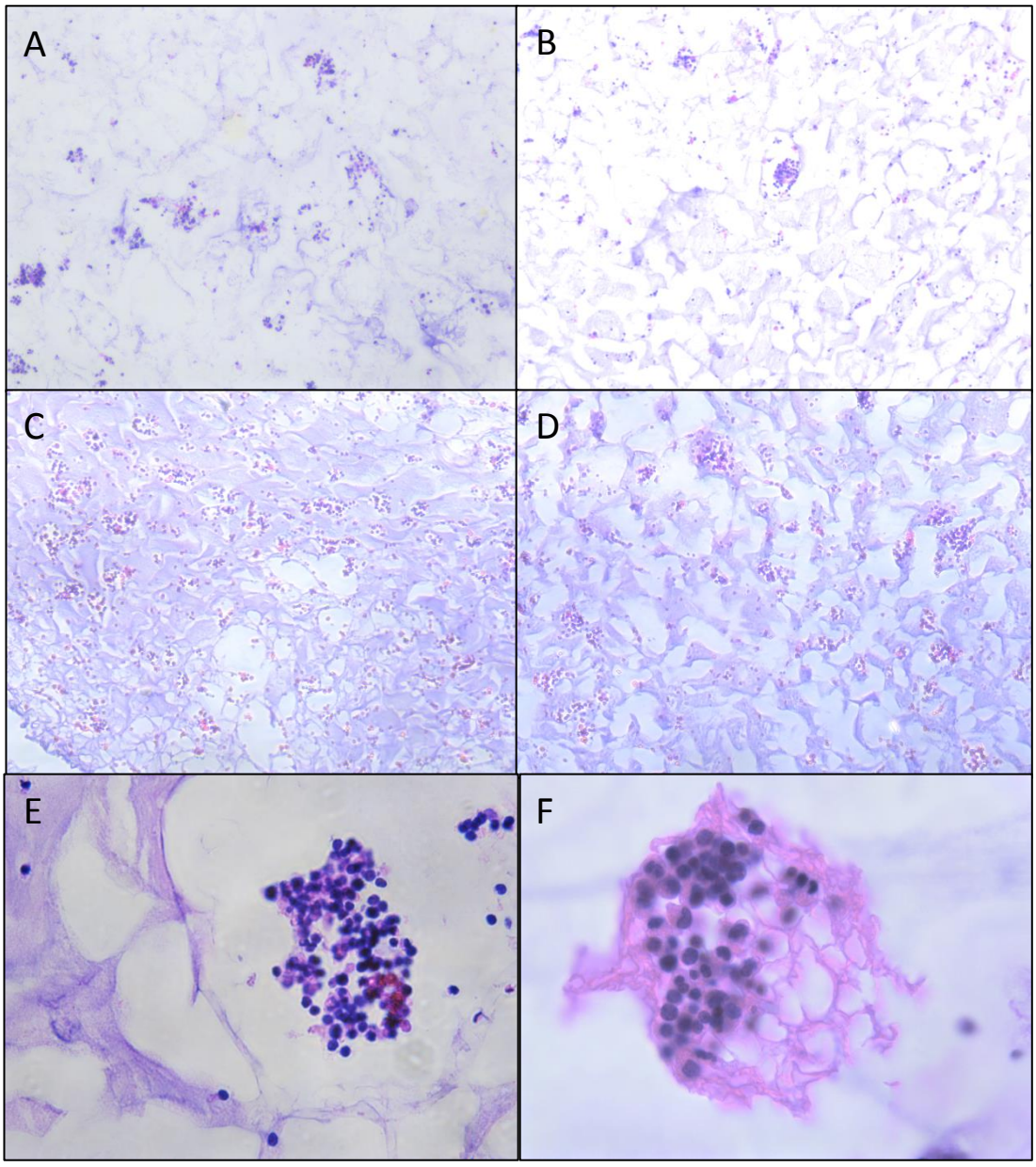

Figure 5.10 Distribution of cells within the AlgiMatrix® following centrifugation. Images A, C, E are from uncentrifuged discs; images B, D, F are from centrifuged discs. Gentle centrifugation does not appear to enhance distribution throughout the disc. Diffuse colonisation is observed throughout the sections using both centrifuged and uncentrifuged methods with two different patient samples. Human PBMCs isolated from fresh bone marrow aspirate were seeded onto two lyophilised AlgiMatrix® discs at a density of $5x10^6$/mL in long-term IMDM culture medium with 10% firming buffer in separate standard 24 well plates. One plate was then subjected to centrifugation at 500 rpm for 5 minutes before both plates were maintained at 5% CO_2, 37°C for seven days with media changes every 3 days before being fixed for 2 hours in 4% neutral buffered formalin, embedded in paraffin, sectioned (10 microns) and stained with haematoxylin and eosin.

5.2.5 Fibronectin to aid adhesion to the AlgiMatrix®

Given the evidence from the previous chapter of MCL cells dependence on interactions with CD40-ligand and accessory cells for survival and proliferation, an experiment was designed to culture both primary MCL cells and stromal cells together using the AlgiMatrix® 3-D system. In this experiment, colonisation and visualisation of discs was performed using PBMCs from a patient with aggressive, nodal MCL together with CD40 ligand-transfected murine fibroblasts.

Primary MCL cells from a proliferative case were selected because it was postulated that cells from a more aggressive case would proliferate more rapidly within the culture system.

Fibronectin (FN) is a large, cell-surface and plasma protein which is important for cell adhesion, migration and proliferation Adherent cells constitutively produce FN and deposit it into the ECM which further aids adhesion and has been demonstrated to stimulate proliferation in human fibroblasts.[151]

In order to enhance adhesion and proliferation within the AlgiMatrix® system, FN was also added at a concentration of 25µg/mL to the seeding solution for this and subsequent experiments.

In order to ensure that the cells retrieved from the culture system at the end of incubation were from the disc and not the floor of the well, the disc was suspended in culture medium on a 5 micron filter and immersed in complete RPMI culture medium within the well of a 6 well plate. At the end of a 10 day culture period, the disc structure was reinforced with barium chloride, fixed and processed as previously described.

CD40-ligand-transfected murine fibroblasts were suspended in complete RPMI medium at a density of $5x10^6$ cells per sponge (density based on the optimum seeding density observed in the previous experiment) containing10% firming buffer as previously described. In addition, 100µL of 1:40 FN was added to the seeding suspension. A lyophilised AlgiMatrix® disc was seeded with 500µL of the cell suspension and the disc was transferred to a 5-micron filter and inserted into a well of a standard 6 well plate before being immersed in complete RPMI medium. The disc was maintained at 5% CO_2, 37^oC for 10 days to allow stromal cell colonisation.

Primary MCL PBMCs were purified from peripheral blood and cryopreserved as previously described. The PBMCs from subject MCL016 (an aggressive MCL case) were thawed and resuspended in RPMI medium at a density of $1x10^7$/mL in before being seeded onto the AlgiMatrix® disc and maintained at 5% CO_2, 37^oC for a further 5 day incubation period. The disc was then transferred to the well of a standard 24 well plate and immersed in 100mM BaCl for 30 minutes prior to fixation for 2 hours in 4% neutral buffered formalin, dehydration, paraffin embedding and sectioning (10 microns per section) and staining with haemotoxylin and eosin.

Aggregates of small lymphocytes with basophilic nuclei admixed with lighter-coloured purple stromal cells are visible in the stained sections demonstrating the feasibility of culturing primary MCLs together with murine stromal cells in the 3-D model (Figure 5-11).

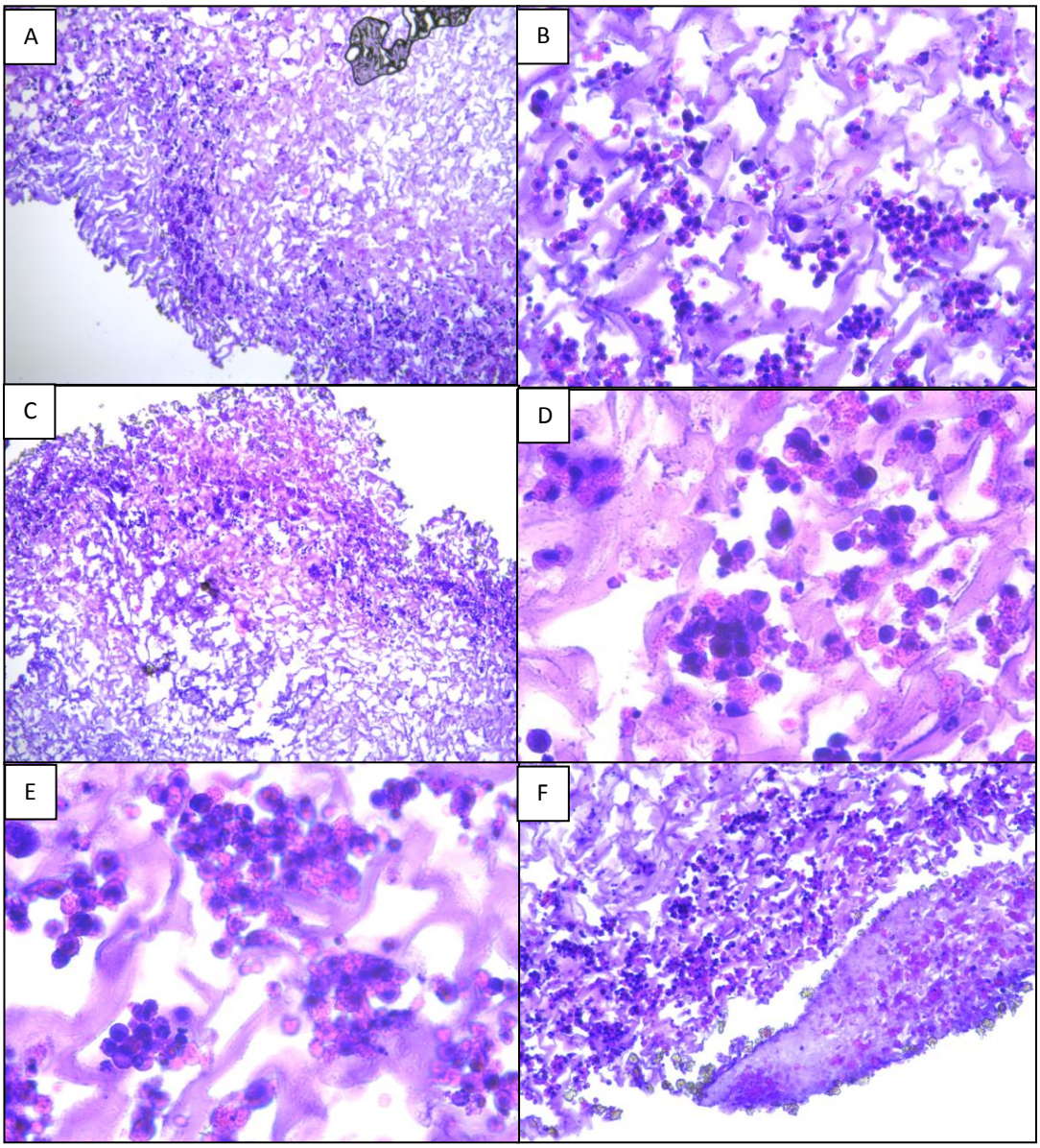

Figure 5.11 Co-culture of murine fibroblasts with primary human MCL cells for 5 days with the addition of fibronectin. MCL cells from subject MCL016 (aggressive, nodal MCL) were cultured with CD40-L transfected murine stroma with fibronectin (25µg/mL) for 5 days on AlgiMatrix® discs in 5 micron filters immersed in complete RPMI culture medium before being reinforced with barium chloride solution, fixed, paraffin embedded and sectioned and stained with haematoxylin and eosin. (Note aggregates of small lymphocytes with basophilic nuclei admixed with lighter-coloured purple stromal cells) (Mag. A x4, B x20, C x4, D & E x40, F x10)

5.3 Cell retrieval

According to the manufacturer, one of the potential advantages of using the AlgiMatrix® system as a model for studying MCL cells in 3-D culture is the option of cell retrieval from the matrix via non-enzymatic degradation of the matrix after culture.[149]

In order to test whether MCL cells could be retrieved from AlgiMatrix® and analysed for cell surface markers, rates of proliferation and apoptosis after culture the following experiment was performed. Two AlgiMatrix® discs were seeded with CD40L-transfected murine stromal cells at a density of $5x10^6$/mL in complete RPMI medium with 10% firming buffer. The sponges were allowed to settle for two hours before 200µL of complete RPMI medium was gently added in order to prevent drying out during incubation. Discs were then incubated for 24 hours at 37°C, 5% CO_2.

Two cell suspensions at a density of $5x10^6$/mL of primary MCL cells from two different cases (MCL16, nodal case and MCL07, leukaemic case) were prepared in complete RPMI media.

The sponges were retrieved from the incubator; excess media was removed from the well of each sponge by careful pipetting. The stromal-seeded discs were then seeded with 500µL of the MCL cell suspension by pipetting onto the disc within the well of the 24 well plate. To a second disc for each case, the disc was seeded with MCL cells alone in RPMI complete medium containing 10% firming buffer as previously described.

All discs were then dynamically seeded by centrifugation (100G for 4 minutes) before being returned to the incubator for 3 days.

On day 5 the sponges were retrieved from the culture wells and transferred to sterile empty wells on the same plate. 1mL of non-enzymatic dissolving buffer (provided by

Gibco ready for use) was added directly onto each disc to fully submerge the disc as per manufacturer's instructions. The discs were dissolved for 5 minutes. The discs visibly degraded within 5 mins and were completely degraded after 10 mins. The now liquid contents of the well were transferred to a sterile centrifuge tube, and 1000µL of complete RPMI culture medium was added before centrifugation at 1600rpm for 5 minutes to pellet the released cells. The supernatant was removed and the cells were resuspended in complete RPMI media and adjusted to an approximate density of $5x10^6$/mL of PBMCs and $5x10^6$/mL of stromal cells.

Three sterile 1.5mL Eppendorf tubes containing the following antibodies and reagents were prepared for each sample:

1. Unstained
2. Isotype controls
3. FITC-AV, CD5 PE and CD19 APC;

100µL from each cell suspension was then added to each tube and incubated in the dark for 20 minutes before flow cytometry was performed.

The forward / side scatter plots and mean fluorescent intensity peaks for cells from subjects MCL07 and MCL16 after cell retrieval from culture in AlgiMatrix® with murine stroma are displayed in Figures 5-12 and 5-13. The cells have been labelled with fluorochrome-labelled anti-CD 5 and 19 antibodies, corresponding isotype controls and annexin V FITC after cell retrieval.

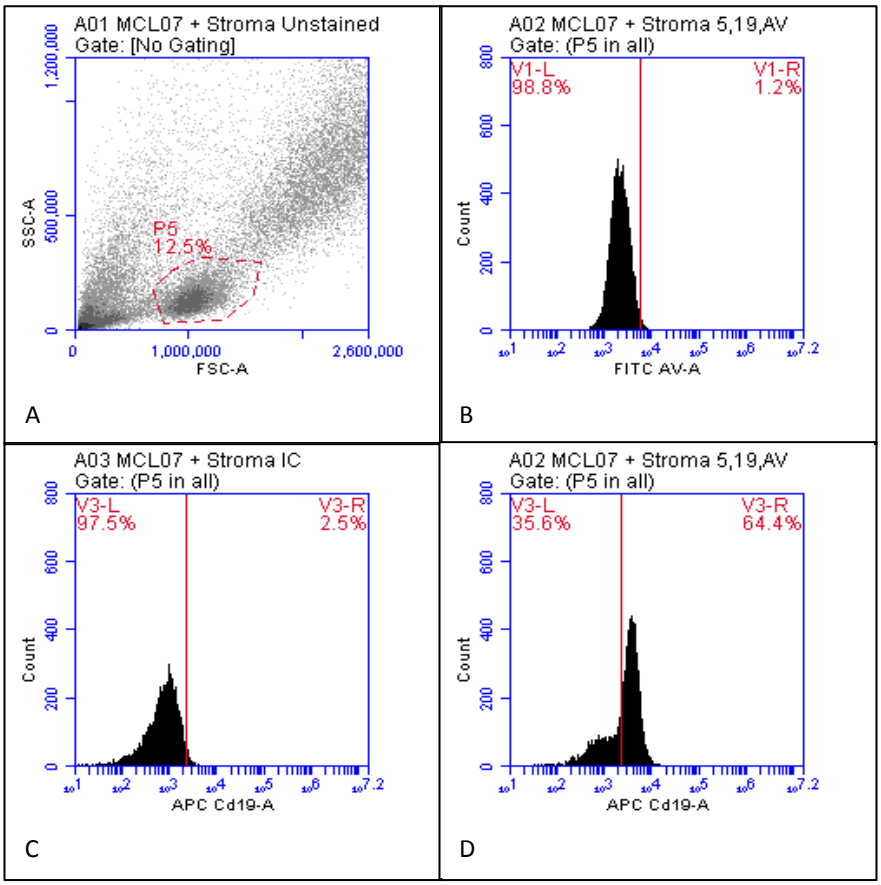

Figure 5.12 MCL peripheral blood mononuclear cells can be retrieved from the AlgiMatrix® disc and visualised by flow cytometry for labelled surface markers and annexin-V expression after co-culture with murine stromal cells. The forward / side scatter plot (A) and mean fluorescent intensity peaks for MCL07 after cell retrieval from culture in AlgiMatrix® with murine stroma are displayed (B-D). The cells have been labelled with APC-conjugated anti-CD19 (D) and corresponding isotype control (C) plus annexin V FITC (B) after cell retrieval from the matrix using non-enzymatic degradation after 3 days co-culture with CD40L-transfected murine stroma. A distinct and viable population of CD19 positive MCL cells can be seen, demonstrating the ability to label and analyse surface markers on PBMCs after culture in the AlgiMatrix® 3-D system.

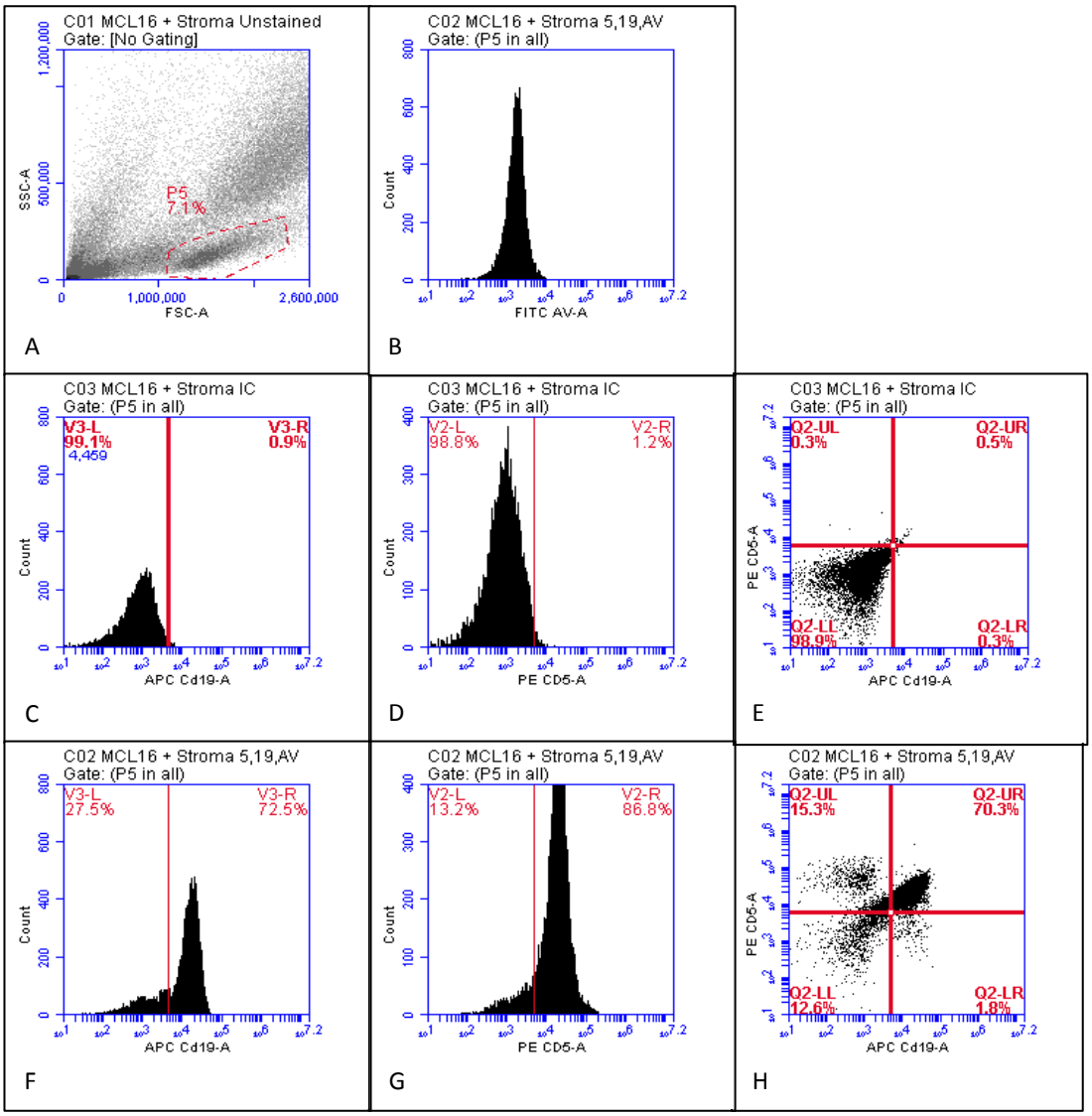

Figure 5.13 Primary MCL cells from subject MCL16 retrieved from the AlgiMatrix® disc and visualised by flow cytometry for labelled surface markers and annexin-V expression after co-culture with murine stromal cells. The forward / side scatter plot (A) and mean fluorescent intensity peaks for MCL16 after cell retrieval from culture in AlgiMatrix with murine stroma are displayed (C-H). The cells have been labelled with APC-conjugated anti-CD19 (F) and PE-conjugated anti-CD5(G) and corresponding isotype controls (C & D) plus annexin V FITC (B) after cell retrieval from the matrix using non-enzymatic degradation after 3 days co-culture with CD40L-transfected murine stroma. A distinct and viable population of CD 5 / 19 positive MCL cells can be seen (H) in contrast to isotype controls (E), demonstrating the ability to label and analyse surface markers on PBMCs after culture in the AlgiMatrix® 3-D system.

A distinct and viable population of CD5 / CD19 positive MCL cells can be observed in Figure 5-13 and CD19 positive cells in Figure 5-12 (MCL07 did not express CD5). This demonstrates that surface markers can be preserved and analysed by flow cytometry on MCL cells retrieved from the AlgiMatrix® system to identify and distinguish the cells from other cells cultured simultaneously.

5.4 Alternative 3D model systems

In addition to the AlgiMatrix® method explored above, the hanging drop method was explored using primary lymphocytes from a patient with CLL. CLL cells were used in this section because, unlike primary MCL cells, there is good evidence that these cells survive and proliferate more readily without stromal support and were therefore deemed more suitable to use as cell type in exploratory experiments.[92]

The hanging drop method involves the culture of large cellular spheroids formed by aggregation of tumour cells from a suspension within a "hanging drop" of liquid media or within a flask of medium which rotates to prevent adhesion.[138] Suspended cells cluster and aggregate and can re-establish contact-dependent interactions.

5.4.1 Hanging Drop Culture

In this experiment a cell suspension of PBMCs from a patient with untreated CLL were ficoll-separated from red cells and plasma and prepared at density of $1x10^6$ cells per mL in complete RPMI media. In order to establish the optimal seeding density for the hanging drops a series of dilutions of the cell suspension were prepared ($2x10^3$, $10x10^3$, $20x10^3$, $30x10^3$, $40x10^3$, $50x10^3$/50µL).

50µL of each dilution was carefully pipetted on to the underside of a 96 well plate within the condensing rings of individual wells. The lid was then gently inverted so the drops hung upside down and stacked on top of another lid before being returned to the incubator. Because the overall drop volume was small, significant evaporation and drying out while being incubated at 37°C, 5% CO_2 was anticipated. The drops were therefore topped up with 20µL of warm RPMI media twice daily (Figure 5-14).

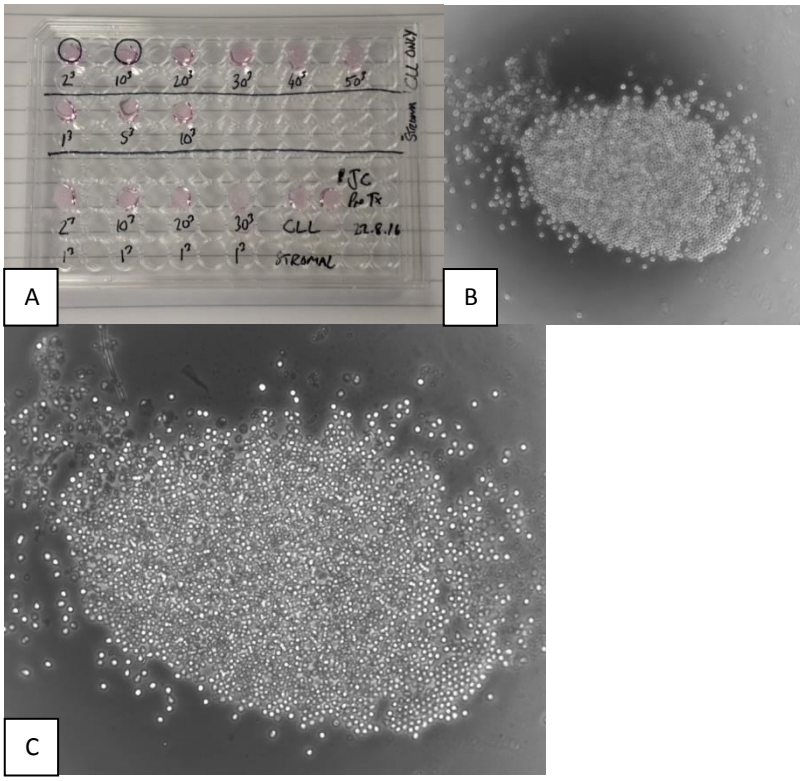

Figure 5.14 Initial hanging drop method experiment with primary CLL cells. Top left: the lid of a 96 well plate with hanging-drops seeded onto the under-side of the lid within the condensing ring of each well (A). B: hanging drop with $1x10^4$ cells visualised by phase-contrast microscopy (10x magnification) after 24 hours of culture. C: hanging drop with $1x10^4$ cells after 24 hours of culture (20x magnification).

An example of the initial hanging drop method experiment is displayed in Figure 5-14. A cell density of $1x10^4$ cells per 50µL appeared to yield a reasonable sized aggregate of CLL cells.

5.4.1.1 Problems Encountered with the Hanging Drop Method

Initially, the drops in the $40x10^3$ and $50x10^3$ wells lost surface tension and ran into the adjacent wells. Therefore a volume of 50µL appears to be vulnerable to loss of surface tension in this system. Secondly, despite twice daily media top-ups, the drops evaporated significantly overnight when cultured by this method.

Maintaining drop integrity whilst performing media top-ups was difficult because media top ups required the surface tension of the drop to be broken when

replenishing with culture medium. It was also difficult to accurately estimate the amount of medium required to replenish the drop: too little increased the risk of excess evaporation overnight; too much risked breaking the surface tension of the drop and causing it to smear across the plate.

Finally, this method required the lid of the 96 well plate to be rested upon the upturned lid of another plate. Because these surfaces were not compatible, risk of upsetting the plate on transfer or in the incubator was high and this could lead to disastrous evaporation. This method was therefore abandoned.

5.4.1.2 Revised Hanging Drop Method

In this method, three separate cell suspensions were prepared in RPMI at a cell density of $3x10^4$/mL, $3x10^5$/mL and $3x10^6$/mL using primary CLL cells from the same untreated subject. Smaller (40µL) drops of CLL cells suspended in RPMI media were carefully pipetted onto the upturned lid of a petri culture dish within the laminar flow cabinet. Provided the drops were not in contact with each other, a large number, 20 – 30 could be pipetted onto the same plate with ease (Figure 5-15).

In order to prevent excess evaporation during incubation, a humidity reservoir of 10mLs of sterile PBS was added to the culture dish before the lid was smoothly and moderately quickly inverted and placed onto the dish before incubation.

The drops were incubated for 48 hours and inspected for CLL cell aggregation / spheroid formation at 24 and 48 hours. Images taken after 24 hours by phase contrast microscopy are displayed below (Figure 5-16).

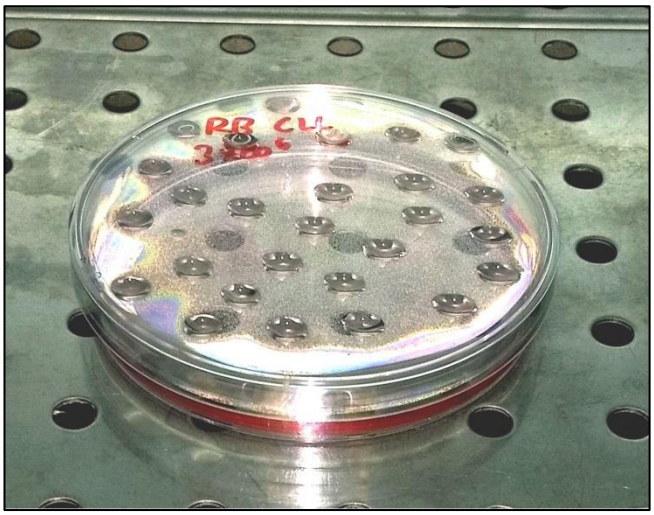

Figure 5.15 Revised hanging drop method in which 40µL drops of CLL cell suspension in RPMI were carefully pipetted onto the underside of the lid of a standard petri dish before careful inversion and replacement on the dish. A 10mL humidity reservoir containing sterile 1x PBS was added to the dish before incubation.

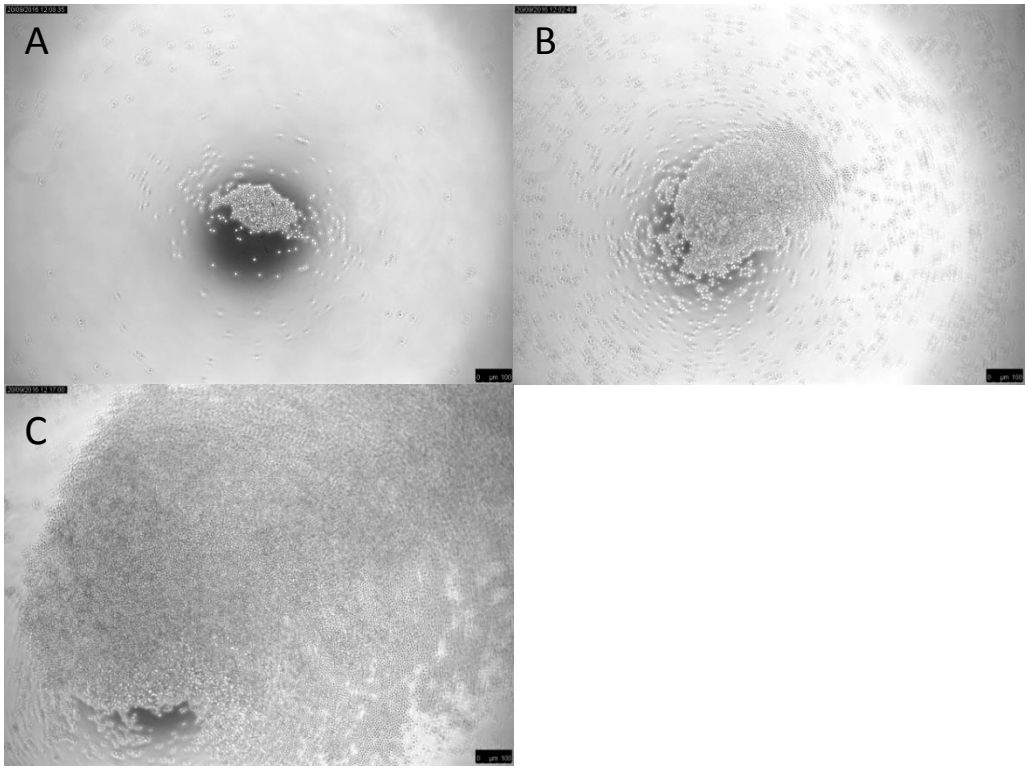

Figure 5.16 Images of hanging drops taken at 24 hours using revised method. Primary CLL cells were ficoll separated and suspended in complete RPMI before dropping onto the underside of a sterile petri-dish lid in 40µL volumes. The lid was inverted and replaced on the dish containing a 10mL humidity reservoir prior to incubation. Cells were suspended at a density of $3x10^4$/mL (A) $3x10^5$/mL (B) and $3x10^6$/mL (C) (magnification 10x).

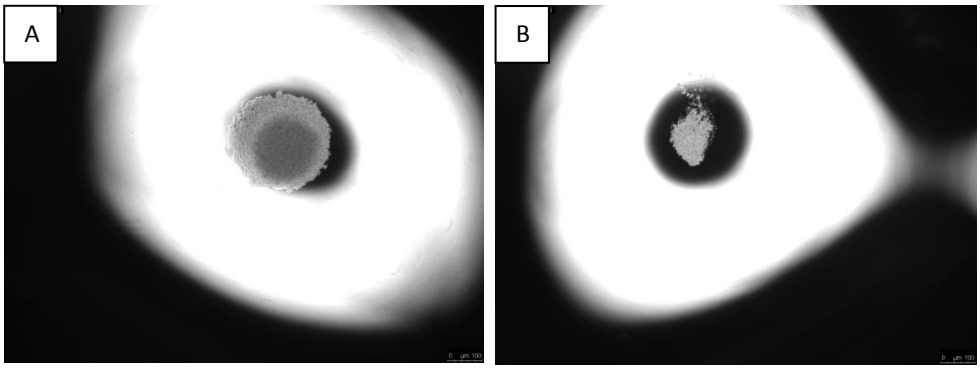

Figure 5.17 Primary CLL cells cultured by revised hanging drop method after 56 hours at density of 3x10^6 (A) and 3x10^5 (B) demonstrate aggregates of cells within the drop. (Cells visualised at 2.5x by phase-contrast light-microscopy).

5.4.1.3 Viability of CLL cells cultured in hanging drops for 5 days using second method

After five days of culture using this method, there was no evidence of significant evaporation or contamination. The lids were inverted in the laminar flow hood and 500µL of sterile PBS was used to wash the drops into the bottom of the angled lid. The resulting cell suspension was collected into a 15mL falcon and a cell count was performed. Negligible numbers of cells were observed in the $3x10^4$/mL suspension. From the $3x10^5$/mL suspension, approximately $5x10^4$ cells were harvested and $1x10^6$ cells were harvested from the $3x10^6$/mL suspension. The resulting cell suspensions were analysed by flow cytometry. The scatter plot characteristics of cells retrieved from hanging drop culture after 5 days are displayed in Figure 5-18. This shows that at both cell densities there is a similar degree of apoptosis/cell death represented on the plots in the area outlined in blue. This suggests that the cell density and culture time requires further optimisation to improve cell viability.

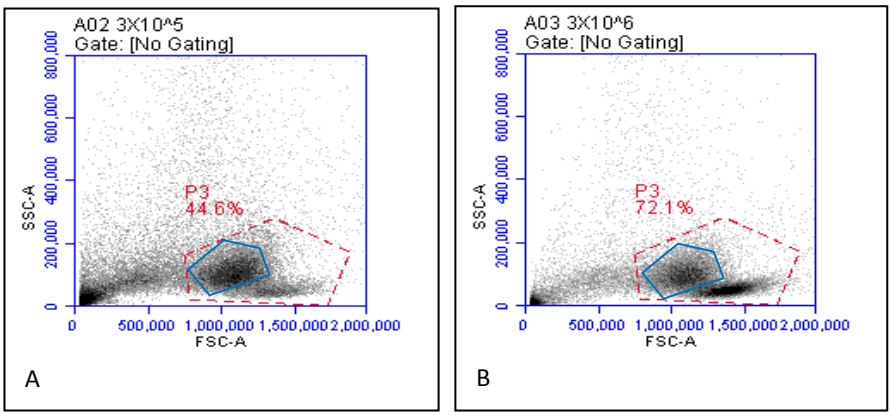

Figure 5.18 Flow cytometry scatter plots for CLL cells reovered from culture in hanging drops. Viability of cells recovered following culture in hanging drops is similar at both cell density concentrations, shown in the plots in the area outlined in blue. Primary CLL cells were cultured for 5 days in hanging drops at different cell densities, cells were harvested and assessed by flow cytometry. Cells cultured at $3x10^5$/mL (A) have similar scatter plot characteristics to those cultured at 3×10^6/ml (B) suggestive of similar rates of apoptosis.

5.5 Discussion

5.1.7 Culturing stromal and MCL cells in 3-D model alters cell morphology and proliferation rates

Observation of phase contrast images of stromal cells cultured in 3-D versus 2-D highlighted differences in both morphology and rates of proliferation. Culture of cells on 2-D surface results in flat cells through simple geometry – there is only one surface on which the cells can adhere resulting in a default, apical-based polarity. The observed stromal cells in the 2-D system were flat spindle shaped cells compared to the development of small spheroidal clusters of cells observed in the 3D system (Figure 5-2). This was effectively demonstrated by phase contrast light microscopy during the culture period but was not clearly demonstrated by the fixed, stained sections, mainly due to a paucity of cells at this stage.

Colonisation and proliferation rates of stromal cells also appeared lower than expected in the 3-D culture system in comparison to the 2-D system, particularly for the murine

stromal cells which proliferate rapidly in 2-D culture. This was an unexpected finding as other studies have demonstrated that 3-D culture increases rates of proliferation of tumour cells, in part due to adhesion-receptor-dependent changes in intracellular signalling.[152,153]

When G519 MCL cells were cultured in isolation within the AlgiMatrix® disc, microscopic phase contrast examination revealed the formation of spheroid clusters after 21 days of culture but proliferation rates within the matrix appeared slower than expected when compared to cells grown in suspension culture (Figure 5-4). The prolonged culture time required also led to deterioration in disc integrity. The disc was rendered extremely fragile and disintegrated during transfer to the paraffin embedding cassette therefore sectioning and staining was not possible.

When human marrow fibroblasts were cultured within the AlgiMatrix® system, although colonisation is apparent (Figure 5-6), cell numbers are poor suggesting the microenvironment is hostile to human stromal cell proliferation. Unfortunately the matrix integrity was again degraded after 6 days culture following the fixation, paraffin embedding and staining process.

When a higher density of cells was used including the whole buffy coat from ficoll separation, multiple aggregates of bone marrow cells were observed throughout the disc after 6 days of culture (Figure 5-7).

The formation of spheroids is a well-recognised characteristic of tumour cells in 3-D cell culture and usually increases proliferation rates and cellular drug resistance through upregulation of transcription pathways through activation of surface adhesion molecules.[128,138,154] Possible explanations for the slow proliferation rates observed were a failure of cells to migrate into and adhere to the matrix during the seeding

stage and a lack of cell-cell contact, both of which are important factors in survival and proliferation of tumour cells in 3-D culture.[155–158]

Higher stromal cell densities for seeding the matrix; the addition of extracellular matrix proteins to aid adhesion, such as fibronectin and different seeding techniques may be required are areas which require further exploration in order to optimise proliferation and survival within this model.

5.5.1 Increasing the seeding cell density from $1x10^6$/mL to $5x10^6$/mL appears to improve colonisation of the AlgiMatrix® 3-D system

The AlgiMatrix® manufacturer recommended using a cell suspension with a density of $1x10^6$ cells/mL to seed the disc.[149] However, initial experiments revealed a paucity of stromal and lymphoid cells within the matrix after culture at this cell density.

In order to address this problem and given the better colonisation of the matrix when a higher concentration of cells (marrow buffy coat) was used, an experiment with a series of cell-suspension densities was performed to establish the optimal seeding density.

A cell density of $5x10^6$/mL yielded optimal results in terms of disc colonisation. Seeding densities above this concentration resulted in dense sheets of cells in the peripheries of the sponge with no significant colonisation of the sponge itself (Figure 5-9).

5.5.2 Centrifugation of the AlgiMatrix® Disc does not appear to improve colonisation

Although increasing the density of the cell suspension used to seed the AlgiMatrix® disc appeared to improve colonisation of the disc, sectioning revealed the centre of the disc remains largely empty of cells when examined by light microscopy. In an

attempt to improve distribution of the cells within the disc, the manufacturer recommended gentle centrifugation of the 24 well-plate holding after seeding.

However, gentle centrifugation (500 rpm for 5 minutes prior to incubation) did not appear to enhance distribution throughout the disc in these experiments. Diffuse colonisation was observed throughout the sections using both centrifuged and uncentrifuged methods with two different patient samples (Figure 5-10).

5.5.3 Co-culture of primary MCL cells with stromal cells is possible within the AlgiMatrix® system

Given the evidence from the previous chapter of MCL cells dependence on interactions with CD40-ligand and accessory cells for survival and proliferation, an experiment was designed to culture both primary MCL cells and stromal cells together using the AlgiMatrix® 3-D system. After a 5 day incubation period, aggregates of small lymphocytes with basophilic nuclei admixed with lighter-coloured purple stromal cells were visible in the stained sections demonstrating the feasibility of culturing primary MCLs together with murine stromal cells in the 3-D model (Figure 5-11).

5.5.4 Optimising AlgiMatrix® disc integrity prior to sectioning and staining

Optimising the conditions for disc fixation, embedding, sectioning and staining was one of the challenges encountered in the 3-D culture model and significant progress was made in fixation and reinforcement of the disc structure.

Fixation times vary depending on tissue thickness and density. In the initial experiments on AlgiMatrix, after 6 days of culture, the disc was fixed with PFH overnight. However, after twelve hours, the tissue was friable and broke up, even with careful handling.

Because there were no calcified or fibrous components in the tissue, a shorter fixation time of 2 hours was tested and appeared to be adequate in terms of balance between maintaining the integrity of the tissue and allowing adequate fixation to prevent degradation of the sections over time. However, because no antigen labelling was performed in these experiments, further work is required in establishing the optimal time for fixation for epitope preservation.

5.5.5 AlgiMatrix® disc reinforcement with barium chloride improved disc integrity

Prolonged incubation times also had detrimental effects on the disc integrity causing deterioration during the fixation and embedding phases. Images from light-microscopy of the stained sections demonstrated suboptimal preservation of the structure following tissue processing (Figure 5-3). With the aim of making the AlgiMatrix® disc more durable throughout the dehydration and paraffin embedding process, the disc was immersed in a 100mMolar solution of barium chloride to reinforce the matrix cross-linkages prior to fixation and paraffin embedding. This appeared to improve the structural integrity of the disc for the fixation, embedding and sectioning steps (Figure 5-8).

Further work is required to establish whether the use this method of matrix reinforcement with barium chloride prior to fixation in its current form has an effect on antigen expression and binding.

5.5.6 Cell retrieval from the AlgiMatrix® disc is possible using non-enzymatic degradation.

After 5 days of co-culture of primary MCL cells with murine stromal cells, the discs were dissolved using non-enzymatic dissolving buffer (*Gibco*). The discs visibly degraded within 5 minutes and were completely degraded after 10 minutes.

Fluorescein associated cell sorting of the resulting cell suspension demonstrated a distinct and viable population of CD5 / CD19 positive MCL cells (Figures 5-12 and 5-13). This demonstrates that surface markers can be preserved and analysed by flow cytometry on MCL cells retrieved from the AlgiMatrix system to identify and distinguish the cells from other cells cultured simultaneously.

5.5.7 Hanging Drop Method

Culturing primary CLL cells within the hanging drop method demonstrated the formation of aggregates of viable cells when the revised method using a 9cm diameter petri dish with a humidity reservoir was used. FACS analysis of cells retrieved from hanging drop culture after 5 days are displayed in Figure 5-17. Despite the significant apoptosis seen in these cultures it shows that viable cells can be recovered. Optimisation of the cell culture conditions, cell density and culture length however is required.

6. CHAPTER 6. Summary and Discussion

This thesis represents a significant body of work on the characterisation of the behaviour of primary cells from what is a relatively rare disease. Compared with other studies in this field, this is one of the largest case sets of primary MCL cases characterised and studied *ex vivo*.

6.1.1 Developing a 2-D model for primary MCL culture

One of the most striking observations from a general perspective is how differently these cases behave *ex vivo*. The observation that, on the whole, survival is better and proliferation rates are lower *ex vivo* in cells from the indolent leukaemic cases is not surprising, given the indolent nature of the disease in these subjects. However there is also significant heterogeneity in the survival and proliferation rates observed in some of the aggressive cases which may underline the fact that characteristics of indolent and aggressive MCL are not very well defined in the literature and outcomes do vary between cases. The marked genetic heterogeneity of MCL has already been alluded to, with some cases carrying the t(11;14) chromosomal aberration in isolation whereas others also carry mutations in key genes such as p53 and SOX-11.[21,22] Future work may include further definition of the genetic and molecular-genetic profile of the cases studied here in order to establish any patterns between molecular genetics, clinical phenotype and rates of survival and proliferation in our *ex vivo* system.

One of the primary aims of this thesis was to develop a model which reflects the *in vivo* lymphoma microenvironment for *in vitro* study. Significant progress has been made in this regard. Initially it was noted that MCL cells from peripheral blood generally require an accessory cell for sustained survival and proliferation, probably due to

stromal cell secretion of pro-survival cytokines such as granulocyte-macrophage colony stimulating factor (GM-CSF), IL-6 and B-cell activating factor.[39,159,160]

Both murine and human stromal layers appear capable of supporting survival and proliferation. However when murine stroma are used, this study has demonstrated that additional CD40 signalling is necessary in order to sustain survival and growth, especially in the nodal, proliferative cases.

The costimulatory signal of the CD40 synapse is well recognised as a necessary signal for the initiation and progression of adaptive immune response and as a necessity for normal B-cell proliferation.[45,62] However previous studies have demonstrated diverse outcomes of malignant B-cells after CD40 ligation. For example, in Burkitt's lymphoma, a tumour of the germinal centre, CD40 ligation results in FAS-induction and initiation of apoptosis.[46] Cell growth is also directly suppressed by CD40 ligation in other aggressive forms of B-cell lymphoma.[47] However, in more indolent forms, such as CLL, CD40 ligation can inhibit apoptosis and prolong cell survival *in vitro*.[48] A positive role for CD40-L in MCL cells has been demonstrated previously in a small number of cases and has been shown to facilitate entry into the S-phase of the cell cycle.[49] In this study, the CD40-ligand appeared critical for sustained survival and proliferation in many but not all of the cases but particularly the nodal / aggressive ones. The reasons for the varied responses to CD40-L observed here are not known, and would be a consideration for future work; however, on the whole, CD40-ligation appears to have a positive effect without any obvious detrimental effects and should probably be incorporated into a model for the study of MCL *ex vivo* when murine stromal cells are used.

The addition of IL-4 is known to stimulate the clonal expansion and continued proliferation of normal B cells in association with CD40 ligation. [62] This may be due to the activation of pro-survival protein transcription.[60,61] However, the impact of IL-4 in B-NHL proliferation is also controversial. In some studies, IL-4 has demonstrated an inhibitory effect on proliferation of human NHL cases.[161] Whereas others demonstrate that proliferation of CLL cells can be induced in the presence of IL-4 and CD40 agonists.[162] In this study, IL-4 with CD40L appears to have a uniformly positive effect and significantly enhances survival of primary MCL cells *ex vivo* supporting and augmenting data already published on a small series of MCL cases and suggesting an ongoing role for IL-4 and CD40-ligation in the development of a model for MCL culture *ex vivo*.[49]

Toll-like receptor-9 ligation did not appear to enhance the culture model for primary MCL cases in this study. In fact, survival was significantly impaired and no significant effect on proliferation was noted. Although TLR9 ligation is well known to increase proliferation in CLL cells,[163,164] the response is mixed in other B-NHL subtypes and previous data sets have shown no increase in proliferation in MCL cells.[165] This, large data set reflects this pattern and it is therefore unlikely that TLR9-ligation would make up part of future work on this model of MCL study.

Only a very limited amount of data is available from this study on the culture of primary MCL cells on human stroma. The results, however, were promising in terms of survival and the use of human stroma as a culture model would definitely be part of the future work.

The higher intrinsic rate of apoptosis exhibited by the primary MCL cells from the more nodal and proliferative clinical cases is an interesting observation and may represent a

more mutated and unstable MCL genotype compared with the more indolent cases. This remains to be established and would be an interesting hypothesis to pursue in future work.

6.1.2 Profiling the cellular adhesion molecules of primary MCL cells

The profiling of CAMs has been performed on primary, peripheral blood MCL cells from 17 cases with paired bone marrow and peripheral blood adhesion profiles in four cases. Again, this is a large case series for MCL, a relatively rare disease, and significantly augments the literature on CAM expression.[28,76]

In this series, CD11a, CD49d and CD54 were consistently expressed at a high level. CD11a, which forms part of the LFA-1 molecule, is thought to facilitate adhesion to FDCs via ICAMs 1-3. LFA-1 is normally expressed by reactive B-cells in lymph nodes and variably expressed in NHL lymphocytes.[110] The relatively high expression of CD11a seen here corresponds with greater expression observed in other nodal diseases such as SLL and DLBCL.[116] This in itself is an important observation in adding to the characterisation of MCL cells.

CD49d, which makes up part of VLA-4, is commonly expressed on resting lymphocytes and monocytes, functioning as a matrix and cellular receptor. The high expression observed in this series is probably to be expected, given VLA-4's role in facilitating lymph node adhesion to FDCs via ICAM-1.[108]

In addition to the baseline adhesion characteristics of MCL, the dynamic increase in expression of CD184 in response to stromal cell co-culture is an important observation which reinforces previously published data on the high level expression of CD184 and VLA-4 by MCL cells.[28] It is thought that this dynamic expression facilitates drug-resistance in MCL through adherence and migration beneath the stromal cell layer, a

phenomenon termed pseudoemperipolesis, which can be blocked by CD184 inhibition or VLA-4 antibodies.[28] The increase of CD54 expression by CD40L is intriguing and may contribute to retention of cells within the tissue microenvironment.

BTK inhibitors have revolutionised the treatment of patients with MCL. However resistance to therapy is observed and complete remissions rare. Improving responses using synergistic drug combinations are being assessed. This study has shown differences in expression of CAM based on clinical phenotype following ibrutinib treatment of MCL cells cultured on human stroma and although results are preliminary could provide targets for therapy to overcome resistance and/ or improve treatment response.

6.1.3 Developing a 3-D model for primary MCL culture

The exploration of a 3-D model for MCL culture *ex vivo* is a novel method. Because this model had not been previously tested in primary MCL, and only limited published data exists for any 3-D culture method for lymphoma cells in general, a relatively high number of variables (seeding suspension composition and density; length of culture time; the addition of supplements; methods for enhancing colonisation and alterations to methods for fixation, staining and embedding) were tested with limited time and materials.

Colonisation of a 3-D matrix does appear possible with both primary MCLs and stromal cells. Interesting changes in morphology of stromal cells were noted, with the formation of discrete spheroids compared with the flat, spindle-shaped cells seen on flat-surface culture and the development of clusters of MCL cells were observed by phase-contrast microscopy. Preservation of disc integrity, a significant challenge, was improved by applying relatively short fixation times and reinforcing the disc structure

by cross linking the matrix with barium chloride. Morphologically recognisable cell colonies were preserved in stained sections of the cultured disc. Importantly, this study has demonstrated that is possible to retrieve and identify MCL cells by flow cytometry after culture within the 3-D system therefore enabling future work to examine dynamic changes to survival, adhesion marker expression and proliferation in 3-D culture by this method. This would be an interesting avenue for future work.

Overview and Future Directions

6.2 The observations demonstrated in this thesis and how these could be developed in future work can be summarised in the following points:

- Cells from subjects with more indolent, leukaemic forms of MCL demonstrate more prolonged survival in ex-vivo culture compared with cells from subjects with a more aggressive, proliferative disease type;
- both murine and human stromal layers are able to support survival and proliferation of primary MCL cells ex-vivo, however, when murine stroma are used, additional CD40 signalling is necessary in order to sustain survival and growth, particularly in cells from subjects with more proliferative MCL;
- the soluble cytokine IL-4 appears to have a synergistic effect with CD40-L on enhancing the survival of MCL cells and could be used in future work to enhance and develop an ex-vivo culture model for primary MCL cells;
- observations from light microscopy of cell culture and cytospin preparations demonstrate that cells from proliferative cases exhibit cell clustering during times of cell division whereas non-proliferating cells do not form tight clusters;
- profiling of cellular adhesion molecules on a large series of MCL cases demonstrates increased surface expression of CD11a and its respective ligand

CD54. This may be relevant to the cell clustering behaviour visualised by light microscopy and may represent a biological rationale for this behaviour as a point of focus for future research;

- early work on a 3-D model has demonstrated the possibility of colonisation of a 3-D alginate matrix with both primary cells and cell lines. Although it remains necessary to overcome several key challenges, such as improving colonisation and cell viability throughout the matrix, important progress has been made, including new methods for cell-seeding, tissue fixation and cell retrieval.

6.3 Conclusions

Primary MCL cells exhibit significant heterogeneity in their ability to survive and proliferate when cultured in an *ex vivo* microenvironment. This reflects the clinical heterogeneity often seen in patients with MCL. Cells from subjects with indolent, leukaemic disease demonstrate a greater ability to survive *ex vivo* but with low proliferation rates. Cells from subjects with aggressive nodal disease generally have higher intrinsic rates of apoptosis associated with higher rates of proliferation. Both survival and proliferation can be significantly enhanced in *ex vivo* culture by the addition of CD40-ligand. This effect appears more marked in primary MCL cells from nodal, clinically aggressive cases. Within the stromal cell co-culture model, survival is improved by the addition of IL-4 whereas TLR-9 stimulation attenuates survival with no significant increase in proliferation.

Primary MCL cells express a characteristic profile of CAMs in which CD11a, CD49d and CD54 were consistently expressed at a high level. The profile of CAM expression differed between peripheral blood and bone marrow and between clinical phenotypes although no individual adhesion molecule expression differed significantly likely as a

result of case numbers. These results together with the increased level of expression of CD184 and CD54 seen in MCL cells when co-cultured on stroma highlight the importance of further studies to understand adhesion molecule expression within tissue microenvironments of MCL. The observation that MCL cells express CD11a and CD54 may be important in relation to the cell-clustering behaviour demonstrated by microscopy in proliferative cases. This could represent an avenue of future work.

The AlgiMatrix® 3-D culture system is a potentially useful model for the study of MCL *ex vivo*. It is possible to culture primary MCL cells within this 3-D system both alone and in association with bone marrow fibroblasts. It is also possible to analyse cellular behaviour within this model after fixation, by paraffin embedding, sectioning and staining and by live cell retrieval and flow cytometry.

Taken together this thesis has contributed new data to this under-explored area on the biology of MCL cells within *in vitro* models of the tissue microenvironment. The study particularly identifies a role for CD40L and links this to the intrinsic clinical variability of the disorder-this dependence may suggest future treatment strategies directed against the CD40 signalling pathway. The success and characterisation of the culture model may allow its future adaptation to explore or develop new treatment strategies in the disorder.

7. Bibliography

1. Zhou Y, Wang H, Fang W. Incidence trends of mantle cell lymphoma in the United States between 1992 and 2004. *Cancer*. 2008;113(4):791-798.

2. Morton LM, Wang SS, Devesa SS, Hartge P, Weisenburger DD, Linet MS. Lymphoma incidence patterns by WHO subtype in the United States, 1992-2001. *Blood*. 2006;107(1):265-276. doi:10.1182/blood-2005-06-2508.

3. Swerdlow SH, Campo E, Harris NL, et al. *WHO Classification of Tumours of Haematopoietic and Lymphoid Tissues*.; 2008.

4. Argatoff LH, Connors JM, Klasa RJ, Horsman DE, Gascoyne RD. Mantle cell lymphoma: a clinicopathologic study of 80 cases. *Blood*. 1997;89(Mcl):2067-2078.

5. Fernàndez V, Salamero O, Espinet B, et al. Genomic and gene expression profiling defines indolent forms of mantle cell lymphoma. *Cancer Res*. 2010;70(4):1408-1418. doi:10.1158/0008-5472.CAN-09-3419.

6. Vegliante MC, Palomero J, Pérez-Galán P, et al. SOX11 regulates PAX5 expression and blocks terminal B-cell differentiation in aggressive mantle cell lymphoma. *Blood*. 2013;121(12):2175-2185. doi:10.1182/blood-2012-06-438937.

7. Jares P, Colomer D, Campo E. Genetic and molecular pathogenesis of mantle cell lymphoma: perspectives for new targeted therapeutics. *Nat Rev Cancer*. 2007;7:750-762. doi:10.1038/nrc2230.

8. Eve HE, Furtado M V, Hamon MD, Rule S a J. Time to treatment does not influence overall survival in newly diagnosed mantle-cell lymphoma. *J Clin Oncol*. 2009;27(32):e189-e190; author reply e191. doi:10.1200/JCO.2009.23.9731.

9. Royo C, Navarro A, Clot G. Non-nodal type of mantle cell lymphoma is a specific biological and clinical subgroup of the disease. *Leukemia*. 2012;26(8):358-366. doi:10.1016/j.jsbmb.2011.07.002.Identification.

10. Rubio-Moscardo F, Climent J, Siebert R, et al. Mantle-cell lymphoma genotypes identified with CGH to BAC microarrays define a leukemic subgroup of disease and predict patient outcome. *Blood*. 2005;105(11):4445-4454. doi:10.1182/blood-2004-10-3907.

11. Cheah CY, Seymour JF, Wang ML. Mantle cell lymphoma. *J Clin Oncol*. 2016;34(11):1256-1269. doi:10.1200/JCO.2015.63.5904.

12. Campo E, Rule S. Mantle Cell Lymphoma – Evolving Management Strategies Address for correspondence : Professor Simon Rule Professor of Clinical Haematology Plymouth University Peninsula School of Medicine and Dentistry Plymouth UK. 2015. doi:10.1182/blood-2014-05-521898.

13. Weigert O, Pastore a, Rieken M, Lang N, Hiddemann W, Dreyling M. Sequence-dependent synergy of the proteasome inhibitor bortezomib and cytarabine in mantle cell lymphoma. *Leuk Off J Leuk Soc Am Leuk Res Fund, UK*.

2007;21(3):524-528. doi:10.1038/sj.leu.2404511.

14. *Romaguera JE, Fayad LE, Feng L, et al. Ten-year follow-up after intense chemoimmunotherapy with Rituximab-HyperCVAD alternating with Rituximab-high dose methotrexate/cytarabine (R-MA) and without stem cell transplantation in patients with untreated aggressive mantle cell lymphoma. *Br J Haematol*. 2010;150(2):200-208. doi:10.1111/j.1365-2141.2010.08228.x.

15. Chen Y, Wang M, Romaguera J. Current regimens and novel agents for mantle cell lymphoma. *Br J Haematol*. 2014;167(1):3-18. doi:10.1111/bjh.13000.

16. Delarue R, Haioun C, Ribrag V, et al. CHOP and DHAP plus rituximab followed by autologous stem cell transplantation in mantle cell lymphoma : a phase 2 study from the Groupe d ' Etude des Lymphomes de l ' Adulte. *Blood*. 2013;121(1):48-53. doi:10.1182/blood-2011-09-370320.The.

17. Tucker D, Rule S. A critical appraisal of ibrutinib in the treatment of mantle cell lymphoma and chronic lymphocytic leukemia. *Ther Clin Risk Manag*. 2015;11:979-990.

18. Sherr CJ. G1 phase progression: Cycling on cue. *Cell*. 1994;79:551-554.

19. Jares P, Colomer D, Campo E. Review series Molecular pathogenesis of mantle cell lymphoma. 2012;122. doi:10.1172/JCI61272.3416.

20. Pérez-galán P, Dreyling M, Wiestner A, Dc W, Pe P. Mantle cell lymphoma : biology , pathogenesis , and the molecular basis of treatment in the genomic era. *Blood*. 2011;117(1):26-38. doi:10.1182/blood-2010-04-189977.

21. Mozos A, Royo C, Hartmann E, et al. SOX11 expression is highly specific for mantle cell lymphoma and identifies the cyclin D1-negative subtype. *Haematologica*. 2009;94(11):1555-1562. doi:10.3324/haematol.2009.010264.

22. Nordström L, Sernbo S, Eden P, et al. SOX11 and TP53 add prognostic information to MIPI in a homogenously treated cohort of mantle cell lymphoma - a Nordic Lymphoma Group study. *Br J Haematol*. 2014;166(1):98-108. doi:10.1111/bjh.12854.

23. Navarro A, Clot G, Royo C, et al. Molecular subsets of mantle cell lymphoma defined by the IGHV mutational status and SOX11 expression have distinct biologic and clinical features. *Cancer Res*. 2012;72(20):5307-5316. doi:10.1158/0008-5472.CAN-12-1615.

24. Grivennikov SI, Greten FR, Karin M. Immunity, inflammation, and cancer. *Cell*. 2010;140(6):883-899. doi:10.1016/j.cell.2010.01.025 [doi].

25. Coussens LM, Werb Z. Inflammation and cancer. *Nature*. 2002;420(6917):860-867. doi:10.1038/nature01322.

26. Candido J, Hagemann T. Cancer-related inflammation. *J Clin Immunol*. 2013;33(SUPPL.1). doi:10.1007/s10875-012-9847-0.

27. Burger J a, Ghia P, Rosenwald A, Caligaris-cappio F. The microenvironment in mature B-cell malignancies : a target for new treatment strategies Review article The microenvironment in mature B-cell malignancies : a target for new

treatment strategies. 2009;114(16):3367-3375. doi:10.1182/blood-2009-06-225326.

28. Kurtova A V., Tamayo AT, Ford RJ, Burger J a. Mantle cell lymphoma cells express high levels of CXCR4, CXCR5, and VLA-4 (CD49d): Importance for interactions with the stromal microenvironment and specific targeting. *Blood*. 2009;113(19):4604-4613. doi:10.1182/blood-2008-10-185827.

29. Burger JA, Ford RJ. The microenvironment in mantle cell lymphoma: Cellular and molecular pathways and emerging targeted therapies. *Semin Cancer Biol*. 2011;21(5):308-312. doi:10.1016/j.semcancer.2011.09.006.

30. Medina DJ, Goodell L, Glod J, Gélinas C, Rabson AB, Strair RK. Mesenchymal stromal cells protect mantle cell lymphoma cells from spontaneous and drug-induced apoptosis through secretion of B-cell activating factor and activation of the canonical and non-canonical nuclear factor ??B pathways. *Haematologica*. 2012;97(8):1255-1263. doi:10.3324/haematol.2011.040659.

31. Medina DJ, Abass-Shereef J, Walton K, et al. Cobblestone-area forming cells derived from patients with mantle cell lymphoma are enriched for CD133+ tumor-initiating cells. *PLoS One*. 2014;9(4):e91042. doi:10.1371/journal.pone.0091042.

32. Trentin L, Cabrelle A, Facco M, et al. Homeostatic chemokines drive migration of malignant B cells in patients with non-Hodgkin lymphomas. *Blood*. 2004;104(2):502-508. doi:10.1182/blood-2003-09-3103.

33. Kurtova A V, Tamayo AT, Ford RJ, Burger J a. Mantle cell lymphoma cells express high levels of CXCR4, CXCR5, and VLA-4 (CD49d): importance for interactions with the stromal microenvironment and specific targeting. *Blood*. 2009;113(19):4604-4613. doi:10.1182/blood-2008-10-185827.

34. Burger JA, Burger M, Kipps TJ. Chronic lymphocytic leukemia B cells express functional CXCR4 chemokine receptors that mediate spontaneous migration beneath bone marrow stromal cells. *Blood*. 1999;94(11):3658-3667.

35. Bürkle A, Niedermeier M. Overexpression of the CXCR5 chemokine receptor, and its ligand, CXCL13 in B-cell chronic lymphocytic leukemia. …. 2007;110(9):3316-3325. doi:10.1182/blood-2007-05-089409.The.

36. Sipkins DA, Wei X, Wu JW, et al. In vivo imaging of specialized bone marrow endothelial microdomains for tumour engraftment. *Nature*. 2005;435(7044):969-973. doi:10.1038/nature03703.

37. Damiano JS, Cress AE, Hazlehurst LA, Shtil AA, Dalton WS. Cell adhesion mediated drug resistance (CAM-DR): role of integrins and resistance to apoptosis in human myeloma cell lines. *Blood*. 1999;93(5):1658-1667. doi:10.1016/0014-4827(72)90265-0.

38. Kim Y, Eom K. Simultaneous Inhibition of CXCR4 and VLA-4 Exhibits Combinatorial Effect in Overcoming Stroma-Mediated Chemotherapy Resistance in Mantle Cell Lymphoma Cells. 2014;14(6):296-306.

39. Medina DJ, Goodell L, Glod J, Gélinas C, Rabson AB, Strair RK. Mesenchymal

stromal cells protect mantle cell lymphoma cells from spontaneous and drug-induced apoptosis through secretion of B-cell activating factor and activation of the canonical and non-canonical nuclear factor κB pathways. *Haematologica*. 2012;97(8):1255-1263. doi:10.3324/haematol.2011.040659.

40. Saba NS, Liu D, Herman SEM, et al. Pathogenic role of B-cell receptor signaling and canonical NF-κB activation in mantle cell lymphoma. *Blood*. 2016;128(1):82-93. doi:10.1182/blood-2015-11-681460.

41. Carbone E, Ruggiero G, Terrazzano G, et al. A new mechanism of NK cell cytotoxicity activation: the CD40-CD40 ligand interaction. *J Exp Med*. 1997;185(12):2053-2060. doi:10.1084/jem.185.12.2053.

42. Basso K, Klein U, Niu H, et al. Tracking CD40 signaling during germinal center development. *Blood*. 2004;104(13):4088-4096. doi:10.1182/blood-2003-12-4291.

43. Liu Y, Joshua DE, Williams GT, Smith CA, Gordon J, MacLennan IC. Mechanism of antigen-driven selection in germinal centres. *Nature*. 1989;Dec 21-28(342):929-931.

44. Holder M, Wang H, Milner A, Casamayor M, Armitage R. Suppression of apoptosis in normal and neoplastic human B lymphocytes by CD40 ligand is independent of Bc1-2 induction. *Eur J Immunol*. 1993;23(9):2368-2371.

45. Elgueta R, Benson M, de Vries V, Wasiuk A, Guo Y, R N. Molecular mechanisms and function of CD40/CD40L engagement in the immune system. *Immunol Rev*. 2009;229(1).

46. Shattner E, Elkon K, Yoo D, et al. CD40 ligation induces Apo-1/Fas expression on human B lymphocytes and facilitates apoptosis through the Apo-1/Fas pathway. *J Exp Med*. 1995;182:1557-1565.

47. Bishop JY, Schattner EJ, Friedman SM. CD40 ligation impedes lymphoblastoid B cell proliferation and S-phase entry. *Leuk Res*. 1998;22(4):319-327. doi:10.1016/S0145-2126(97)00173-2.

48. Romano MF, Lamberti A, Tassone P, et al. Triggering of CD40 Antigen Inhibits Fludarabine-Induced Apoptosis in B Chronic Lymphocytic Leukemia Cells. *Blood*. 1998;92(3):990-995.

49. Castillo R, Mascarenhas J, Telford W, Chadburn a, Friedman SM, Schattner EJ. Proliferative response of mantle cell lymphoma cells stimulated by CD40 ligation and IL-4. *Leukemia*. 2000;14(2):292-298. http://www.ncbi.nlm.nih.gov/pubmed/10673747.

50. Wortis HH, Teutsch M, Higer M, Zheng J, Parkert DC. B-cell activation by crosslinking of surface IgM or ligation of CD40 involves alternative signal pathways and results in different B-cell phenotypes. *Proc Natl Acad Sci U S A*. 1995;92(April):3348-3352.

51. Isaza-Correa JM, Liang Z, van den Berg A, Diepstra A, Visser L. Toll-like receptors in the pathogenesis of human B cell malignancies. *J Hematol Oncol*. 2014;7(1):57. doi:10.1186/s13045-014-0057-5.

52. Boeglin E, Smulski CR, Brun S, Milosevic S, Schneider P, Fournel S. Toll-Like receptor agonists synergize with CD40L to induce either proliferation or plasma cell differentiation of mouse B cells. *PLoS One*. 2011;6(10). doi:10.1371/journal.pone.0025542.

53. Peng SL. Signaling in B cells via Toll-like receptors. *Curr Opin Immunol*. 2005;17(3):230-236. doi:10.1016/j.coi.2005.03.003.

54. Li X, Jiang S, Tapping RI. Toll-like receptor signaling in cell proliferation and survival. *Cytokine*. 2010;49(1):1–9. doi:10.1016/j.cyto.2009.08.010.Toll-like.

55. Ruprecht CR, Lanzavecchia A. Toll-like receptor stimulation as a third signal required for activation of human naive B cells. *Eur J Immunol*. 2006;36(4):810-816. doi:10.1002/eji.200535744.

56. Bohnhorst J, Rasmussen T, Moen SH, et al. Toll-like receptors mediate proliferation and survival of multiple myeloma cells. *Leuk Off J Leuk Soc Am Leuk Res Fund, UK*. 2006;20:1138-1144. doi:10.1038/sj.leu.2404225.

57. Rabin EM, Mond JJ, Ohara J, Paul WE. B Cell stimulatory factor 1 (BSF-1) prepares resting B cells to enter S phase in response to Anti-IgM and lipopolysaccharide. *J Exp Med*. 1986;164(August):517.

58. Le Gros G, Ben-Sasson SZ, Seder R, Finkelman FD, Paul WE. Generation of interleukin 4 (IL-4)-producing cells in vivo and in vitro: IL-2 and IL-4 are required for in vitro generation of IL-4-producing cells. *J Exp Med*. 1990;172(3):921-929. doi:10.1017/CBO9781107415324.004.

59. Paul WE. Interleukin-4: A Prototypic Immunoregulatory Lymphokine. *Blood*. 1991;77(9):1-19.

60. Lemaire C, Andréau K, Sidoti-de Fraisse C, Adam A, Souvannavong V. IL-4 inhibits apoptosis and prevents mitochondrial damage without inducing the switch to necrosis observed with caspase inhibitors. *Cell Death Differ*. 1999;6(8):813-820. doi:10.1038/sj.cdd.4400556.

61. Dancescu M, Rubio-Trujillo M, Biron G, Bron D, Delespesse G, Sarfati M. Interleukin 4 protects chronic lymphocytic leukemic B cells from death by apoptosis and upregulates Bcl-2 expression. *J Exp Med*. 1992;176(5):1319-1326. doi:10.1084/jem.176.5.1319.

62. Banchereau J, de Paoli P, Vallé A, Garcia E, Rousset F. Long-term human B cell lines dependent on interleukin-4 and antibody to CD40. *Science*. 1991;251(4989):70-72. doi:10.1126/science.1702555.

63. Rush J, Hodgkin P. B cells activated via CD40 and IL-4 undergo a division burst but require continued stimulation to maintain division, survival and differentiation. *Eur J Immunol*. 2001;31(4):1150-1159.

64. Wang ML, Rule S, Martin P, et al. Targeting BTK with ibrutinib in relapsed or refractory mantle-cell lymphoma. *N Engl J Med*. 2013;369(6):507-516. doi:10.1056/NEJMoa1306220.

65. Chang BY, Francesco M, De Rooij MFM, et al. Egress of CD19(+)CD5(+) cells into peripheral blood following treatment with the Bruton tyrosine kinase inhibitor

ibrutinib in mantle cell lymphoma patients. *Blood*. 2013;122(14):2412-2424. doi:10.1182/blood-2013-02-482125.

66. Furtado M, Wang M, Munneke M, McGreivy J, Beaupre DM, Rule SA. Ibrutinib associated lymphocytosis corresponds to bone marrow involvement in mantle cell lymphoma. *Br J Haematol*. 2015;170:123-138.

67. Bernard S, Danglade D, Gardano L, et al. Inhibitors of BCR signalling interrupt the survival signal mediated by the micro-environment in mantle cell lymphoma. *Int J Cancer*. 2014;0(May):1-14. doi:10.1002/ijc.29326.

68. Kim C, Ye F, Ginsberg MH. Regulation of Integrin Activation. *Annu Rev Cell Dev Biol*. 2011;27(1):321-345. doi:10.1146/annurev-cellbio-100109-104104.

69. Tamkun JW, DeSimone DW, Fonda D, et al. Structure of integrin, a glycoprotein involved in the transmembrane linkage between fibronectin and actin. *Cell*. 1986;46(2):271-282. doi:10.1016/0092-8674(86)90744-0.

70. Campbell ID, Humphries MJ. Integrin Structure , Activation , and Interactions. 2015:1-15.

71. Springer T a. Adhesion receptors of the immune system. *Nature*. 1990;346(6283):425-434. doi:10.1038/346425a0.

72. Hynes RO. Integrins - A Family of Cell-Surface Receptors. *Cell*. 1987;48:549-554 ST-Integrins-A Family of Cell-Surface. doi:10.1016/0092-8674(87)90233-9.

73. Plow EF, Haas TA, Zhang L, Loftus J, Smith JW. Ligand binding to integrins. *J Biol Chem*. 2000;275(29):21785-21788. doi:10.1074/jbc.R000003200.

74. Matos DM, Rizzatti EG, Falcão RP. Adhesion molecule profiles of B-cell non-hodgkin's lymphoma in the leukemic phase. *Brazilian J Med Biol Res*. 2006;39:1349-1355.

75. Tan SM, Hyland RH, Al-Shamkhani a, Douglass W a, Shaw JM, Law SK. Effect of integrin beta 2 subunit truncations on LFA-1 (CD11a/CD18) and Mac-1 (CD11b/CD18) assembly, surface expression, and function. *J Immunol*. 2000;165(5):2574-2581. doi:10.4049/jimmunol.165.5.2574.

76. Matos DM, Rizzatti EG, Garcia a. B, Gallo D a P, Falcão RP. Adhesion molecule profiles of B-cell non-Hodgkin's lymphomas in the leukemic phase. *Brazilian J Med Biol Res*. 2006;39(10):1349-1355. doi:10.1590/S0100-879X2006001000011.

77. Boyd A, Dunn SM, Fecondo J V. Regulation of expression of a human intercellular adhesion molecule (ICAM-1) during lymphohematopoietic differentiation. 198AD;73(7):1896-1903.

78. Csanaky G, Matutes E, Vass JA, Morilla R, Catovsky D. Adhesion receptors on peripheral blood leukemic B cells. A comparative study on B cell chronic lymphocytic leukemia and related lymphoma/leukemias. *Leuk Off J Leuk Soc Am Leuk Res Fund, UK*. 1997;11(3):408-415. doi:10.1038/sj.leu.2400582.

79. Stauder R, Greil R, Schulz TF, et al. Expression of leucocyte function-associated antigen-1 and 7F7-antigen, an adhesion molecule related to intercellular adhesion molecule-1 (ICAM-1) in non-Hodgkin lymphomas and leukaemias:

possible influence on growth pattern and leukaemic behaviour. *Clin Exp Immunol*. 1989;77(2):234-238.

80. Wingren AG, Parra E, Varga M, et al. T cell activation pathways: B7, LFA-3, and ICAM-1 shape unique T cell profiles. *Crit Rev Immunol*. 1995;15(3-4):235-253. doi:10.1615/CritRevImmunol.v15.i3-4.30.

81. Veltroni M, De Zen L, Sanzari MC, et al. Expression of CD58 in normal, regenerating and leukemic bone marrow B cells: implications for the detection of minimal residual disease in acute lymphocytic leukemia. *Haematologica*. 2003;88(11):1245-1252.

82. Angelopoulou MK, Kontopidou FN, Pangalis GA. Adhesion molecules in B-chronic lymphoproliferative disorders. *Semin Hematol*. 1999;36(2):178-197.

83. Boyum A. Isolation of mononuclear cells and granulocytes from human blood. Isolation of monuclear cells by one centrifugation, and of granulocytes by combining centrifugation and sedimentation at 1 g. *Scand J Clin Lab Invest Suppl*. 1968;97:77-89.

84. Radtke S, Görgens A, Liu B, Horn PA, Giebel B. Human mesenchymal and murine stromal cells support human lympho-myeloid progenitor expansion but not maintenance of multipotent haematopoietic stem and progenitor cells. *Cell Cycle*. 2016;15(4):540-545. doi:10.1080/15384101.2015.1128591.

85. Issaad C, Croisille L, Katz A, Vainchenker W, Coulombel L. A Murine Stromal Cell Line Allows the Proliferation of Very Primitive Human CD34 +. *Blood*. 1993;81(1):2916-2924.

86. Andrews R, Singer J, Bernstein I. PRECURSORS OF COLONY FORMING CELLS IN HUMANS CAN BE DISTINGUISHED FROM COLONY-FORMING CELLS BY EXPRESSION OF THE CD33 AND CD34 ANTIGENS AND LIGHT SCATTER PROPERTIES In the hematopoietic stem cell hierarchy , the earliest cell is pluripotent and capable of. 1989;169(May).

87. Thalmeier K, Meissner P, Reisbach G, Falk M, Brechtel A, Dörmer P. Establishment of two permanent human bone marrow stromal cell lines with long-term post irradiation feeder capacity. *Blood*. 1994;83(7):1799-1807.

88. Nicol A, Nieda M, Donaldson C, et al. Cryopreserved human bone marrow stroma is fully functional in vitro. *Br J Haematol*. 1996;94(2):258-265.

89. Ruan J, Hajjar K, Rafii S, Leonard JP. Angiogenesis and antiangiogenic therapy in non-Hodgkin's lymphoma. *Ann Oncol*. 2009;20(3):413-424. doi:10.1093/annonc/mdn666.

90. Ning ZQ, Norton JD, Li J, Murphy JJ. Distinct mechanisms for rescue from apoptosis in Ramos human B cells by signaling through CD40 and interleukin-4 receptor: Role for inhibition of an early response gene, Berg36. *Eur J Immunol*. 1996;26(10):2356-2363. doi:10.1002/eji.1830261013.

91. Andersen NS, Larsen JK, Christiansen J, Pedersen LB, Christophersen NS, Geisler CH. Soluble CD40 ligand induces selective proliferation of lymphoma cells in primary mantle cell lymphoma cell cultures. 2016;96(6):2219-2226.

92. Grdisa M. Influence of CD40 ligation on survival and apoptosis of B-CLL cells in vitro. *Leuk Res*. 2003;27(10):951-956. doi:10.1016/S0145-2126(03)00028-6.

93. Beà S, Valdés-Mas R, Navarro A, et al. Landscape of somatic mutations and clonal evolution in mantle cell lymphoma. *Proc Natl Acad Sci U S A*. 2013;110(45):18250-18255. doi:10.1073/pnas.1314608110.

94. Eve HE, Furtado M V, Hamon MD, Rule SA. Time to treatment does not influence overall survival in newly diagnosed mantle-cell lymphoma. *J Clin Oncol*. 2009;27(32):e189-90; author reply e191. doi:JCO.2009.23.9731 [pii]\r10.1200/JCO.2009.23.9731.

95. Hernandez L, Fest T, Cazorla M, et al. P53 Gene Mutations and Protein Overexpression Are Associated With Aggressive Variants of Mantle Cell Lymphomas. *Blood*. 1996;87(8):3351-3359. http://www.ncbi.nlm.nih.gov/pubmed/8605352.

96. Katz T, Shivtiel-Arad S, Saadi H, et al. Different Sources of Stromal Cells Diversely Affect Survival and Trafficking of Mantle Cell Lymphoma Cells. In: *Blood*.Vol 126.; 2015:2670-2670. http://www.bloodjournal.org/content/126/23/2670.

97. Ding W, Nowakowski GS, Knox T, Boysen J, Maas M, Schwager S. Bi-directional Activation between Mesenchymal Stem Cells and CLL B-Cells: Implication for CLL Disease Progression. *BrJHaematol*. 2009;147(4):471-483.

98. Liu Y, Joshua DE, Williams GT, Smith C, Gordon J, MacLennon I. Mechanism of antigen-driven selection in germinal centres. *Nature*. 1989;21-28(342):929-931.

99. Pettitt AR, Moran EC, Cawley JC. Homotypic interactions protect chronic lymphocytic leukaemia cells from spontaneous death in vitro. *Leuk Res*. 2001;25(11):1003-1012. doi:10.1016/S0145-2126(01)00067-4.

100. Burger J a. Nurture versus Nature: The Microenvironment in Chronic Lymphocytic Leukemia. *Hematology*. 2011;2011(1):96-103. doi:10.1182/asheducation-2011.1.96.

101. Bosch F, López-Guillermo A, Campo E, et al. Mantle cell lymphoma: presenting features, response to therapy, and prognostic factors. *Cancer*. 1998;82:567-575.

102. Ferrer A, Salaverria I, Bosch F, et al. Leukemic involvement is a common feature in mantle cell lymphoma. *Cancer*. 2007;109(12):2473-2480. doi:10.1002/cncr.22715.

103. Orchard J, Garand R, Davis Z, et al. A subset of t(11;14) lymphoma with mantle cell features displays mutated IgVH genes and includes patients with good prognosis, nonnodal disease. *Blood*. 2003;101(12):4975-4981. doi:10.1182/blood-2002-06-1864.

104. Nodit L, Bahler DW, Jacobs S a., Locker J, Swerdlow SH. Indolent Mantle Cell Lymphoma With Nodal Involvement and Mutated Immunoglobulin Heavy Chain Genes. *Hum Pathol*. 2003;34(10):1030-1034. doi:10.1053/S0046-8177(03)00410-6.

105. Kienle D, Kröber A, Katzenberger T, et al. VH mutation status and VDJ rearrangement structure in mantle cell lymphoma: Correlation with genomic

aberrations, clinical characteristics, and outcome. *Blood*. 2003;102(8):3003-3009. doi:10.1182/blood-2003-05-1383.

106. Camacho F, Algara P, Rodriguez A. Molecular heterogeneity in MCL defined by the use of specific VH genes and the frequency of somatic mutations. *Blood*. 2003;101(12):4042-4046. doi:10.1182/blood-2002-06-1864.

107. Del Giudice I, Messina M, Chiaretti S, et al. Behind the scenes of non-nodal MCL: Downmodulation of genes involved in actin cytoskeleton organization, cell projection, cell adhesion, tumour invasion, TP53 pathway and mutated status of immunoglobulin heavy chain genes. *Br J Haematol*. 2012;156(5):601-611. doi:10.1111/j.1365-2141.2011.08962.x.

108. Koopman G, Parmentier HK, Schuurman HJ, Newman W, Meijer CJ, Pals ST. Adhesion of human B cells to follicular dendritic cells involves both the lymphocyte function-associated antigen 1/intercellular adhesion molecule 1 and very late antigen 4/vascular cell adhesion molecule 1 pathways. *J Exp Med*. 1991;173(6):1297-1304. http://www.pubmedcentral.nih.gov/articlerender.fcgi?artid=2190833&tool=pmcentrez&rendertype=abstract.

109. Baldini L, Cro L, Calori R, Nobili L, Silvestris I, Maiolo AT. Differential expression of very late activation antigen-3 (VLA-3)/VLA-4 in B-cell non-Hodgkin lymphoma and B-cell chronic lymphocytic leukemia. *Blood*. 1992;79(10):2688-2693. http://www.ncbi.nlm.nih.gov/entrez/query.fcgi?cmd=Retrieve&db=PubMed&dopt=Citation&list_uids=1586717.

110. Medeiros LJ, Weiss LM, Picker LJ, et al. Expression of LFA- I in Non-Hodgkin's Lymphoma. *Cancer*. 1989;63:255-259.

111. Roossien FF, De Rijk D, Bikker A, Roos E. Involvement of LFA-1 in lymphoma invasion and metastasis demonstrated with LFA-1-deficient mutants. *J Cell Biol*. 1989;108(5):1979-1985.

112. Honigberg L a, Smith AM, Sirisawad M, et al. The Bruton tyrosine kinase inhibitor PCI-32765 blocks B-cell activation and is efficacious in models of autoimmune disease and B-cell malignancy. *Proc Natl Acad Sci U S A*. 2010;107(29):13075-13080. doi:10.1073/pnas.1004594107.

113. Buggy JJ. Bruton Tyrosine Kinase (BTK) and its role in B-cell malignancy. *Int Rev Immunol*. 2012;32(2):119-132.

114. Dal Porto JM, Gauld SB, Merrell KT, Mills D, Pugh-Bernard AE, Cambier J. B cell antigen receptor signaling 101. *Mol Immunol*. 2004;41(6-7):599-613. doi:10.1016/j.molimm.2004.04.008.

115. Maas A, Hendriks RW. Role of Bruton's Tyrosine Kinase in B Cell Development. *Dev Immunol*. 2001;8:171-181. doi:10.1155/2001/28962.

116. Inghirami G, Wieczorek R, Bang-Ying Z. Differential expression of LFA-1 molecules in non-Hodgkin's lymphoma and lymphoid leukemia. *Blood*. 1988;72(4):1431-1344.

117. Bulian P, Shanafelt TD, Fegan C, et al. CD49d is the strongest flow cytometry-

based predictor of overall survival in chronic lymphocytic leukemia. *J Clin Oncol*. 2014;32(9):897-904. doi:10.1200/JCO.2013.50.8515.

118. Yellin MJ, Winikoff S, Fortune SM, et al. Ligation of CD40 on fibroblasts induces CD54 (ICAM-1) and CD106 (VCAM-1) up-regulation and IL-6 production and proliferation. *J Leukoc Biol*. 1995;58(2):209-216. http://www.ncbi.nlm.nih.gov/pubmed/7543921.

119. Rushworth SA, Bowles KM, Barrera LN, Murray MY, Zaitseva L, MacEwan DJ. BTK inhibitor ibrutinib is cytotoxic to myeloma and potently enhances bortezomib and lenalidomide activities through NF-κB. *Cell Signal*. 2013;25:106-112. doi:10.1016/j.cellsig.2012.09.008.

120. Herman SEM, Mustafa RZ, Gyamfi J a, et al. Ibrutinib inhibits BCR and NF-κB signaling and reduces tumor proliferation in tissue-resident cells of patients with CLL. *Blood*. 2014;123(21):3286-3295. doi:10.1182/blood-2014-02-548610.

121. Zheng X, Ding N, Song Y, Feng L, Zhu J. Different sensitivity of germinal center B cell-like diffuse large B cell lymphoma cells towards ibrutinib treatment. *Cancer Cell Int*. 2014;14(1):32. doi:10.1186/1475-2867-14-32.

122. Chen S-S, Chang BY, Chang S, et al. BTK inhibition results in impaired CXCR4 chemokine receptor surface expression, signaling and function in chronic lymphocytic leukemia. *Leukemia*. 2016;30(4):833-843. doi:10.1038/leu.2015.316.

123. Pampaloni F, Reynaud EG, Stelzer EHK. The third dimension bridges the gap between cell culture and live tissue. *Nat Rev Mol Cell Biol*. 2007;8(10):839-845. doi:10.1038/nrm2236.

124. Jiguet Jiglaire C, Baeza-Kallee N, Denicola?? E, et al. Ex vivo cultures of glioblastoma in three-dimensional hydrogel maintain the original tumor growth behavior and are suitable for preclinical drug and radiation sensitivity screening. *Exp Cell Res*. 2014;321(2):99-108. doi:10.1016/j.yexcr.2013.12.010.

125. Petersen OW, Rønnov-Jessen L, Howlett AR, Bissell MJ. Interaction with basement membrane serves to rapidly distinguish growth and differentiation pattern of normal and malignant human breast epithelial cells. *Proc Natl Acad Sci U S A*. 1992;89(19):9064-9068. doi:10.1073/pnas.90.6.2556c.

126. Wang F, Weaver VM, Petersen OW, et al. Reciprocal interactions between beta1-integrin and epidermal growth factor receptor in three-dimensional basement membrane breast cultures: a different perspective in epithelial biology. *Proc Natl Acad Sci U S A*. 1998;95(25):14821-14826. doi:10.1073/pnas.95.25.14821.

127. Huebsch N, Arany PR, Mao AS, et al. Harnessing traction-mediated manipulation of the cell/matrix interface to control stem-cell fate. *Nat Mater*. 2010;9(6):518-526. doi:10.1038/nmat2732.

128. Pickl M, Ries CH. Comparison of 3D and 2D tumor models reveals enhanced HER2 activation in 3D associated with an increased response to trastuzumab. *Oncogene*. 2009;28(3):461-468. doi:10.1038/onc.2008.394.

129. Rhodes N, Srivastava J, Smith R, Longinotti C. Metabolic and histological analysis of mesenchymal stem cells grown in 3-D hyaluronan-based scaffolds. *J Mater Sci Mater Med*. 2004;15(4):391-395.

130. Kirshner J, Thulien K, Kriangkum J, Motz S, Belch A, Pilarski L. In a patient with biclonal Waldenstrom macroglobulinemia only one clone expands in three-dimensional culture and includes putative cancer stem cells. *Leuk Lymphoma*. 2011;52(2):285-289.

131. Bruce A, Evans R, Mezan R, et al. Three-dimensional microfluidic tri-culture model of the bone marrow microenvironment for study of acute lymphoblastic leukemia. *PLoS One*. 2015;10(10):1-16. doi:10.1371/journal.pone.0140506.

132. Steimberg N, Mazzoleni G, Ciamporcero E, et al. In Vitro Modeling of Tissue-Specific 3D Microenvironments and Possibile Application to Pediatric Cancer Research. *J Pediatr Oncol*. 2014;2(July):40-76. doi:10.14205/2309-3021.2014.02.01.5.

133. Lu P, Weaver VM, Werb Z. The extracellular matrix: A dynamic niche in cancer progression. *J Cell Biol*. 2012;196(4):395-406. doi:10.1083/jcb.201102147.

134. Paszek MJ, Zahir N, Johnson KR, et al. Tensional homeostasis and the malignant phenotype. *Cancer Cell*. 2005;8(3):241-254. doi:10.1016/j.ccr.2005.08.010.

135. Rutkowski JM, Swartz MA. A driving force for change: interstitial flow as a morphoregulator. *Trends Cell Biol*. 2007;17(1):44-50. doi:10.1016/j.tcb.2006.11.007.

136. Mueller-Klieser W. Three-dimensional cell cultures: from molecular mechanisms to clinical applications. *Am J Physiol - Cell Physiol*. 1997;273(4):C1109-C1123. doi:10.2307/3010125.

137. Holopainen I. Organotypic Hippocampal Slice Cultures: A Model System to Study Basic Cellular and Molecular Mechanisms of Neuronal Cell Death, Neuroprotection, and Synaptic Plasticity. *Neurochem Res*. 2005;30(12):1521-1528.

138. Kelm JM, Timmins NE, Brown CJ, Fussenegger M, Nielsen LK. Method for generation of homogeneous multicellular tumor spheroids applicable to a wide variety of cell types. *Biotechnol Bioeng*. 2003;83(2):173-180. doi:10.1002/bit.10655.

139. Rossi MI, Barros AP, Baptista LS, et al. Multicellular spheroids of bone marrow stromal cells: a three-dimensional in vitro culture system for the study of hematopoietic cell migration. *Braz J Med Biol Res*. 2005;38(10):1455-1462. doi:S0100-879X2005001000002 [pii]\r/S0100-879X2005001000002.

140. Debnath J, Muthuswamy SK, Brugge JS. Morphogenesis and oncogenesis of MCF-10A mammary epithelial acini grown in three-dimensional basement membrane cultures. *Methods*. 2003;30(3):256-268. doi:10.1016/S1046-2023(03)00032-X.

141. Girard YK, Wang C, Ravi S, et al. A 3D Fibrous Scaffold Inducing Tumoroids: A Platform for Anticancer Drug Development. *PLoS One*. 2013;8(10).

doi:10.1371/journal.pone.0075345.

142. Kleinman HK, Martin GR. Matrigel: Basement membrane matrix with biological activity. *Semin Cancer Biol*. 2005;15(5 SPEC. ISS.):378-386. doi:10.1016/j.semcancer.2005.05.004.

143. Hoffman R. Histocultures and Organ Cultures. *eLS*. http://onlinelibrary.wiley.com/doi/10.1038/npg.els.0002573/full.

144. Guneta V, Soon Tan N, Chan SK, et al. Comparative study of adipose-derived stem cells and bone marrow-derived stem cells in similar microenvironmental conditions. *Exp Cell Res*. 2016;348(2):155-164.

145. Cardoso TC, Sakamoto SS, Stockmann D, et al. A three-dimensional cell culture system as an *in vitro* canine mammary carcinoma model for the expression of connective tissue modulators. *Vet Comp Oncol*. 2016:n/a-n/a. doi:10.1111/vco.12202.

146. Andersen T, Auk-Emblem P, Dornish M. 3D Cell Culture in Alginate Hydrogels. *Microarrays*. 2015;4(2):133-161. doi:10.3390/microarrays4020133.

147. Engbring JA, Kleinman HK. The basement membrane matrix in malignancy. *J Pathol*. 2003;200(4):465-470. doi:10.1002/path.1396.

148. Autengruber a, Gereke M, Hansen G, Hennig C, Bruder D. Impact of enzymatic tissue disintegration on the level of surface molecule expression and immune cell function. *Eur J Microbiol Immunol (Bp)*. 2012;2(2):112-120. doi:10.1556/EuJMI.2.2012.2.3.

149. Gibco, Life-Technologies. *AlgiMatrix ™ 3D Culture System*.; 2013.

150. Haug A, Smidsrod O. The Effect of Divalent Metals on the Properties of Alginate Solutions. *Acta Chem Scand*. 1965;19:341-351. doi:10.3891/acta.chem.scand.19-0341.

151. Sottile J, Hocking DC, Swiatek PJ. Fibronectin matrix assembly enhances adhesion-dependent cell growth. *J Cell Sci*. 1998;111 (Pt 1:2933-2943.

152. Lin R, Chang H. Recent advances in three-dimensional multicellular spheroid culture for biomedical research. *Biotechnol J*. 2008;3:1172-1184.

153. Kim SH, Turnbull J, Guimond S. Extracellular matrix and cell signalling: The dynamic cooperation of integrin, proteoglycan and growth factor receptor. *J Endocrinol*. 2011;209(2):139-151. doi:10.1530/JOE-10-0377.

154. Desoize B, Jardillier JC. Multicellular resistance: A paradigm for clinical resistance? *Crit Rev Oncol Hematol*. 2000;36(2-3):193-207. doi:10.1016/S1040-8428(00)00086-X.

155. Boudreau N, Sympson C, Werb Z, Bissell MJ. Suppression of ICE and Apoptosis in Mammary Epithelial Cells by Extracellular Matrix. *Science (80-)*. 1995;10(267):891-893. doi:10.1124/dmd.107.016501.CYP3A4-Mediated.

156. Bates RC, Buret A, Van Helden DF, Horton MA, Burns GF. Apoptosis induced by inhibition of intercellular contact. *J Cell Biol*. 1994;125(2):403-415.

doi:10.1083/jcb.125.2.403.

157. Meredith JE, Fazeli B, Schwartz MA. The extracellular matrix as a cell survival factor. *Mol Biol Cell*. 1993;4(9):953-961. doi:10.1091/mbc.4.9.953.

158. Fujita N, Kataoka S, Naito M, et al. Suppression of T-Lymphoma Cell Apoptosis by Monoclonal Antibodies Raised against Cell Surface Adhesion Molecules. *Cancer Res*. 1993;53(20):5022-5027.

159. Guba BSC, Sartor C, Gottschalk LR, Ye-hu J, Mulligan T, Emerson SG. Bone marrow stromal fibroblasts secrete interleukin- 6 and granulocyte-macrophage colony-stimulating factor in the absence of inflammatory stimulation: Demonstration by serum-free bioassay, enzyme-linked immunoabsorbant assay and reverse transcriptase pol. 2015;80(5):1190-1199.

160. Taichman RS, Emerson SG. Human osteoblasts support hematopoiesis through the production of granulocyte colony-stimulating factor. *J Exp Med*. 1994;179(5):1677-1682. doi:10.1084/jem.179.5.1677.

161. Defrance T, Fluckiger a C, Rossi JF, Magaud JP, Sotto JJ, Banchereau J. Antiproliferative effects of interleukin-4 on freshly isolated non-Hodgkin malignant B-lymphoma cells. *Blood*. 1992;79(4):990-996. http://www.ncbi.nlm.nih.gov/pubmed/1737107.

162. Crawford DH, Catovsky D. In vitro activation of leukaemic B cells by interleukin-4 and antibodies to CD40. *Immunology*. 1993;80(1):40-44. http://www.pubmedcentral.nih.gov/articlerender.fcgi?artid=1422112&tool=pmcentrez&rendertype=abstract.

163. Jahrsdörfer B, Hartmann G, Racila E, et al. CpG DNA increases primary malignant B cell expression of costimulatory molecules and target antigens. *J Leukoc Biol*. 2001;69(1):81-88.

164. Decker T, Schneller F, Kronschnabl M, et al. Immunostimulatory CpG-oligonucleotides induce functional high affinity IL-2 receptors on B-CLL cells: Costimulation with IL-2 results in a highly immunogenic phenotype. *Exp Hematol*. 2000;28(5):558-568. doi:10.1016/S0301-472X(00)00144-2.

165. Jahrsdorfer B, Mühlenhoff L, Blackwell SE, et al. B-Cell Lymphomas Differ in their Responsiveness to CpG Oligodeoxynucleotides B-Cell Lymphomas Differ in their Responsiveness to CpG Oligodeoxynucleotides. 2005;11:1490-1499. doi:10.1158/1078-0432.CCR-04-1890.